Combined *Power* and Process – an ***Exergy*** Approach

Revised Edition

Frederick J. Barclay

Exergy Exergy Exergy

Professional Engineering Publishing

Combined Power and Process

An Exergy Approach

by

Frederick J Barclay

Professional Engineering Publishing Limited
London and Bury St Edmunds, UK

First published 1995
Revised Second Edition 1998

ISBN 1 86058 129 3

A CIP catalogue record for this book is available from the British Library.

Printed in the United Kingdom at the University Press, Cambridge, UK.

About the Author

Fred Barclay's extensive and varied career began with various posts with Rolls-Royce, the Navy, BTH, CEGB, and AWRE: he redesigned the latter's Herald reactor. In 1963 he became the Manager of the Dragon International Reactor Experiment at AEE, Winfrith where he successfully completed the commissioning and construction of the plant sections.

Between 1966 and 1968 he was the Manager of Engineering Development, Dounreay. Here he solved the liquid metal superheat problem, developed reactor acoustic equipment, investigated parallel channel instability, sub-cooled bubble collapse, and cavitation in electromagnetic pumps.

In 1968 Fred Barclay was appointed the Head of Dounreay Fast Reactor, and controller of Overseas Irradiations. This post gave him the opportunity to operate and utilize the world's major fast neutron irradiation reactor and power plant, including programming of in-core liquid metal boiling experiments at the end of reactor life.

From 1977–1982 he worked as the Manager of Engineering, Prototype Fast Reactor, UKAEA Dounreay Nuclear Establishment. He was responsible for crucial repair and rescue of leaking sodium-heated steam generators, as well as the diagnosis of fundamental design errors.

From 1982–1986 Fred was employed as the Acting Director for the Abu Dhabi Water and Electricity Department, United Arab Emirates. This involved work on a 3000 MWe, 1 500 000 tone/day power and desalination project.

Since July 1986 Fred Barclay has worked as a successful independent consultant. Clients have included the Abu Dhabi government, the Institution of Mechanical Engineers, and Legal and General Insurance.

Related Titles of Interest

Title	Editor/Author	ISBN
Engineering Profit from Waste – V	IMechE Conference Transactions 1997–4	1 86058 102 1
The Regenerator and the Stirling Engine	Allan J Organ	1 86058 010 6
Process Machinery – Safety and Reliability	William Wong	1 86058 046 7
Heat Transfer	IMechE Conference Transactions 1995–2	0 85298 950 4
CHP 2000: Co-Generation for the 21st Century	IMechE Conference Transactions 1998–1	1 86058 141 2
Journal of Power and Energy	Proceedings of the Institution of Mechanical Engineers – Part A	ISSN 0957/6509

For the full range of titles published by Professional Engineering Publishing contact:

Sales Department
Professional Engineering Publishing Limited
Northgate Avenue
Bury St Edmunds
Suffolk
IP32 6BW
UK

Tel: 01284 763277
Fax: 01284 704006

This book is dedicated to my wife Mary Cissella without whom it could not have been written.

O, Mary I'm your lovelorn lad,
A glaikit gormless loon,
Wi' scarce a glim o'commonsense,
Tae mark me fae a goon.

Ah dinna ken the straight road hame,
Ma heid's a scratchit birlie,
Wi' one thing constant goin' roon,
That your'e ma fated girlie.

Wi' wordies nice and phrases right,
Wad I woo thee i' the moon,
And tell thee in the 'witched light,
That I wad wed thee soon.

Foreword

If you are a practising mechanical or chemical engineer involved from time to time in the analysis of power or process systems, then this book has been written for you, but not for the student or the beginner. The author's principal aim – by argument and example – is to promote the advantages which accrue from applying Second Law analysis.

Simple analysis of such systems is based on the First Law of Thermodynamics in which work and heat are interchangeable and conservative. Using the Système International (SI), 1 Watt second (work) = 1 Joule (heat) and the equality applies regardless of the direction of the process of conversion.

In Second Law analysis account must be taken of the irreversible nature of Joule's experiment, namely

$$1 \text{ Watt second (work)} \rightarrow = 1 \text{ Joule (heat)}$$

whereas

$$1 \text{ Joule (heat)} \neq 1 \text{ Watt second (work)}$$

There is a heat equivalent of mechanical power, but there is no unique mechanical power equivalent of heat, as explained by Carnot a long time ago, and the original mechanical work cannot be recovered unaided. The author argues that the time-honoured expression for engine efficiency work/heat input is immediately thrown into question because instead of being a ratio of similar quantities it is a relation between 'chalk and cheese'.

In part, the dilemma results from the use of the word **energy** in a general sense both for heat and for mechanical work. Accordingly, the author uses the term **exergy** for that property of the system which is the maximum work obtainable through bringing the system into equilibrium with its surroundings. The fact that the system was not originally in equilibrium could have been caused by initial differences in pressure or temperature, or in concentration, or the potential for a chemical reaction. The former two can be associated with thermo-mechanical **exergy** and the latter two with chemical **exergy**.

Armed with this necessary additional terminological clarification, the author satisfactorily tackles in turn the efficiencies of relatively simple

systems such as open-cycle engines and fuel cells before analysing the performance of a wider range of complex systems, moving from the generality of thermo-electrical–chemical systems to such specific multiple systems as combined heat and power (CHP), combined power and desalination, heat-pump-based distillation, and 'topping' fuel cells.

Those readers with a greater interest in identifying and tracking down cycle losses and in the economic implications, rather than in efficiency as such, will also find much of value.

The necessary thermodynamics is addressed at the outset and particularly the entropy function, essential to the understanding of the concepts both of exergy and irreversibility. The book draws attention to the fact that the second law is an approximation. Because of thermal fluctuations no equilibrium is really steady and, moreover, the concept of reversibility has its limitations; the fluctuations will not repeat between forward and reverse.

The author quickly arrives at his main mission of providing a series of worked examples aimed at persuading engineers of the utility of exergy analysis. In chemical engineering the thermo-mechanical practice of comparing real and reversible systems does not work well. Accordingly, pinch technology, which some claim to be exergy analysis with a difference, and which accepts unavoidable irreversibilities, is considered. While noting the novelty and strength of pinch technology in certain contexts the author also highlights its shortcomings in others.

All in all the book encapsulates much of the great depth of knowledge and extensive experience of Mr Barclay and, in addition to leading the assiduous reader to the point where most conceivable power and process systems can be analysed, he has much of interest to say about deriving further value from the methodology promoted.

Dr Tom Patten

Author's Introduction to the Second Edition

The main feature of this second edition is a rewrite of the chapters on fuel cells, recognizing the rapid advance of the technology. The equilibrium theory is given in much greater detail, and leads to a modified definition of fuel chemical exergy (reflects on Chapters 1, 3, and 6). Moreover, the origin of fuels in photosynthesis is discussed as of interest in its own right, and as an illustration of the separation of work and heat in equilibrium and near-equilibrium chemical reactions. Both equilibrium and practical fuel cells conform to the latter description. Combustion is a far from equilibrium reaction, which precludes electrochemistry, destroys the Gibb's potential completely, and leaves a variable residue of Carnot limited energy (thermo-mechanical exergy), depending on the arrangement of the combustion equipment.

The first chapter is slightly improved, and throughout the book sins of omission and commission have been rectified – no doubt accompanied by new imperfections!

In photosynthesis, work-rich molecules are created, and nature operates prodigiously to conserve this work. From a second law viewpoint, animal life is a means of conserving exergy in light-created molecules. The animal is endowed with senses to guide it with minimum effort to its food, using a superb isothermal engine, elegantly fuelled by adenosine triphosphate, and superbly controlled for peaks of effort, and economical waiting. Likewise the insect, the bird, and the fish; everything that moves and is alive. The scene is enriched by predators and scavengers, all conservators, second-law coordinated.

Part of the atmospheric pollution problem is the evolutionary changes being forced on animal and vegetable life by increasing the carbon dioxide to oxygen ratio. The irreversible effects on primitive C3 plants will not match those on more evolved C4 plants, with modified carbon dioxide fixation. Removal of links in the conservation chain by extinction of species could be consequential in the event of nature having insufficient redundancy. Nature's example is that combustion is a technology of last resort.

Frederick J Barclay
April 1998

Introduction

'Yes, it used to be so, but we have changed all that'
Molière

Simplicity and elegance, sense of proportion and balance, and competitive cheapness are sought-after attributes of engineering projects. Good qualitative thinking is a prerequisite to be reinforced by sound quantitative analysis. The discovery of a first facet of the pervasive second law of thermodynamics by Carnot, prior to Joule's experimental elucidation of the first law, should have given a head start to the balanced application of both laws to the analysis of projects involving power generation, thermal processes, chemical reactions, electrolysis, osmosis and the like. The publication of textbooks on second law exergy analysis and associated thermoeconomics is rather gradually generating practical applications. This book attempts to accelerate the process. It highlights chosen applications, and attempts interdisciplinary integration. The analysis demonstrates the fresh and altered sense of proportion obtainable from exergy methods. The solutions are sometimes quite different and obviously both the traditional and the new analyses cannot both be true. A historical unfolding approach results in heat engine theory leading into thermochemistry. The latter two topics need a unified exergetic approach, for successful power and process analysis, leading to systems with integrated flow sheets of optimum performance. The historical calculation system leading to plant integration is known as 'pinch point analysis', a technology which has been called by its main protagonist, Linnhoff 'exergy analysis with a difference' (**21**). This book aims to contribute to the possible unification implied by the last sentence. For example in the simple case of power and desalination, both the power output and the water output can be measured in megawatts, added and compared to the megawatts of exergy in the fuel to give a combined efficiency. Water and electricity production efficiency can be compared. Such calculations can be extended to multi-process integrated plants.

In the realm of economics, energy is currently thought to be a traded good; an unfortunate banker's misapprehension. The real traded good is exergy, and it is hoped to make this clear.

The Système International units used in this book have limitations for exergy analysis. Joule's experiment was reversible: 1 Watt.sec of stirring work converts to 1 Joule of energy. The reverse statement should be along the lines, 1 J = η_C. Watt.sec. If the stirring occurs at the ambient temperature the Carnot efficiency $\eta_C = 0$.

Gibbs asserted that the functions U+PV=H, E–TS=F, and H–TS=G, should be called thermodynamic potentials. Moreover it will be obvious to all, that PV is a reversible work quantity, and for consistency so should the other components of the three potentials, and the potentials themselves. The SI makes the potentials in kJ/kg look like specific energies. A unit of work is needed – perhaps the Carnot. In this book the issue of units is half fought by quoting exergies in Watt seconds. Exergy is a generalized thermodynamic potential.

Notation

f	Fugacity = pressure of ideal gas; adapts real gas to work with ideal gas relationships. See (**42**)
g	Specific Gibb's potential $kWsmol^{-1}$ (or $\bar{G}$ if following a different author)
h	Specific enthalpy $kJmol^{-1}$
K	Equilibrium constant of a chemical reaction
K	Temperature, degrees Kelvin
m	Mass flow kgs^{-1}
P	Pressure, bar (Pascal/10)
Q	Heat $J = m\partial u/\partial t$
R	Universal gas constant
s	Time, seconds
u	Specific internal energy $kJmol^{-1}$
v	Specific volume m^3
V	Volume, m^3
z	kmoles fuel in a $mixture_{eq}$

Greek symbols

γ	$= \partial u/\partial t$, specific heat, $kJmol^{-1}$
γ_{co}	CO fraction in a mixture
ϕ	Function in Gas Tables (qv) for calculation of entropy changes, from: $S_2-S_1+\Phi_2-\Phi_1\ R\ln(P_2/P_1)$
η	Efficiency, dimensionless ratio
ξ	Specific exergy $kWsmol^{-1}$

NB: Work or exergy quantities are allocated Ws, not J, to distinguish work from heat. This is an unorthodox practice, which reiterates to the reader, the fact that 1 Ws = 1J (Joule's Experiment), but 1J at ambient temperature is of zero work content. 1J is not equal to 1 Ws. Sometimes it is necessary to distinguish steam parameters from water by using upper case letters for steam (H, S), and lower case for water, (h, s).

Subscripts

o	Relating to standard conditions, 298.15K, 1 bar
oo	Relating to environmental conditions, e.g. concentrations
ch	Chemical
t	Thermomechanical
Ct	Carnot
eq	Equilibrium
p	Refers to equilibrium constant on partial pressure basis
f	Refers to equilibrium constant on partial fugacity basis

Fuel cell abbreviation

AFC	Alkaline Fuel Cell = Bacon Cell and Descendants
PAFC	Phosphoric Acid Fuel Cell
SPFC	Solid Polymer Fuel Cell = Proton Exchange Membrane Fuel Cell
MCFC	Molten Carbonate Fuel Cell
SOFC	Solid Oxide Fuel Cell

Preface

It is a pleasure to acknowledge my debt to the following writers who provided my foundations in thermodynamics: J A Ewing, C Sieppel, J H Keenan, J D Fast, R A Gaggioli, and T J Kotas.

Contents

Chapter 1

Notes on Thermodynamics

'I like work; it fascinates me. I can sit and look at it for hours.
I love to keep it by me: the idea of getting rid of it nearly breaks my heart.'
Jerome K Jerome

1.1 What is equilibrium?

A cosmologist might seek to defer this question. When grappling with it, a mechanical engineer, like Carnot, is likely to sketch a piston and cylinder, so defining a system and a boundary separating the system from the environment. A chemist might select a bottle containing a pure liquid and a solution separated by a semi-permeable membrane. The physical chemist has an advantage, however, in having access within his own discipline to the 1873 seminal paper of J Willard Gibbs, 'On the equilibrium of heterogenous substances' (**1**). On the foundations provided by Carnot and Clausius this reference broadened out the second law greatly. Modern interpretive renditions are given in (**6**) (**13**) (**14**) (**23**) and (**42**). Located as he is in a matrix of professions, our mechanical engineer, concerning with gaseous working fluids, can consult the physicists and study the Maxwell–Boltmann statistics (**2**) (**3**) (**42**) of a perfect gas of idealized elastic molecules colliding with each other and the system boundary, in a perpetual isotropic flux with a known distribution of molecular speeds, as sketched in Fig. 1.1.

A dip into statistical mechanics and its microstates, will reveal a picture of very infrequent anisotropic microstates in which, for example, all molecules are proceeding in one direction, or all concentrated at one corner of the system boundary. These latter pictures perturb the notion of an infinitely slow reversible compression or expansion of an isotropic fluid by means of a piston. The latter notion survives because of the extremely low probability of any particular microstate (**2**). It is

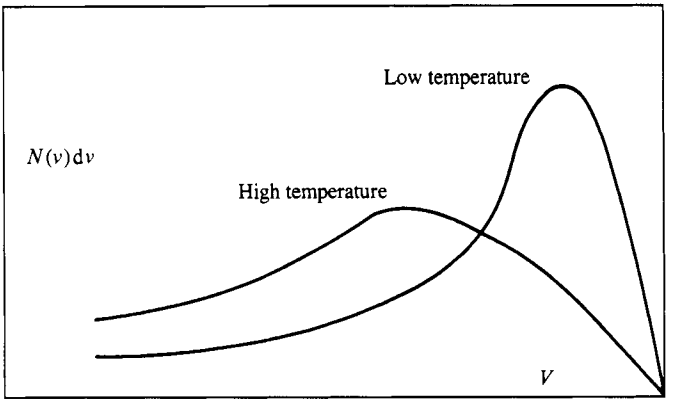

Fig 1.1 Maxwell–Boltzmann distribution

reasonable, but not quite rigorous, to think of a reversible expansion as a continuous series of isotropic equilibrium states through which a reversed piston can cause retracing of the path to the start. The perfectly uniform, homogeneously isotropic state is as improbable as that in which all molecules are moving in one direction. There are, however, very many almost isotropic states through which the piston can progress. A retraced path would pass through a similar, but not precisely identical, series. Equilibrium in a gas is, then, a flickering fluctuating phenomenon. All equilibria, even in solids, are subject to thermal fluctuations. Nothing is quite steady; indeed the well-known Brownian motion in which air-suspended pollen particles can be seen being buffeted to and fro, demonstrates not only this unsteadiness, but also the near isotropy of the most states. The effect on the pollen of all molecules proceeding in one direction would be obtrusive, but is unlikely ever to be witnessed (**2**).

Analysis of the thermal performance of an engineered system comprises a comparison between the real system and an idealized reversible system. It is immediate necessary to assert that the reversible cycle must be carefully chosen, otherwise the practical device may be a failure. In the case of the simple open-cycle gas turbine, the ratio of turbine work to compressor work must be high to achieve a reasonable net output.

Our chemist's bottle constitutes the beginning of the analysis of the desalination process (**22**); reverse osmosis and distillation can take place therein reversibly.

1.2 What is energy?

Energy is a word much used in everyday speech. To be tired or to be energetic describes one's capacity to influence the human predicament, to cause change. Everyday usage is that electrical energy makes the vacuum cleaner motor rotate. This usage does not gel with the scientific definition of energy, which cannot be created or destroyed. The molecules of gas in our piston and cylinder can do work on the piston if their pressure is higher than the environment (the atmosphere). However, from our Maxwell–Boltzmann picture it is clear that both the gas and the outside air molecules have energy by virtue of their speed of translation (kinetic energy). Since the molecules are travelling in all directions their kinetic energy is not useable, but can be tapped readily if a pressure or temperature difference exists. A difference in composition as, for example, between combustion gas and air can also, in principle, be tapped using perm-selective membranes. In this discussion a distinction is emerging between energy which is utilizable and energy which is unavailable. In modern thermodynamics, utilizable energy is called 'exergy' (**18**). The everyday user of the word 'energy' would, if accurate, use the word 'exergy', the broadest definition of which is 'the potential to cause change'. A colloquial term for 'exergy analysis' is 'lost work analysis'. Exergy is destructible, as is its parent – work. Colloquially, exergy is 'the go of things'!

Molecular science reveals (**2**) (**4**) (**7**) (**20**) that there is vibrational, rotational, and electronic energy within molecules, some of which, during an expansion process emerges – via collisions – as molecular translational speed. In thermodynamics the molecular energy and kinetic energy (speed) are lumped as internal energy, with the symbol U. U is indestructible. Remarkably, if the gas in our cylinder is left for a very long time and then inspected, it will be unchanged. The myriad collisions in the conservative process will have produced no dust or debris. The Maxwell–Boltzmann statistics will be unaltered.

The kinetic energy of a bullet is imparted, so that its target can be destroyed, in the dissipation of the kinetic energy (strictly speaking kinetic exergy). Other examples of energy which is totally available are the kinetic energy of a rotating flywheel, the potential energy of an elevated body of water, or the familiar motive power of electricity. The availability is total only with frictionless apparatus. In practice, while work is being done, heat is generated by friction; in alternative words motive power is destroyed and lost as an ambient temperature energy flow.

In power and process analysis, account must be taken of the degree to which energy is utilizable or available. Parasitic processes like friction, which reduce the work utilization, must be in the accounting system. Nuclear reaction energy appears in practice as the internal energy of a working fluid, which is only partly utilizable.

An example which attracts unsophisticated attention is the very large amount of energy in the cooling water of steam power station condensers. Such energy is almost in equilibrium with the environment and is of trivial thermodynamic availability or economic value. Cooling water energy is largely a consequence of waste incurred when heat is taken in from the fuel at a limited temperature, as dictated by the restricted properties of engineering materials and by finite mechanical arrangements.

1.3 What is heat?

Everyday personal experience is of being warmed up or chilled by the climate or by the services of a building. The nerves sense and the mind appreciates that one's flesh is gaining or loosing something. The microscopic scene is of colliding air and flesh molecules communicating internal energy to each other; an outward flow is chilling and an inward flow is warming. Heat is an energy flow. Specific heat is $\partial U/\partial t$.

Returning to the piston and cylinder system, the discussion has been of series of equilibrium states. The introduction of valves, ignition sparks, fuel, shaped pistons – the paraphernalia of the internal combustion engine – changes the scene. Ignition of the fuel/air mixture initiates the combustion chain reaction, creating a spreading hot zone in a gas systematically in motion as a result of inlet valve action and shaped piston movement. The resulting currents of internal energy and currents of molecules are superposed on the Maxwell–Boltmann isotropic flux. They are the symptoms of disequilibrium. The spreading out of internal energy in a temperature gradient by collision processes is an alternative attempt at a definition of the word 'heat' (in gases). The dispersion of the molecular currents into eddies, and finally into an isotropic flux, results in increased internal energy; the system has been heated. Again, everyday experience tells us that radiation plays a part. The physicists are ready with quantum theory (**4**) to explain electron energy level jumps in radiation emitting and absorbing molecules. Heat again becomes a spread of internal energy. In thermodynamics, increments of the spread over a time interval are given the symbol $\mathrm{d}Q$. Increments of $\mathrm{d}Q$ and of $\mathrm{d}W$ entering the system increase its internal energy.

$$\begin{aligned} dQ + dW &= dU \\ dQ &= dU - dW \\ &= dU + P\,dV \end{aligned} \tag{1}$$

($dW = -P\,dV$ by the sign convention that entry to the system is positive; but dV, a contraction, is negative.) In the case of an adiabatic expansion process consisting of a series of isotropic states, clearly $dQ = 0$, and hence $dW = -dU$ yielding a possible method of measuring or calculating internal energy, relative to an arbitrary datum. Qualitatively it is clear that the internal energy is a property of the molecules. In the real expansion discussed above, dQ is an arbitrary variable influenced by practical engine details. As dQ increases dW decreases. Neither are unique to the molecules. More rigorously the same result is obtained in textbooks by showing that dU is a perfect differential; dQ and dW are not perfect differentials; in the limit with isotropy conserved, they are reversible increments; and U is a thermodynamic potential.

In the real expansion, mention of cooled cylinder walls were avoided. In the absence of energy flow through the system boundary the expansion is termed 'adiabatic irreversible'. 'Adiabatic' means no energy flow through the system boundary. In an isothermal expansion there is an organized flow of energy through the control surface into the system. If a reversible isothermal expansion were to be achieved it would be slow – a series of small heat inputs, minimally disturbing the isotropic molecular flux. Such dQs qualify in the limit, for the special title dQ reversible, 'dQ rev' for short.

1.4 What is entropy?

Carnot's heat cycle, when based on a perfect gas, comprises four operations, all reversible, using a piston and cylinder engine, a heat source and heat sink of idealized capabilities. With source and sink out of action the first operation is adiabatic compression according to the perfect gas law $PV^{\gamma} = C$. The second operation is isothermal expansion to the perfect gas law $PV = C$. The heat source is in action, exactly compensating the lowering of the temperature which would otherwise occur due to expansion. The equilibrium isotropic flux of gas molecules is maintained during a succession of dQ rev inputs. In terms of real components such a process is particularly difficult to conceive, but is an acceptable limit for the purposes of discussion. The third operation is adiabatic expansion with source and sink inactive, and the fourth is isothermal compression with the heat sink active. The cycle is arranged to finish where it started.

In (**2**) (**3**) and (**4**), for example, it is shown that the efficiency of the Carnot cycle based on a perfect gas is $(T_1 - T_0)/T_1$. If the heat source of the Carnot cycle feeds via a conducting metallic layer through a temperature difference $T_2 - T_1$ without affecting the internal reversibility of the sequences in the working fluid, then it can be asserted that without the metallic layer the efficiency would have been $(T_2 - T_0)/T_2$. With reference to an element of heat dQ, the loss of work output due to reduced temperature operation is

$$dQ[1 - T_0/T_2 - 1 + T_0/T_1] = T_0[dQ/T_1 - dQ/T_2] \tag{2}$$

In words, the conduction of heat through a temperature difference leads to a loss of work, which is a function of dQ/T. Since T_2 exceeds T_1, both sides of (2) are positive.

The efficiency of the Carnot cycle is $(T_1 - T_0)/T_1 = (Q_1 - Q_0)/Q_1$ from which by symmetry

$$Q_1/T_1 = Q_0/T_0 \tag{3}$$

Equation (3) can be dubbed as Carnot's sense of proportion. If the heat intake is Q_1, then the rejected heat is predetermined as $Q_1 T_0/T_1$ to close the cycle. Q_1 and Q_0 are both series of increments of dQ rev, so that $Q_1/T_1 = \int dQ_1 \text{rev}/T_1$.

The point of this discussion is that simple manipulations of Carnot cycle theory make the functions dQ/T and dQ rev$/T$ appear. Then they require name (entropy) and meaning – the achievement of Clausius. In the Carnot cycle the working fluid reversible entropy growth during isothermal expansion is equal to the entropy reduction during isothermal compression. Moreover, during reversible adiabatic compression no heat enters the system and no heat is generated within the system: $dQ = dQ/T = 0$. In one rotation of the heat cycle $\oint dQ \text{ rev}/T = 0$. If, for example, during isothermal compression, there had been some heat generated, that is disturbance of the isotropic equilibria by flow or uneven temperature, then at the end of the stroke there would have been an entropy growth ΔS, and an inevitable increase in heat rejected, $T_0 \Delta S$, for which the accepted term is an internal irreversibility. An external irreversibility occurred in the temperature degradation in the metallic layer described in equation (2). Entropy is, perhaps, the most significant concept since the wheel. Irreversible entropy growth is a general feature of real systems, and is fundamental to all statements of the second law. Many students have been put off from understanding entropy by teaching techniques involving arbitrary introduction of the function. Readers should study alternative introductions to entropy in textbooks,

e.g. (**2**) (**5**) (**6**) (**15**) (**16**) (**17**) (**23**) (**42**) since entropy growth and irreversibility are the cornerstones of exergy analysis, as applied in this book. Article 1 of (**17**) has a fresh vigorous non-historical approach to entropy and thermodynamics and may appeal. The word 'entropy' has spread via statistical mechanics into information theory where, for example, the maximum entropy method is a technique for the deconvolution of image signals, (**12**). In some future rationalization, an introduction to entropy may be presented which starts at the information theory end and arrives finally at heat engines. The beginnings of such an approach are visible in article 17 of (**17**). Meanwhile the author favours the approach via historical unfolding starting with Carnot, but helped along by modern physics; a process of increasing disillusionment, approaching understanding gradually.

None of the above has revealed articulately that entropy, like internal energy, is a property capable of being tabulated, plotted on a temperature entropy chart, or incorporated in an equation of state to allow a computer to reproduce its values. Indeed the assertion that Q is not a property makes explanation essential. Consider the process of reversibly heating, at constant pressure, some gas in a piston and cylinder assembly. An increment $\mathrm{d}Q$ rev must enter the gas at temperature T from a source at T, in such a way as not to disturb the equilibrium isotropic flux of molecules. In reality there has to be a small temperature difference available.

The transaction is in summary

$$\mathrm{d}Q\,\mathrm{rev} = \mathrm{d}U\,\mathrm{rev} + P(\mathrm{const})\,\mathrm{d}V\,\mathrm{rev} = T\mathrm{d}S\,\mathrm{rev}.$$

Between any two equilibrium states there is an infinity of reversible paths involving, for example, adiabatics, isothermals, and intermediate alternatives. The specification of constant pressure, however, means that there is but one unique path. Moreover, with a practised eye the differential of the enthalpy function $H = U + PV$ at constant pressure can be recognized

$$\mathrm{d}H = \mathrm{d}U + P\mathrm{d}V = V\mathrm{d}P$$

with, at constant P

$$V\mathrm{d}P = 0 \tag{4}$$

Hence $\mathrm{d}Q\mathrm{rev}/T = \mathrm{d}H\ \mathrm{rev}/T$ (at constant P). This result indicates, since H and T are both properties, that $\mathrm{d}Q\mathrm{rev}/T$ may be a property. More convincing is the argument from the operation of the Carnot cycle, in which for the two adiabatics $\mathrm{d}Q = 0 = \mathrm{d}Q/T = \mathrm{d}S$, and hence $S = \text{constant}$.

For the two isothermals $Q_1/T_1 1 = Q_1/T_1 = \int dQ\text{rev}/T$. Hence $\oint dQ$ rev/T Carnot $= 0 = \oint dS$. Hence the value of S at the start of the cycle repeats itself. In contrast, since $Q_1 > Q_0$ there is no function Q repeating itself. Q is not a property. Since all reversible cycles amount to assemblies of elementary Carnot cycles, their $\oint dS\text{rev} = 0$.

1.5 What is enthalpy?

The compound property enthalpy has been introduced above without explanation, while heating a non-flowing gas at constant pressure. Most engines and processes use a steady flow of working fluid(s). The enthalpy property is used intensively in analysing steady flow. Both U and PV are to be thought of as properties, of which $\oint \text{Carnot} = 0$. The learning process is to investigate what H does in various unit operations.

Consider first a frictionless reversible adiabatic water pump, supporting at its outlet a column of water of height Z, overflowing very slowly. The inlet and outlet enthalpies are H_1 and H_2, respectively. At the pump outlet the water is hotter and slightly compressed, and able to expand up the column losing internal energy and temperature as it rises, until its condition at the top of the column is H_1. Across the pump $H_2 - H_1 = \Delta H = \Delta U + P\Delta V + V\Delta P = \Delta Q + V\Delta P = V\Delta P$ for an adiabatic reversible pump. If ΔP is in metres of water and V in m^3 then $H_2 - H_1$ clearly represents the pump's work. If some churning losses are introduced in the pump, $\Delta Q = T\Delta S$ will assume a positive value. If $V\Delta P$ is kept constant, and H_1 is the same, increased shaft work will be needed to supply both $V\Delta P$ and ΔQ. H_2 will increase accordingly. The increase $H_2 - H_1$ now represents pump work plus pump losses, that is the required shaft input. H is a thermodynamic potential (**1**).

A relatively compressible working fluid such as air in a compressor, is no different in principle, but columns of air, say 20 atmospheres tall, introduce conceptual difficulties and compressibility effects in columns which cannot be ignored. Nevertheless $H_2 - H_1$ = compressor work + compressor losses.

In the case of a turbine $H_1 - H_2$ represents the shaft power per unit mass flow. $H_1 - H_2$ shrinks as the turbine losses increase with blade or seal erosion, i.e., H_2 increases.

In the heating of a constant pressure flow in a frictionless pipe the term $V\text{d}P$ in $\text{d}H = \text{d}U + P\text{d}V + V\text{d}P$ is zero and $\text{d}H = \text{d}Q$. If the process is real with a frictional pressure drop, then the power needed to push the flow along, appears in the flow as additional heat $\text{d}Q'$; and $H_2 - H_1 = \int(\text{d}Q + \text{d}Q')$. The above unit operations can be assembled into a Rankine cycle

steam engine, the performance of which can be evaluated by using enthalpy values from a set of steam tables, in an enthalpy balance. Since the enthalpy differences in the constant pressure heating in the steam generator and the constant pressure cooling in the condenser reveal the heat input and heat rejected, the calculation can also be called a heat balance, without loss of rigour.

Arbitrary introduction of a property such as $U + PV$, is usually less satisfying than an evolutionary approach. Figure 1.2 is a flow sheet for a steady flow Carnot cycle, accompanied by its temperature entropy diagram.

Not only is the flow steady, but all thermodynamic properties have steady, time invariant, values at any fixed point in the cycle. The diameters of the ducts between each of the four main circuit components are such that the velocity of each unit mass of gas is constant, the kinetic energy in each duct is the same. The four machines occupy the horizontal plane of the paper, so that there is no change in elevation or potential energy. The isotropic flux of perfect gas molecules as seen by a moving observer slides past the smooth duct walls unmodified, in the absence of friction. At the top left corner of the circuit between isotropic compression and isothermal expansion is a redundant component introduced for discussion. A tall vertical cylindrical frictionless inverted concentric riser/down comer tube is indicated by the twin circles. At each of its bottom ends the thermodynamic state is identical.

How does the analysis of this system differ from the piston and cylinder non-flow engine?

Start with the riser tube! As the gas ascends the riser its pressure falls, it expands, it loses internal energy, it gains potential energy, and it must

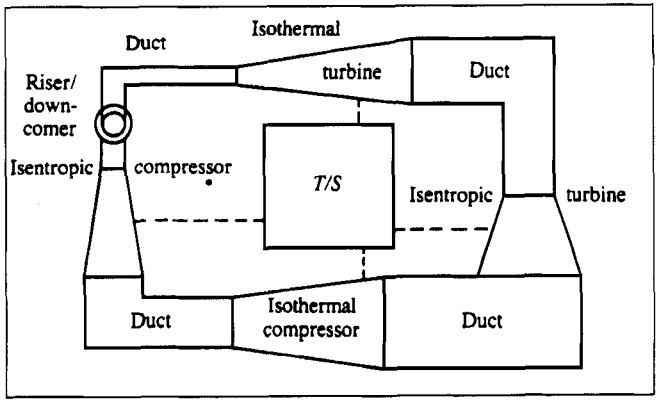

Fig 1.2 Steady flow Carnot cycle

accelerate in the parallel sided duct and gain kinetic energy. Moreover, each unit mass of gas has to displace the one ahead of it, sweeping ahead volume V at pressure P, or doing work PV. Note, however, that PV is not work leaving the system via the control surface. What is being described is a reversible interchange in which internal energy is converted into potential and kinetic energy (gZ and $v^2/2$) and into PV, which needs a name. There is no consensus, see (**6**) and (**17**) with flow energy, flow work, and flow function. So in this book the name 'displacement property' will be used. An alternative description of PV is to consider it as the reversible work needed to introduce a small packet of fluid into a large body of fluid without significantly increasing the pressure, i.e. $\int^{V} P\mathrm{d}V = PV$. If PV is not reversible it will not have a unique value and will not be a property. The reader is advised to look at a number of presentations in texts available. The sequence in the down comer is the inverse of that in the riser and the outlet properties are identical to those at the inlet.

Moving to the isothermal expansion turbine inlet, the total enthalpy is $U_1 + P_1V_1 + v^2/2$ and at the outlet $U_2+P_2V_2+v^2/2$. The duct sizes have been arranged so that the kinetic energy terms are equal, and cancel out in a subtraction. Note particularly that in a subtraction, the arbitrary constant associated with internal energy disappears. The expansion law is PV=Constant so the PV terms are equal and cancel in subtraction. In the end $\Delta H=\Delta U=\Delta W$.

In the isentropic expansion turbine the kinetic energy terms again cancel by arrangement. Since $PV^{\gamma}=C$ the displacement property PV varies through the turbine. Since $P_1V_1/P_2V_2=T_1/T_2$, then PV shrinks as U and T increase. In the isothermal compressor PV and U are again constant, so fixing the isentropic compressor inlet enthalpy. A balancing interchange between U and PV occurs, so that the difference between the negative expansion work and the positive compression work is the same as in the piston and cylinder case. (The sign convention follows equation (1).) The latter reasoning, while instructive, is redundant, since all reversible cycles working between the same temperature limits have the same efficiency.

1.6 Entropy growth and irreversibility

If the components of the engine in Fig. 1.2 are endowed with some imperfections, friction in ducts, viscosity in the gas, and churning losses in the turbines and compressors the consequences are profound. If it is asserted that the temperature at some point has a value, that is an approximation because there is no equilibrium. Practically speaking,

temperature sensors must be located with care, and circumspectly interpreted so as to get the best measurement (no news to instrument engineers). The same applies to any other measurable property. In compressors and turbines the working fluid will be heated by the degradation of shaft work. Less heat input will be needed to achieve isothermal expansion, and more cooling will be needed to achieve isothermal compression. In the formerly isentropic turbines the conversion of shaft work into heat will result in a steady entropy growth as the working fluid moves through the machines. In the ducts, the pressure will fall in the direction of flow. Although all sorts of engineering approximate solutions to frictional flow are possible, the flow problems can be attacked via the Navier–Stokes equations – a feat which computers have just made expensively possible (**8**). However, as Feynman states in (**4**) physics cannot solve analytically the problem of turbulent flow in a pipe. (See below at Fig. 1.7.) The temperature entropy diagram of Fig. 1.2 has to be modified to that of Fig. 1.3, to show entropy growths.

Each individual entropy growth, for example that associated with the duct between any two machines in the flow sheet, dictates an increase in heat rejection via the isothermal compressor, of magnitude $T_0\Delta S$. Such an increase in heat rejected is called an 'irreversibility'; once the entropy growth has been incurred the loss is final and not recoverable by any means whatsoever. However, if a variable loss exists such as the pressure drop across a valve, adjustment of the valve will affect all other losses in the system. In heat engine processes (as distinct from chemical processes) there are two principal types of irreversibility, based on entropy growths due to pressure drop, and on entropy growths due to the passage of

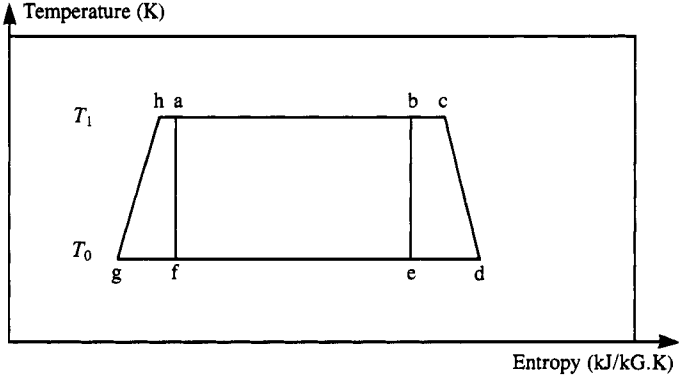

Fig 1.3 Imperfect Carnot cycle

energy through a temperature difference without work being extracted, see equation (2). Pressure drop represents wasted fan or compressor power. Temperature degradation represents loss of engine shaft power. See (**10**) and (**11**) for useful historical elaboration on the topic of irreversibility.

Within a turbo-machine the existence of blade tip leakage paths alongside expansion passages causes the two forms of irreversibility to merge, only mixed entropy growth being observable. In Fig. 1.3 the condition line of the adiabatic compressor slopes upward to the right and the adiabatic turbine condition line slopes down to the right because of entropy growth. In the isothermal turbine, part of the entropy growth is due to external heating and the remainder due to destruction of shaft work in the blade system. In the isothermal compressor the cooling duty represents loads due to the sum of all the separate entropy growths in the ducts and in the other three turbo-machines, plus the entropy growth in its own blade passages.

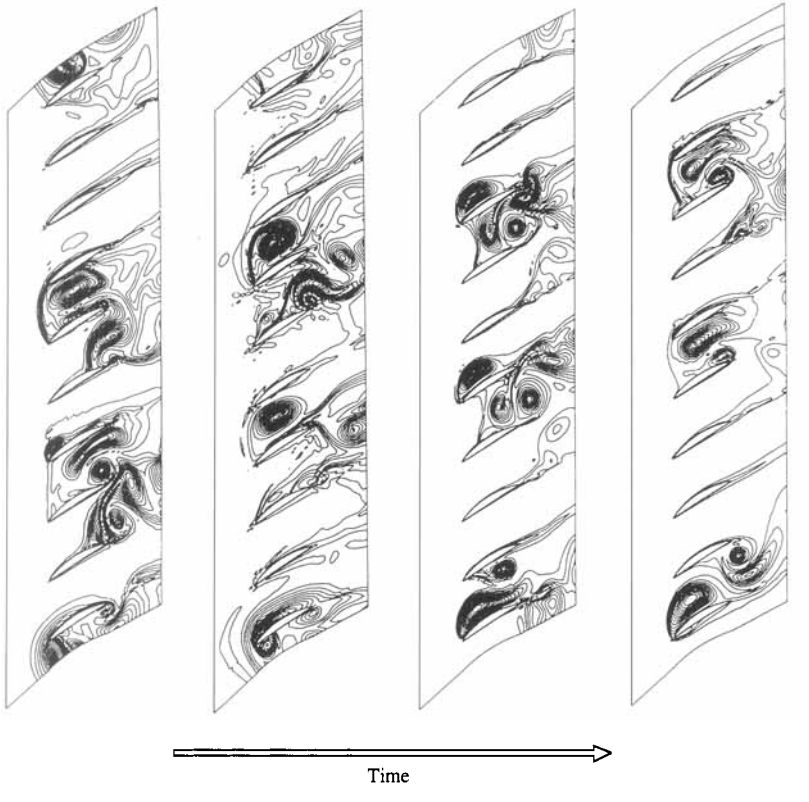

Fig 1.4 Entropy contour plots of flow in a rotating stall of a subsonic blade row

In a real gas turbine compressor, orderly flow guided by the blading is achieved using a large number of stages. In off design conditions, say at below 47.5 Hz in a 50 Hz power generating machine, a disorderly condition called 'rotating stall' sets in. This condition is portrayed in Fig. 1.4, which shows the antithesis of the orderly isotropic flows discussed in connection with Maxwell–Boltzmann statistics. The figure is due to Dr Li He of the University of Durham. The entropy contours in the figure are of course related to flow vorticity. Entropy growth is portrayed.

A word of warning is needed about illustrations such as Fig. 1.7, based on Navier–Stokes solvers. The derivation of the Navier–Stokes equations is based on a parallelipiped of homogeneous fluid, and its properties. However, as every pond-skating insect finds, the liquid at a pond surface has different properties than the bulk. The protons at the surface, cannot, as in the bulk, interact with those above them, and turn sideways for companionship. The interfacial liquid has modified properties. Qualitatively, therefore, one would expect a Navier–Stokes solver to struggle with the problem of a dripping tap, or a multi-jet nozzle. Computers produce numbers, which are not always solutions.

In (**24**) the author has drawn attention to interfacial exergy phenomena (heterogeneous surfaces) which could improve the heat and mass transfer in power and desalination plants.

1.7 Thermomechanical exergy

The term 'thermomechanical exergy' is an internationally agreed (**18**) term for the compound property $\xi_t = H - T_0 S$, another thermodynamic potential. Previous names include 'utilizable energy', 'available enthalpy', and 'availability'. Dropping of these older terms is part of a broad scheme, which includes chemical exergy (to be discussed later), both terms being for use in steady flow processes. Since both U and S have arbitrary zeros, arithmetic involves setting a reference state, $H_0 - T_0 S_0$ and using differences like $H - T_0 S - (H_0 - T_0 S_0)$, so as to eliminate unknown arbitrary constants. Note that properties in this book from (**19**) and (**20**) are mutually consistent. This is necessarily so since the exhaust gases in the gas tables contain steam, referred in the steam tables, to the triple point.

In the reversible steady flow Carnot cycle of Fig. 1.2 the entropy increase in the isothermal turbine is $S_2 - S_1$, which determines the rejected heat $T_0 S_2 - T_0 S_1$. The rejected heat from the reversible cycle can also be called the external irreversibility. It represents degradation from unachievable infinite temperature. The temperature rise, even after

stoichiometric combustion, is limited. Moreover, dissociation of the combustion products eventually sets a limit which is impossible to bypass using air preheating. However, if, for example, hydrogen is oxidized in a reversible, standard-conditions, fuel cell, then, as will be made clear later, there will be a work output (fuel chemical exergy, Chapter 4), equivalent to a Carnot cycle with an infinite top temperature. For that reason some writers refer to combustion as 'crude oxidation', distinct from reversible isothermal fuel cell oxidation.

An alternative way of thinking about the Carnot cycle is that its input is the increment of thermomechanical exergy $\Delta\xi_t = \Delta H - T_0\Delta S$. The first term is the heat input and the second the heat rejected. Since the engine is reversible and perfect, its output of shaft work is also $\Delta\xi_t$. In a heat pump the action is reversed. The exergy output is the shaft work input.

The property $T_0\Delta S$ represents reversible entropy change and reversible heat rejection. The heat input to the steady flow Carnot cycle is $H_2 - H_1$. Hence the work output is $H_2 - T_0S_2 - (H_0 - T_0S_1) = \xi_t^2 - \xi_t^1 = \xi_t$; t being the international symbol for thermomechanical exergy. (Two terms + and – $\{H_0 - T_0S_0\}$ cancel out.) Having glimpsed the answer, it is appropriate to return to the beginning and the piston and cylinder non-flow system of Fig. 1.5.

A piston and cylinder system contains a gas, and is enveloped in an environment of the same gas. The environment is in equilibrium at P_0, T_0, etc. The system fluid is at P_1, T_1, etc., and the thermomechanical exergy of the system is defined as its maximum theoretical capability to deliver work to the piston. There is no question of chemical disequilibrium, as for example between combustion gas and air. The points 1 and 0, are shown on the associated temperature entropy diagram, which has no scales and is for any gas. The piston is constrained to reach equilibrium by isentropic expansion, followed by isothermal

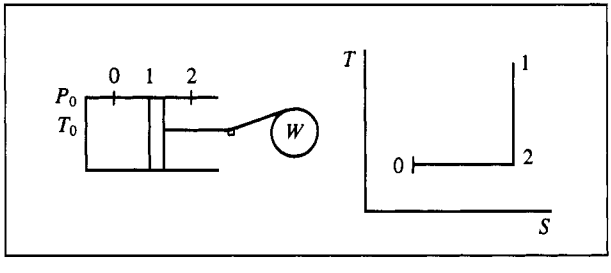

Fig 1.5 Thermomechanical exergy

compression with reversible heat exchange with the environment at T_0. Any other sequence involves irreversible heat exchange with the environment, through a finite temperature difference. Using the sign convention of equation (1), that work dW done on the system is positive, dQ, dS, and dU entering the system are also positive so that, for example, Rankine cycle feed pump work is positive. Then in Fig. 1.5 during:
(a) isentropic expansion

$$dW = dU, \text{ and } W = -(U_2 - U_1), \text{ while } S_1 = S_2. \tag{5}$$

(b) isothermal compression

$$dW = -dU + dQ, \text{ and } W = +(U_0 - U_2) - T_0(S_0 - S_1) \tag{6}$$

(c) piston displacement work against P_0

$$W = -P_0\{(V_2 - V_2) + (V_0 - V_2)\} \tag{7}$$

Hence

$$\begin{aligned} \text{net work} &= U_1 - U_0 + T_0(S_1 - S_0) - P_0(V_0 - V_1) \qquad (8)\\ &= U_1 + P_0V_1 - T_0S_1 - (U_0 + P_0V_0 - T_0S_0)\\ &= \text{Absolute thermomechanical exergy}\\ &= \xi_t \qquad (9) \end{aligned}$$

Note that the above argument can be extended to deduce the Carnot efficiency, independent of the working gas properties. The thermodynamic temperature can then be defined. With a perfect gas as working fluid the zero value of dU during isothermal compression, would simplify the algebra of the above calculation. In a steady flow system such as Fig. 1.2, a point somewhere in the isentropic turbine would correspond with point 1 in Fig. 1.5, the turbine work from 1 would be $H_2 - H_1$, and the isothermal compressor work $T_0(S_2 - S_0) - (H_2 - H_0)$. Then

$$\xi_t = H_1 - T_0S_1 - (H_0 - T_0S_0) = H_1 - H_0 - T_0(S_1 - S_0) \tag{10}$$

equals steady flow thermomechanical exergy. Note that in this case there is no equivalent of the environment side of the piston. The above argument can be further extended by making the piston system contain nitrogen, and the surrounding air Fig. 1.6.

Then at pressure and temperature equilibrium at the completion of the isentropic and isothermal expansions to P_0 and T_0, the nitrogen is still in disequilibrium with the air because of the difference in composition between the two. If the nitrogen had access to the air, it would diffuse and be diluted. Work would be required to re-separate the nitrogen and

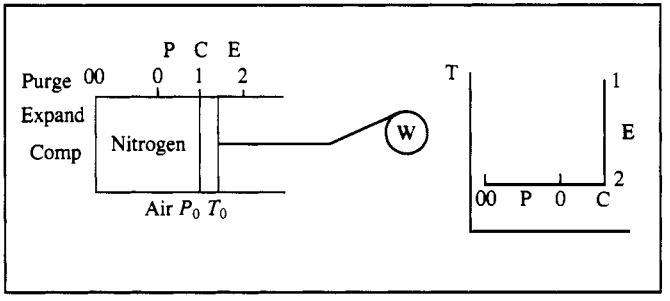

Fig 1.6 Single substance thermomechanical plus chemical exergy

indeed commercial, electricity-consuming, membrane-based apparatus can be purchased for the purpose.

Reversible dissipation of the nitrogen concentration in the cylinder must yield work. The simplest reversible process is as follows, in Fig. 1.6. Withdraw the piston isothermally (0 to 00), until the pressure inside the cylinder is equal to P_{00} the partial pressure of nitrogen in the atmosphere. Replace the cylinder wall by a membrane permeable to nitrogen only. Allow the piston to move inwards, displacing the nitrogen into the atmosphere via the membrane, where it encounters no change of concentration or partial pressure in the infinite environment, see Table 1.1. Also in Chapter 4 is the extension of the argument to steady flow elevated temperature and pressure chemical reactions in 'Van't-Hoff boxes'; employing membranes and circulators to control reactants and products, and isothermal enclosures interacting with Carnot cycles, to maintain reaction temperature.

1.8 Chemical exergy

Exergy theory is a fusion of mechanical engineering and chemical engineering thermodynamics, and also a fusion of first and second law analysis. Chemical thermodynamic analysis without the second law and Gibbs potential (**1**) is a non-starter. Hence second law analysis is firmly entrenched in industrial chemistry, production metallurgy, and chemical engineering, (**2**) (**13**) (**73**). Accordingly it is possible to find factories, comprising power and process systems, with first law analysis of the power system and second law analysis of the chemical processes, and more seriously, mismatched economics. This book has the objective of improving on the preceding situation, which has lasted overlong since the 1870s, when second law analysis was pioneered by such names as

Table 1.1 Work increments, 0 to 00 (Fig. 1.6)

Piston withdrawal isothermal expansion work
$(dW = -dU + dQ) = -(U_0 - U_{00}) + T_0(S_0 - S_{00})$
Piston withdrawal displacement work on atmosphere $= -P_0(V_0 - V_{00})$
Piston purge stroke displacement work (nitrogen via membrane) $= +P_{00}(V_{00})$
Atmospheric work on piston during purge stroke $= -P_0 V_{00}$
Combining these, the net work $= -(U_0 + P_0 V_0 - T_0 S_0)$
$+(U_{00} + P_{00} V_{00} - T_0 S_{00})$ (11)
= Chemical exergy ξ_c; to be further discussed below.

Maxwell, Tait, Guoy, and Gibbs himself. Modern pioneers such as Keenan, Gaggioli, Heywood, Aherne, and Kotas, are being rather slowly recognized, with significant monetary consequences. In chemical engineering Linnhoff *et al.* have been rather more successful, Chapter 7.

Chemical and mechanical engineering thermodynamics both start with the Carnot cycle. Chemical engineering, however, has to deal mainly with chemical reactions in steady flow systems, having inlet streams of reactants, chemically and physically reactive substances, and outlet streams of reaction products. The words 'physically reactive' are not idly used, the diffusion of one substance into another being of fundamental importance. Chemical engineering and combustion engineering have to deal with the thermodynamics of variable composition. The chemical exergy of a fuel undergoing oxidation in an equilibrium chemical reaction is discussed in Chapter 4; Fig. 4(a) cannot be extrapolated to the circumstances of an equilibrium chemical reaction.

In industrial or natural chemical processes, the reactions may involve the break up of large natural molecules into smaller ones, or vice versa the build up of complex molecules from simple ones (photosynthesis). Since chemical bonds are, at base, matters of forces, atom-to-atom and atom-to-electron, work must be interchanged. The reaction temperature may have to be controlled by supplying or extracting heat with a thermomechanical exergy content. As may be deduced from first principles, or seen from the easily available temperature entropy charts of steam or carbon dioxide, the entropy of gas molecules exceeds that of liquids, which in turn exceeds that of orderly crystalline solids. To move from the liquid to the vapour state a large isothermal energy flow (latent heat) is required, which dictates a related reversible entropy increase. When, in a chemical reaction, the status of the products is compared with that of the reactants, solid, liquid, or gas, an immediate judgement may be made, without thermodynamic data, as to the reversible entropy change being positive or negative – subject to the

reaction being at equilibrium. A non-equilibrium reaction (combustion) has a large irreversible entropy change, due to destruction of the Gibbs potential G.

The separation of pure solvent from a solution, or the separation of one isotope from another also requires work (or heat with an exergy content). Witness the electricity consumption of uranium separation plants or of reverse osmosis desalination plants, or the steam consumption of multi-stage flash distillation plants.

In (**1**) Gibbs gives an example of thinking from the general to the particular in producing a theory to account for the preceding descriptive matter. Presumably he saw links from particular example to particular example in his unrevealed process of synthesis. Accordingly in the present book particular examples are used as a teaching method, against a background of a glimpsed general theory, a circular approach.

In exergy analysis, the end of the beginning is equation (12), for the total specific exergy, broken down into thermomechanical and chemical components, for a set of heterogeneous substances (gas mixture). Equation (12) is an elaboration of equations (10) and (11) for a single substance, the thermomechanical exergy of which was extracted in isentropic expansion, and the chemical exergy of which was extracted during an isothermal interaction with the environment. The meaning and uses of equation (12) need to be elaborated. It disregards those work potentials associated with capillarity, electricity, and magnetism, for example, which are of limited relevance to power and processes, and sums up the main agents of change.

$$\xi = \xi_t + \xi_c = [(h - h_0) - T_0(s - s_0)] + [\Sigma_i n_i(\mu_{i0} - \mu_{i00})] \tag{12}$$

The Σ term at the right is the as yet unfamiliar chemical energy ξ_0, for a set of heterogeneous substances. The set does not include chemically reactive substances such as fuels, which by convention are stored at standard conditions P_0 and T_0. Fuels are not present in the environment, but the products of their oxidation are, e.g. steam and carbon dioxide. Species i is present as n_i moles, in a set of species. The molar chemical potential of species i is μ_i, where

$$\mu_i = (\partial G/\partial n_i)TP_{i'}$$

and

$$G = H - TS \tag{13}$$

i' signifies that the composition is held constant in respect of the set of species, with the exception that the n_i varies. Variation of n_{ii} influences

the relative concentrations of the other components. Note that μ_0 is a chemical potential at the environment pressure and temperature, and μ_{00} is a value at the dead state, for example at the concentration of substance i in the atmosphere. $G=H-TS$ is Gibbs potential, central to physical chemistry, which is clearly a relative of the thermomechanical exergy, of equation (10).

Also (see (**14**)).

$$\mu=(\partial U/\partial n_k)SV_{k'}=(\partial H/\partial n_k)SP_{k'}=(\delta A/\delta n_k)TP_{k'} \tag{13a}$$

The difference in electrical potential between two points represents the work done in moving a unit electric charge from point to point. Since the thermodynamic functions $H=U+PV$, $G=H-TS$, $\xi_t=H-T_0S$, as differences, can represent the maximum available work, they can, by analogy, be called potentials, following Gibbs; albeit they are not, at first sight, potentials of a field, as is the electric potential, or the hydrodynamic potential. Synthesis of Gibb's function begins with equation (1) in second law form

$$T\mathrm{d}S=\mathrm{d}U-\mathrm{d}W(\text{irrev or rev}) \tag{14}$$

Equation (13) applies to a piston and cylinder system. 'Rev' implies $T\mathrm{d}S=\mathrm{d}Q$, and $\mathrm{d}W=-P\mathrm{d}V$. 'Irrev' implies entropy growth, e.g. by temperature degradation or by friction between piston and cylinder; $T\mathrm{d}S$ may exceed $\mathrm{d}Q$, and $P\mathrm{d}V$ may exceed $\mathrm{d}W$.

$$\mathrm{d}H=\mathrm{d}U+P\mathrm{d}V+V\mathrm{d}P$$

From (14)

$$0=\mathrm{d}U+P\mathrm{d}V-T\mathrm{d}S \text{ (reversible)}$$

$$\mathrm{d}(TS)=S\mathrm{d}T+T\mathrm{d}S$$

and combining these

$$\mathrm{d}(H-TS)=V\mathrm{d}P-S\mathrm{d}T=\mathrm{d}G$$

$$G=H-TS \tag{15}$$

1.9 Thermomechanical plus chemical exergy of a single substance

The net work of equation (11), can now be written as $-G_0+G_{00}=-n\bar{G}_0+n\bar{G}_{00}$ (overbar signifies molar), and since $\partial/\partial n.n\bar{G}=\mu=\bar{G}$, then for a single substance the final term of equation (13) reduces to the left hand side of equation (11). Note that the net work was obtained during an isothermal interaction with the environment.

1.10 Membrane equilibrium (solution/pure liquid)

If a beaker of fresh water is immersed gently in the sea, the temporary interface between pure liquid and solution will progressively disappear. The high concentration of water molecules diffuses into the sea, and the high concentration of salts diffuses into the pure water. To undo this spontaneous process, work will have to be done, the magnitude of which is independent of the way the fresh water was prepared, by nature or by man.

Figure 1.7 is the equilibrium diagram of a solution and pure water, separated by a perm-selective membrane capable of passing water molecules only.

The water is soluble in and diffuses through the membrane, according to the most favoured model. If the solution is sea water, which is of practical importance, then the dissolved salts are, ideally, insoluble in the membrane and incapable of passing through it.

With the enclosure, the temperature is maintained uniform at T_0, by contact with the environment (the air, the sea). In this important type of isothermal interaction with one reservoir, Carnot's limitation is not involved. However, the second law certainly remains involved since any imperfection involves entropy growth and irreversibility.

To obtain a diffusion balance across the membrane the sea water must be compressed isothermally until its water molecule concentration is the same as in the pure water, the extent of the compression being known as the osmotic pressure, h metres of sea water in Fig. 1.7. Note that the compressibility of the electrolytic solution is not the same as that of pure water. Reference (7) discusses the theory of electrolytes.

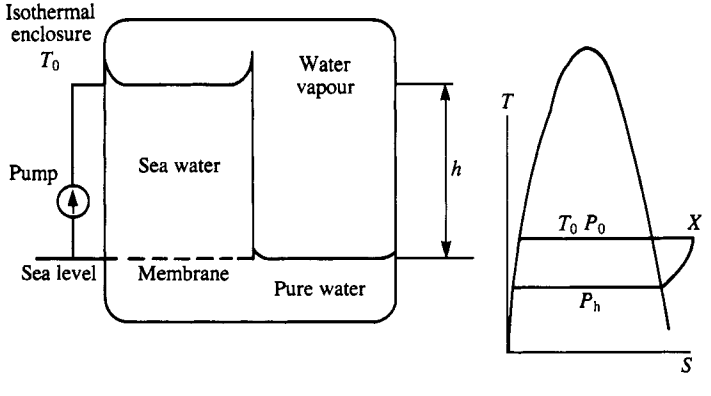

Fig 1.7 Equilibrium water solution

The vapour pressure at the pure water surface must exceed that at the salt water surface by h metres of (variable density) water vapour. The boiling point at the salt water surface is elevated by the salt content, and depressed by the elevation h. In the water vapour at the water surface the conditions are P_0 and T_0. As the elevation increases along the corresponding isothermal on the temperature/entropy diagram, starting at the saturation line and moving into the superheat field, there is an intersection X with the isobar P_h. The intersection X represents the vapour condition at the sea water surface. The sea water is in equilibrium with superheated steam, immediately above and immediately below its surface, where the steam is in solution. Proceeding down through the sea water the superheat declines to zero at the membrane where there is equilibrium between the pure water immediately below, and the sea water immediately above the membrane. The condition for equilibrium in this diagram is that it is isothermal. However, at any interface, that is the membrane or one of the two liquid surfaces, the function $G = H - TS$ is constant immediately above and below the interface. See equation (20) below.

If the pump P is used (compression followed by expansion) to elevate a very small amount of sea water by h and inject it at T_0, then the balance will be upset. Two things will happen. Vapour will evaporate from the sea water surface and condense on the fresh water surface (distillation). Water molecules will permeate the membrane from salt side to fresh side (reverse osmosis). A new balance will be reached. Fresh water is obtainable by draining down the fresh water compartment to its previous sea level, leaving a slightly increased salt content in the sea water compartment. The latter inconsistency disappears in the infinitesimal limit, or can be modified using the steady flow apparatus of Fig. 1.8, which again becomes consistent when operating infinitely slowly.

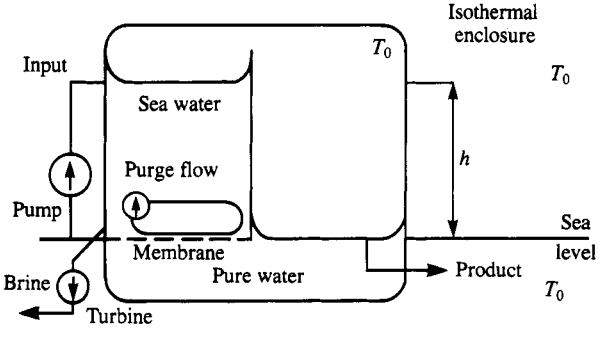

Fig 1.8 Steady flow desalination

It will become clear below that the isothermal pump work of P per mole is a chemical exergy. It represents an amount of reversible work done per mole in elevating water from an equilibrium or 'dead' state (reduced water concentration) in the environment (the sea) to a higher concentration or chemical potential in pure water, at the same elevation. Note that reverse osmosis and distillation require the same minimum work input per mole, since any difference would allow work to be derived by coupling the two processes. Moreover, the loss incurred on dispersing fresh water in the sea must have a unique value, implying that all desalination methods have the same minimum work per unit of fresh water, subject of course to the same initial solution concentration. To choose between desalination processes requires, *inter alia*, a knowledge of the losses, (minimum 500 percent in practice).

To elevate 1 m^3 of average sea water through its osmotic pressure of 2.5 mPa requires $2.5/3.6 = 0.694$ kWh which produces $1/1.0345$ m^3 of fresh water. Hence minimum work to produce 1 m^3 of fresh water $= 0.694 \times 1.0345 = 0.718$ kWh. The relatively concentrated water of the Arab Gulf requires $0.718 \times 45000/34483 = 0.936$ kWh.

In Figure 1.8 all conditions are steady. The salt concentration is constant by virtue of a large flow into and out of the sea water compartment. The inflow of sea water minimally exceeds the very slightly concentrated outflow, due to fresh water extraction. The resulting power imbalance is the penalty for obtaining a supply of fresh water, of higher chemical potential than sea water. The characteristics of this process are that sea water at P_0 and T_0, is being converted reversibly into fresh water at P_0 and T_0 by excess pump work. The fresh water has absorbed and stored the excess pump work, which could be recovered by reversing the flow directions and flow imbalance in Fig. 1.8, and calling it an osmotic engine.

The purge flow of Fig. 1.8 assists the dispersal of salt pile up at the membrane during desalination. The latter phenomenon is called 'concentration polarization' and is a form of irreversibility important in real membrane devices. Any unrestricted dispersion of a concentration entails an entropy growth, and an irreversibility, called a 'mixing loss'. Alternatively, there is a reduction of the diffusion rate due to a smaller than ideal concentration difference across the membrane, which reduces the output. An inconsistency of both Figs 1.7 and 1.8 is that natural sea water is saturated with dissolved air, which would have to be removed before entry to the isothermal enclosure. In other words an extra exergy input is required to separate the components of the mixture. However, sea water without gas has a trivially higher chemical potential than with

gas (see numerical treatment later). Note also that the process of discharging brine to the sea throws away some (difficult to use) exergy.

When, as in practice, the processes of reverse osmosis and distillation are carried out separately, only distillation requires air extraction, a plus point for reverse osmosis.

Solvent/solution equilibrium now has to be reworked in terms of exergy and the chemical potential, to illustrate general rather than particular thinking.

In Figure 1.7 with elevated pumping the pump work is the isentropic enthalpy increase $V\mathrm{d}P$ across the pump. If m is the sea water flow, then the pump work

$$V\mathrm{d}p = \rho_s m\pi \ (\rho_s = \text{sea water density}, \pi = \text{osmotic pressure}) \tag{16}$$

Use of the function ξ_t would yield the same answer, since a difference of two values of $(H-T_0S)-(H_0-T_0S_0)$ under isentropic conditions is an enthalpy difference. The thermomechanical exergy comes into its own when the machines are irreversible. The shaft power is automatically broken down into the useful part which compresses within the pump, and the lost part which represents churning rather than orderly flow. In Fig. 1.8 with isothermal pumping, there is heat flow at T_0 (with zero exergy content) to and from the environment, at the pump and turbine. Given that the process is reversible these two flows must balance. The exergy account is

Compressor:

$$H-T_0S-(H_0-T_0S_0)=W_c=\Delta G_c=H-H_0-T_0(S_0-S) \tag{17}$$

Turbine:

$$-\{H'-T_0S'-(H'-T_0S'_o)\}=W_T=-\Delta G_T=-\{H'-H'_o-T_0(S'_o-S')\} \tag{18}$$

(The turbine uses slightly more concentrated sea water, with slightly different thermodynamic properties. It also has a slightly smaller mass flow.)

In reversible conditions the heats to and from the environment must balance. The excess of the compressor work above the turbine work cannot be dissipated in reversible conditions, and has to appear as chemical exergy in the fresh water, there being no other output. Since both the isothermal and elevated pumping schemes are reversible, the fresh water output of each must be the same.

At the membrane, when there is equilibrium, the net driving force must be zero; the chemical potential of the fresh water must equal that of the fresh water component of the sea water. The salt in the sea water

lowers its chemical potential, whilst the elevated pressure raises the chemical potential of the sea water by an equal compensating amount.

$$\mu_{f^*}(p) = \mu_f(X_s, p+\pi) \tag{19}$$

Subscript 'f' is for fresh water, superscript * implies a pure substance, X_s is the total mole fraction of sea salts.

The effect of pressure and of temperature on the chemical potential may be analysed as follows. From (14)

$$dG = V dP - S dT = V(\partial G/\partial P)T - S(\partial G/\partial T)P,$$

since G is a perfect differential. At constant temperature $dG = V dP$. Moreover, $\mu = (\partial G/\partial n)P,\ T$, for a pure substance, and $G = ng_m$, whence $(\partial G/\partial n)P,\ T = g_m$. Hence $\mu_f(p+\pi) - \mu_f(p) = \int p\pi V_m dP$. The latter integral indicates the required isothermal compression of the water molecules in the sea water to achieve a balance of chemical potential across the membrane, by raising the sea water pressure or depth to π. The chemical potential is said to be a generalized driving force, and it can be asserted that in the particular case investigated, that it controlled the diffusion of water through the membrane. Moreover, the concentration distribution appears as the scalar field in which the pressure component of the chemical potential operates.

The foregoing has involved the last term in equation (11) without its Σ, and with only one substance involved. Clearly a more elaborate problem is needed to exploit equation (12) to the full. Meanwhile a little more can be extracted from the current problem.

The vapour/water equilibrium at the fresh water surface in terms of chemical potential in molar specific properties is

$$\mu_{w^*} = h_w - T_0 s_w$$

and

$$\mu_{v^*} = h_w + L - T_0(s_w + L/T_0) = h_w - T_0 s_w = \mu_{w^*} \tag{20}$$

The chemical potential is the same on both sides of the surface, and is moreover the same as that under the membrane, which is in turn the same as that above the membrane.

At the sea water surface the vapour pressure is reduced (and the boiling point elevated) because of the salt content. At near atmospheric pressure the sea water surface is impermeable to sea salts, which are insoluble in low pressure steam, hence distillation technology. In the neighbourhood of the critical pressure the salts have some solubility in steam, a very different situation, met in the high pressure steam

generators of power plants, and which leads to salt carryover to turbine blades.

At the sea water surface, the reduction of chemical potential relative to the membrane or to the fresh water surface can be calculated along the vapour route or the sea water route, and the two must be equal. The expression $dG = VdP - SdT$ is convenient. Moreover, the temperature is constant and $SdT = 0$. For each isothermal route $\Delta G = \Delta H = \int V dP$. Since the value of π is well known, the water route is easily calculable. Just as there is no way of using the pressure difference between the sea bed and the surface, so also there is no way of using the difference of the pressure component of the chemical potential. See reference (**14**). Except in geology, it is unusual for the gravitational field to be relevant.

The modern technology of pervaporation, which can for example be used to separate alcohol from a water–alcohol mixture, is a membrane technology. For example alcohol evaporation can occur at the surface of a hydrophobic/organophillic membrane (alcohol is soluble in such a membrane, water insoluble) exposed at its opposite surface to a water alcohol mixture with its temperature maintained to supply the latent heat of evaporation. To maintain a flux through the membrane the alcohol vapour must be pumped away, so that equilibrium is prevented between the liquid alcohol in the membrane and the surrounding vapour. In the foregoing examples involving phase separation at membrane surface, the chemical potential (equation (20)) takes account not only of concentration difference, but also of the gross physical differences between vapour and liquid molecules, which affect the relevant specific entropies and enthalpies.

A water–alcohol mixture provides an introduction to partial molar thermodynamic properties. The addition of a spoonful of water to a barrel of alcohol produces a still smaller increase in the volume of the mixture. The water molecules, enveloped in alcohol, take up a reduced space. Their concentration and, therefore, their chemical potential is higher than simple thinking would indicate. In a mixture of the kind used in the pervaporation process immediately above, with a little alcohol in a lot of water the alcohol volume variation as a function of mixture strength is complex, with a minimum at about 8 percent, see (**42**) Fig. 7.1. The situation at a minimum, at which the addition of a little alcohol causes the same effect as the removal of the same amount, generates an interest in the function $(\partial V_a/\partial n_a)T, P, n_w$. Subscript 'a' denotes alcohol, and 'w' denotes water; n is a number of mols. The function is called the partial molar volume. In the pervaporation process, the chemical potential or partial molar Gibbs function $(\partial G_a/\partial n_a)T, P, n_w$ is of interest.

It is a simple example of the general case introduced in equation (12), and included in the final chemical exergy term of equation (1).

Enough thermodynamics has now been discussed to support an analysis of combined heat and steam power, combined steam power and multi-stage flash desalination, and a combined gas/steam cycle supplying heat to processes. Membranes will recur as components of Van't Hoff boxes, theoretical devices which support isothermal reversible equilibrium chemical reactions, Chapter 4.

Chapter 2

Exergy Analysis of a Simple Steam Power and Desalination Plant

'Yet I doubt not through the ages one increasing purpose runs,
And the thoughts of men are widened with the process of the suns'
Alfred, Lord Tennyson

2.1 Plant description

The plant selected for analysis is of 1960s design. The turbine is equipped with an extraction governor, enabling the supply of constant pressure bled steam over the widest achievable range of electrical loads. The plant heat cycle will be analysed in two modes, producing electricity only, and producing power and fresh water from the sea, by multi-stage flash distillation. Figure 2.1 is the flow sheet for electricity production.

The turbine has modest steam conditions and a simple feed heating system, in line with an era of very low fuel costs. The flow sheet shows the usual parameters of pressure, temperature, dryness fraction, enthalpy (kJ/kG), and mass flow. In addition the mass flow at each node is multiplied by the local value of ξ_t(kWs/kG), derived from Table 2.1, to give the mass exergy $M\xi_t$(kW); exergy in Watt-seconds of motive power, enthalpy in Joules, convertible to motive power according to exergy content. The Système Internationale (S.I.) defines 1 W = 1 J/sec, but in Joules experiment, the conversion is irreversible. One J/sec cannot be reconverted to 1 W of work. Accordingly, the first law oriented S.I. needs some evolution, for second law analysis.

2.2 Plant performance

It is between the de-aerator outlet and the superheater outlet, in the water tubes and steam tubes of the steam generator, that the main

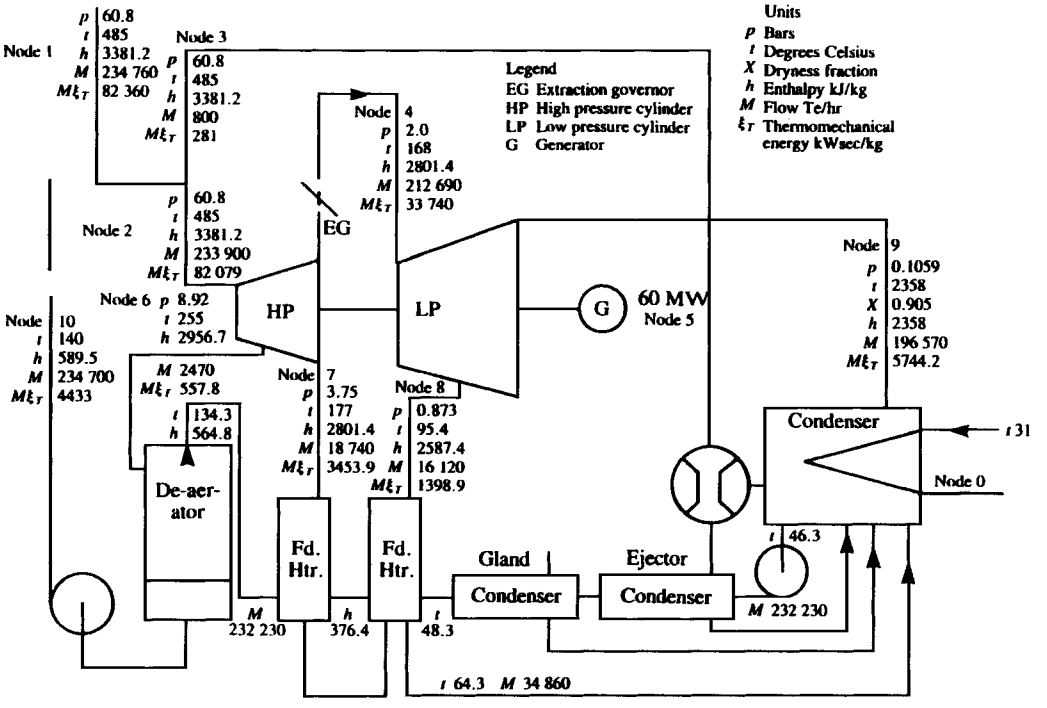

Fig 2.1 Electricity production

entropy growth and loss of the heat cycle occurs, namely the external irreversibility. The latter entropy growth determines the minimum possible heat rejection to the condenser in the absence of entropy growths in imperfect components within the heat cycle. The external irreversibility can be minimized by pushing up the final feed temperature and the superheat temperature, and by introducing steam reheat. At the present state of materials technology the steam temperature cannot approach the temperature of the near stoichiometric combustion gases. In turn, if the materials technology were not a limitation, then dissociation of the combustion gases would be encountered. The theoretical cycle efficiency cannot reach 100 percent, since impossible infinite temperatures are needed. The reader may wish to anticipate the problem – that there has to be a basis for comparing the performance of the emergent fuel cell (not subject to Carnot's limitation) and the long-established heat engine. Both suffer entropy growth dictated by the second law. See Chapter 4, for an introduction to fuel chemical exergy.

The power of exergy analysis to break down and separate the losses is beginning to appear, e.g. Table 2.1 highlights the loss in the valve of the extraction pressure governor. At its full electrical output position, close to fully open, it nevertheless has to have a control margin in hand and, therefore, causes a significant pressure drop, with an associated irreversibility of 5459 kW. The latter exergy destruction is a significant part of the net 60 MW output. Everything costs something: notably control. Given the refined data, or the detailed calculations, the losses can be broken down to any required extent. For example, every bled steam pipe must have a pressure drop which results in exergy destruction, calculated in exactly the same way as that in the extraction governor. The losses due to temperature degradation within a feeder heater can be calculated by summing the mass exergies in the streams entering and leaving the heater. Designer's economic balances can then decide whether it would be cheaper to obtain a thermodynamic benefit by fattening the bled steam pipes and their valves or by enlarging or improving the heat transfer surfaces. Note that without the extraction governor, the bled steam pressure at the lowest pressure feed heater would be raised, and its duty increased. Possibly the distribution of duties is ideal at the design point, in the absence of an extraction governor. Hence the introduction of the extraction governor may have caused an additional irreversibility, due to non-ideal distribution.

The condenser irreversibility of 5744 kW is an important result. Condensing power plants are often denigrated for rejecting large amounts of heat; the condenser is seen to be a cause of low efficiency;

Table 2.1 Calculations for Fig. 2.1 (t_0 = 31 °C sat)

Node	h (*kJ/kg*)	$h-h_0$ (*kJ/kg*)	s (*kJ/kg K*)	$t_0(s-s_0)$ (*kJ/kg*)	ξ_t (*kWs/kg*)	$M\xi_t$ (*kW*)
0	130 (h_0)		0.451 (s_0)	304 t_0		
1	3381.2	3250.2	6.987	1986.9	1263.3	82 381
2	3381.2	3250.2	6.987	1986.9	1263.3	281
3	3381.2	3250.2	6.987	1918.5	1320.2	82 079
4	2801.4	2671.4	7.360	2220.4	391.9	33 741
5	Generator output					
6	2956.7	2826.7	7.075	2013.7	813	557.8
7	2801.4	2671.4	7.056	2007.9	663.5	3454
8	2587.4	2457.4	7.407	2145.7	312.4	1398.9
9	2358.0	2228.0	7.434	2122.8	105.4	5744.2
10	589.5	459.5	1.739	391.5	68	4433

Exergy input (node 1–node 10) = 82 360 – 4433 = 77 927 kW
Exergy output (electricity) = 60 000kW
Internal irreversibility = 77 927 – 60 000 = 17 927 kW
External irreversibility $= T_0(S_1 - S_{10})M$
$= 304 \times 5.243 \times 234\ 760/3600 = 107\ 605$ kW
Condenser irreversibility = 5744 kW
Internal efficiency = 60 000/77 927 = 77%
Overall efficiency (work output/heat input)
= 60 000/ (17 927 + 104 037 + 60 000) = 33%

attempts are made to avoid the condenser by extraction to processes, with irreversibilities, and with heat rejection, which both get overlooked. The reasons for heat rejection from the condensing cycle are to be found in the various irreversibilities, notably the external irreversibility resulting from the metallurgically limited mean heat intake temperature. Efficiency can only be improved by reducing irreversibility, alias avoiding exergy destruction. Condensers are rather efficient low loss heat exchangers, with minimal irreversibility. The reader should note that the calculated irreversibility for the condenser in Table 2.1 ignores the small mass exergy in the condensate. The foregoing remarks on efficiency will be amplified in the paragraphs to follow.

2.3 Combined power and desalination

In the 40–100 percent range of electrical outputs between 24 and 60 MW the extraction governor can maintain the Node 7 low pressure cylinder outlet pressure at approximately 3 bar ±, at a desalination steam flow of 8500 kG/hr. (See Fig. 2.2.)

This flow drives the brine heater of the multi-stage flash desalination plant to be discussed later. The new heat or energy balance at 24 MW minimum electrical output (below which the turbine exhaust tends to overheat) shows a decrease in stop valve flow, due to reduced electrical output, which is offset by bleeding of steam to drive the brine heater of the distiller. The de-aerator needs more steam to deal with additional condensate from the brine heater. The extraction governor valve has to close substantially to maintain the heavier extraction of steam, so that the low pressure turbine inlet pressure and throughout are both greatly reduced. Some of the heat rejection duty of the turbine condenser is transferred to the heat rejection stages of the distiller. Note that the energy balance is an essential underlay to the exergy account. The latter has the function of breaking down the losses and pointing the way towards optimization whilst the plant is under design. The exergy account puts the desalination efficiency on the same thermodynamic basis as the heat engine and gives a unified sense of proportion. In this particular instance, it will be made clear that distillation produces an exergy output in the form of elevated chemical potential of pure water. The pure water, in terms of irreversibility, is expensively obtained, compared to the electricity from the turbine which the desalination steam could alternatively produce. The desalination process must carry not only its internal losses, but also the losses in the extraction governor which exists on behalf of desalination.

Table 2.2 shows that the part load efficiency, when credit is taken for the desalination steam mass exergy, is just below that in the electricity-only figure in Table 2.1. The heat cycle is distorted by extraction governor throttling; the low pressure cylinder being starved of steam with a throughput of less than half the extraction steam; there is little feed heating in the lowest pressure feed heater, dictating additional heating in the next heater and in the de-aerator. However, the extraction steam, which would have taken part in electricity generation, does not in this (unrealistic) calculation suffer any losses of exergy. In reality it takes part in a distillation process, which produces a small output of exergy (raised chemical potential of pure water relative to salt water), with very large thermal degradations in heat exchange, temperature drop in

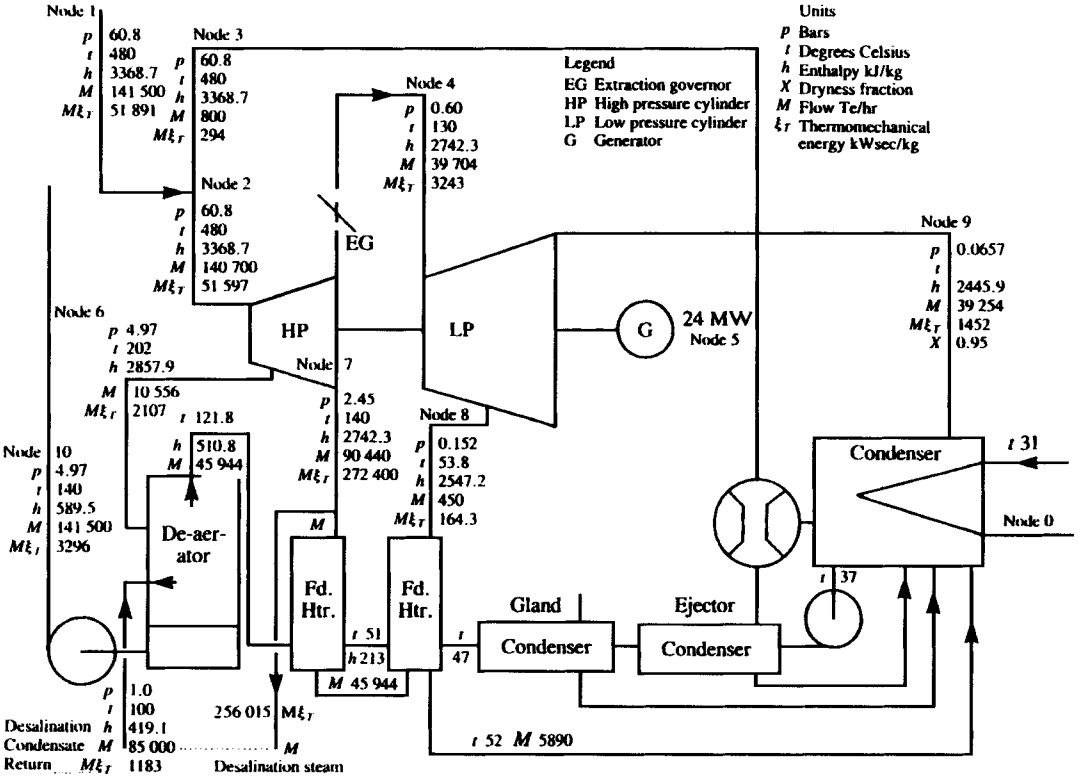

Fig 2.2 Water and electricity production

Table 2.2 Calculations for Fig. 2.2

Node	$h-h_0$ (*kJ/kg*)	s (*kJ/kg K*)	h (*kJ/kg*)	$t_0(s-s_0)$ (*kJ/kg*)	$X\xi_t$ (*kWs/kg*)	$M\xi_t$ (*kW*)
0		0.451 (s_0)	130 (h_0)	304 (t_0)		
1	3238.7	6.762	3368.7	1918.5	1320.2	51 891
2	3238.7	6.762	3368.7	1918.5	1320.2	51 597
3	3238.7	6.762	3368.7	1918.5	1320.2	294
4	2612.3	7.755	2742.3	2220.4	391.9	3243
5 Electrical output						
6	2727.9	7.061	2857.9	2009.4	718.5	2107
7	2612.3	7.115	2742.3	2025.9	586.4	14 732
8	2417.2	7.862	2547.2	2252.9	164.3	20
9	2415.9	7.960	2445.9	2282.7	133.2	1452
10	459.5	1.739	589.5	391.5	68.0	3296
11	289.1	1.303	419.1	259.0	30.1	1183

Exergy input (node 1–10) = 51 891 – 3296 = 48 595 kW
Exergy output (electricity) = 24 000 kW
Exergy output (desal. steam) = 85 000 (586.4 – 30.1)/3600 = 13 134 kW
Internal irreversibility = 48 595 – (24 000 + 13 134) = 11 461 kW
External irreversibility = $T_0(s_1 - s_{10})M$
= 340(6.672 – 1.739)141 500)/3600 = 67 127 kW
EG throttling = 39 704/3600(718.5 – 586.4) = 1457 kW
Condenser irreversibility = 1452 kW
Internal efficiency = (24 000 + 13 134)/48 595 = 76.4%
Overall efficiency (work output/heat input)
= 37 134/(11 461 + 67 127 + 37 134) = 32%

flashing, boiling point elevation, and pumping losses. The efficiency of the integrated power and desalination process is therefore much lower than the 33 percent of the electricity-only processes (a figure a 24 percent is calculated in Table 2.4, as adversely influenced by a desalination efficiency of 4 percent, Table 2.3. Competing desalination processes such as reverse osmosis (**29**) or vapour compression (**30**) which get their exergy from electricity, without distorting the power plant, are nowadays having some market successes based on better thermodynamic performance, but some doubts arise from lack of operating experience. These alternatives were not available when the plant being analysed was procured.

The most efficient new desalination processes consume at least five times as much exergy as is dictated by the equilibrium diagram of Fig. 1.7,

Table 2.3 Multi-stage flash desalination efficiency calculation

	h (kJ/kg)	$h-h_0$ (kJ/kg)	s ($kJ/kg\,K$)	$t_0(s-s_0)$ (kJ/kg)	ξ_t (kW/kg)	$M\xi_t$ (kW)
0	130 (h_0)		0.451 (s_0)	304 (t_0)		
Main steam	2712	2582	7.098	2021	561	24 621
Condensate	415	285	1.293	103	182	7988
Ejector steam	2800	2670	6.510	1844	826	1067
Condensate	169	39	0.576	38	1	13
Electrical consumption						8000
Distilled water 947 × 0.936*						886
Exergy input = 25 699 kW		Exergy output = 886 kW			Efficiency = 3.45%	

* 1 cubic metre of pure water has an elevated chemical exergy of 0.713 kWh relative to normal sea water, and 1.5 times that, relative to Gulf sea water, of 50 percent higher concentration (osmotic pressure 25 bar × 1.5).

and the older less efficient MSF, twenty-five times as much. A heat engine process, displaced by a desalination process, would have consumed only a fraction more than its reversible version.

At full electrical output, the turbine efficiency is a maximum, whilst the desalination plant is unaffected, so that the overall power and desalination efficiency improves, but cannot attain the efficiency of power production only, which is relatively reversible.

2.4 Multi-stage flash desalination

The references (**25**) and (**26**) were seminal to the topic of multi-stage flash desalination, which after thirty years still dominates the Middle-Eastern and remote island market for fresh water from the sea, see Fig. 2.3.

A stream of heated brine is cooled in a series of flash chambers each of which has its output of flash steam led via a demister to a bank of condenser tubes. The condensed flash steam is the output of the distiller. The brine-cooled condensers are connected in series, so that each flash steam flow encounters a condensing surface at the same temperature difference below its saturation temperature. Brine emerging from the hottest condenser is raised in temperature in a brine heater which discharges to the hottest flash box.

The bottom end of the series terminates in some condensers which have sea water coolant and serve to reject the heat put into the system by the brine heater and by pumps. As the bores of the condenser tubes tend to

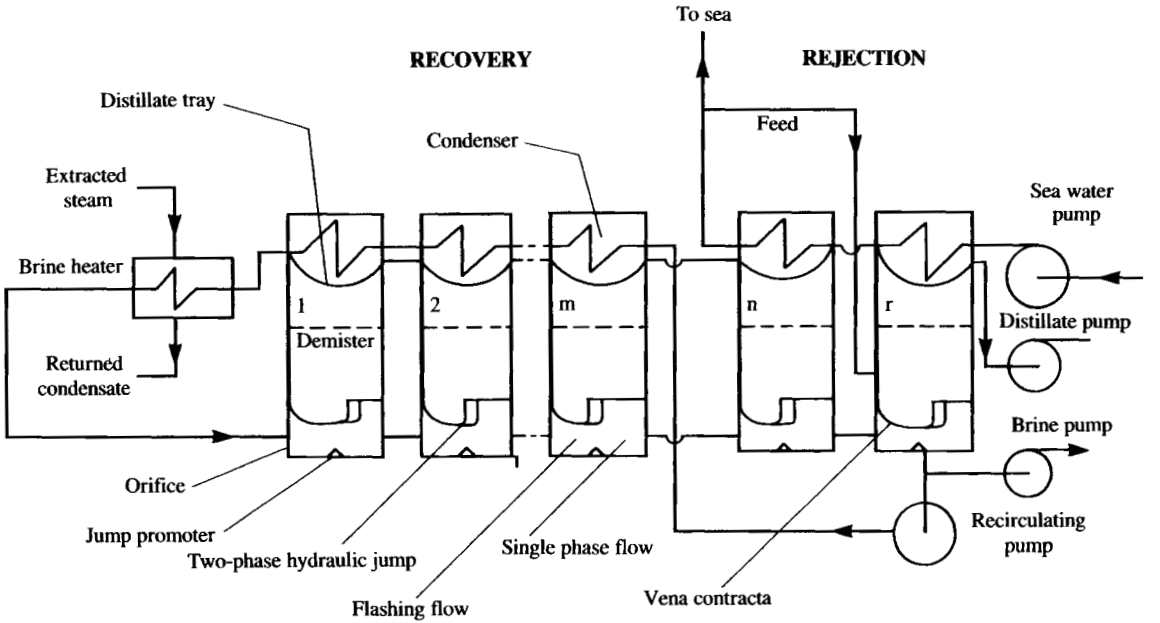

Fig 2.3 Multi-stage distiller

accumulate scale to the impediment of heat transfer, a surface-active antiscalant is circulated in the flowing brine, which interferes with, and slows down, nucleation and scale build up. Abrasive balls are circulated in the brine to aid the antiscalant. The chemicals involved improve continuity of operation and allow the water output to be forced up. They have been developed to be effective up to 120 °C, and are costly. Economy in their use is achieved by providing a brine recirculation pump, which rotates the antiscalants to consume more of their activity, before discharge to the sea in the concentrated brine. A separate de-aerator, working on the incoming sea water, is provided. Due to casing leakage, and because the main de-aerator is not perfect in its action, continuous de-aeration of the whole equipment is used, so that non-condensable gas accumulation at the surface of condenser tubes is minimized. Moreover, at start up the whole distiller and its de-aerator must be evacuated using a so-called hogging ejector. Smooth and controllable flashing depends on the presence in the brine of enough dissolved air to allow bubble nucleation – an objective which is usually achieved through the practical limitations of de-aeration equipment. The incoming sea water from an intake tailored to local conditions, is chlorinated, screened for trash, weed, and life, then settled to remove sand. In fortunate cases beach wells in sand, or well-fractured rock, may minimize the need for engineered pre-conditioning equipment. The energy balance of an MSF distiller involves the steam tables, thermodynamic properties of brine as a function of concentration, including boiling point elevations, and proprietary experimental information on the partial completion of the flashing process, in a commercial design of flash box. Users, however, are beginning to undertake these calculations and to publish them, (**27**).

A rather tidy design of flash box is shown in Fig. 2.3. Brine enters via an orifice, and the flow profile is a conventional 'vena contracta', after which flashing commences. In the base of the flash box a piece of angle iron is sufficient to precipitate a two-phase hydraulic jump, which increases the head and depth ahead of the orifice leading to the next flash box, and suppresses flashing. The process repeats with all flash boxes at one level.

By calculating the inlet thermochemical mass exergy and the outlet chemical mass exergy, the efficiency of the process can be arrived at with no knowledge of its internals.

A typical 1970s design of MSF distiller has the following parameters:
Main steam supply, T 123.5 °C, P 2.23 bar, M 158 000 kg/hr.
Condensate return T 98 °C, P 8.21 bar.
Ejector steam supply, T 204 C, P 14.2 bar, M 4 649 kg/hr.

Condensate return T 40 C, P 8.21 bar.
Electricity supply 8MW for recirculation and cooling water pumps etc.
Distilled water production T 40 °C, P 4.15 bar, M 947 000 kg/hr.

The reader is left to reduce this efficiency further by debiting the extraction governor irreversibility to desalination. It is inconsistent to include auxiliary power in desalination efficiency, but not in turbine efficiency. The station output can be reduced by about 10MW, and the figures adjusted accordingly, without improving the illustration.

An efficiency of 4 percent gives an opportunity for alternative systems such as reverse osmosis and vapour compression to compete, to achieve better overall economy by better exergy utilization. After thirty years of multi-stage flash distillation, plants of that type are still being built and in steadily increasing sizes, but with ever stiffer competition. Known large-scale reliability is difficult to displace! Moreover, exergy utilization is only part of the techno-economic story.

In the above calculation the de-aeration process and the desalination process have been lumped together, on the understanding that the product water is re-aerated for potability. It should be possible, however, to look separately at the efficiency of de-aeration, since the removal of gas means an increase in chemical potential of the purified liquid, leading to the possibility of calculating the minimum work to de-aerate a large flow of liquid. However, the solubility of air in water is very low – about 5.1×10^{-4} mol N_2/kg and 2.6 mol O_2/kG) at standard conditions (**7**) – and the effect on the water molecule concentration is trivial. Accordingly, practical de-aeration can be regarded as a throwaway process in which the incoming exergy is destroyed completely. That conclusion is reinforced by the fact that steam jet ejectors are used, which are based on the wasteful mechanism of entrainment. The process is attractive because of simplicity and reliability, which are outstanding virtues in drinking water production in arid climates.

The loss of exergy in the MSF distiller by conversion of pumping power to internal energy at pump temperature is 8 MW. The remaining, even heavier, losses must comprise degradation in heat exchanger walls (condensers, and brine heater) together with non-equilibrium flash chamber processes, such as flash pressure and temperature drop, and incomplete flash, taking account of boiling point elevation, pressure drop in demisters, and the like. A break-down of these irreversibilities has been published in (**27**) for a recirculating MSF distiller and in (**28**) for a simple non-recirculating MSF distiller. Simplifications were made to allow for lack of comprehensive thermodynamic data on sea water at all relevant concentrations, pressures and temperatures.

The exergy input/output ratio of 25/1 compares badly with the figure of about 6/1 for modern reverse osmosis(RO) or 5/1 for low temperature vapour compression(VC) processes (**29**) (**30**). Two factors operate: firstly efficiency calculations are not often based on exergy analysis; secondly fuel economy is only part of the compromise. However the RO and VC processes are compared on the basis of electricity consumption; virtually exergy analysis.

Neither process causes losses in the power plant as does the MSF distiller.

Table 2.4 is an extension of Table 2.2; the efficiency of the combined power and desalination process is assessed.

An inefficient distillation process has displaced a relatively efficient heat engine process.

If the extraction steam had been utilized in manufacturing industry to produce artefacts such as concrete castings, or plastic mouldings with zero recoverable exergy then the combined efficiency would fall a little further to 24 000/103 113 = 23.3 percent. If all the electricity were used for machining metal, again with zero recoverable exergy, then the efficiency would fall to zero. Such throwaway processes cannot be characterized thermodynamically. They must be dealt with empirically, for example number of machined screws/kWhr, with a market price per screw. Power and desalination is rather a special case where there is a non-throwaway process within the power plant.

In the commercial presentation of combined heat and power, a calculation is often made of 'the fuel utilization factor'. When stack losses are deducted, the remaining flow of energy from the fuel is divided between heat and power production, on the (erroneous) basis that 'all heat going to a process is used'. The fuel utilization factor, approximately 90 percent, is then misquoted as being the efficiency. As a result, it is concluded erroneously that combined heat and power is two or three times as efficient as a condensing, electricity only, generating plant. As energy is indestructible all the heat supplied to a building must eventually

Table 2.4 Power and desalination efficiency

Extraction flow is 85 000 kG/hr with a mass exergy of	13 134 kw
At 4% efficiency the distiller output mass exergy is	525 kw
Total exergy output is, therefore	24 525 kw
Adjusted internal efficiency falls to 24 525/48 595	= 50% (77%)
Adjusted overall efficiency falls to 24 525/(11 461 + 67 127 + 24 525)	= 24% (32%)

leak to the environment. The heat supply can be minimized by insulation, by stale air to fresh air heat exchangers, and by an optimized air change rate, with controllable variables adjusted to building occupancy and climatic change. No matter what is done, however, it remains true that heat input equals heat rejected. Accordingly it is clear that the fuel utilization factor is insensitive to building technology improvements, or on a broader basis it is totally insensitive to the kinds of process to which the CHP plant supplies heat.

On the other hand CHP is clearly a major improvement on the plants which it usually replaces, namely low pressure steam generators and a utility power supply. That is because the low pressure steam generator has a rational efficiency of around 20 percent (**31**) due to degradation of the fuel heat down to a steam saturation temperature of the order of 150 °C. In other words most of the fuel chemical exergy is immediately destroyed. CHP on the other hand uses the fuel heat at engine temperature, with minimum degradation. There is some significant degradation in heat exchange between the engine exhaust and the exhaust heat recovery boiler, which has to be looked at in optimization studies, but this pales into insignificance beside the exergy destruction in a low pressure steam generator. For a large-scale chemical plant requiring a heat supply to a group of processes, a CHP scheme allied to competent process integration is unlikely to have a rival, albeit the fuel utilization factor will misrepresent its performance, which has to be on the basis of exergy output/exergy input.

Within the topic of process integration the heat pump has a niche. In the special case of a single low temperature process such as whisky distillation, or desalination, a heat pump may displace steam generators completely, and compete with CHP. A balanced sense of proportion is possible if plant efficiencies are compared on an exergy basis. On that basis CHP and pure electricity generation are competing processes with marginal efficiency differences, and appropriate economic niches. In a CHP plant electricity is likely to be sensibly utilized for motive power, whilst heat will be derived from steam with little degradation. By contrast, the utilization of electrical power from a utility supply is likely to involve doubtful and wasteful non-motive power forms of use. Such processes are a large and important problem deserving detailed reappraisal by the fuel efficiency community.

Chapter 3

A Modern Combined Cycle-Based CHP Scheme

'Fear no more the heat o' the sun,
Nor the furious winter's rages'
William Shakespeare

3.1 Introduction

The availability of natural gas has led to the construction of combined cycle plants in which exhaust heat recovery is accomplished by steam generators with up to three steam pressures and reheated steam. The complexity is in aid of temperature profile matching between the exhaust gas cooling curve, and the steam heating curve, so as to minimize degradation. The gas turbines are likely to have combustion chamber steam injection or specially designed low NO_X (pollutant oxides of nitrogen) burners. Minimum oxidation of nitrogen is a matter of coolest possible, best mixed combustion, for the dry route. For the wet route steam injection contributes both to cooling and to mixing. For both routes NO_X production increases as the square root of the absolute combustion pressure. Like metallurgical limitations, NO_X production is a factor working against higher flame and turbine entry temperatures. The oxides of nitrogen are NO, NO_2, N_2O_4, N_2O_3, and N_2O_6; hence the shorthand NO_X (**34**)–(**36**).

A medium-sized uncomplicated example of combined cycle technology (under construction in 1993) is chosen to illustrate the energy and exergy flows. Details are by courtesy of British Nuclear Fuels plc. The plant is based on Frame 6 gas turbines supplied under General Electric licence by the GEC Alsthom subsidiary of European Gas Turbines. As gas turbine manufacturers are reticent about the design of

the hot end of their machines, for example blade cooling air flows, turbine entry temperatures and the like, the analysis below uses estimates which are good enough to illustrate a textbook argument. The gas turbines exhaust into double pressure heat recovery steam generators, (EHRBs), which provide 83 bar HHP turbine steam and, via turbine bleeds, 22 bar steam for injection into the combustion chambers to minimize NO_X production, and 6 bar LP process steam. The choice of steam injection requiring 100 percent make-up implies access to low cost make-up water, and indeed a feature of the site processes is that they also return no condensate to the steam generators. River water make-up is, therefore, substantial – via ion-exchange beds – into a special de-aerating blister on the condenser.

Figure 3.1 is a skeleton flow sheet, and shows three gas turbines with individual EHRBs and a single auxiliary boiler, which secures the continuity of supply of process steam. Additional process steam security is provided by two steam pressure-reducing valves in series which bypass the turbine high-pressure cylinder, and supply back up 13 bar HP and 6 bar LP process steam. The normal supply of LP steam is from the HHP turbine exhaust; the HP steam (rather than being extracted) is throttled HHP steam, the latter being a design compromise resulting from turbine arrangement considerations, and the effect on bled steam conditions of electrical load variations. The achievement of control has had its cost in terms of exergy destruction. Further details are given in the flow sheet of Fig. 3.2.

The compressor of the gas turbine takes in moist air at the ISO design point of 1013 mBar, 60 percent RH, 15 °C. In the combustion chamber there is steam injection, and the combustion reaction produces further steam and carbon dioxide from the largely methane fuel. The resulting exhaust gas is, therefore, a mixture of oxygen (15 percent dry basis), nitrogen, carbon dioxide, and water vapour (steam), with NO_X kept below 60 ppmvd (d signifies dry basis ignoring steam in exhaust gas). The exhaust gas is cooled from 541 °C to around a measured 110 °C at the stack, by the double pressure EHRB. An exergy destruction occurs due to the temperature difference between gas during cooling and steam during evaporation. A Q-Carnot diagram (**10**) is used below, to describe this irreversibility as a quantifiable area, Fig. 3.3.

The numerical link between the gas and the steam turbines is that the heat input to the steam, is the heat extracted from the gas turbine exhaust. Since the twin steam cycles receive heat at a lower temperature than the exhaust gas rejects heat, there must be an entropy growth and an irreversibility $T_0\Delta S$ due to temperature degradation during heat

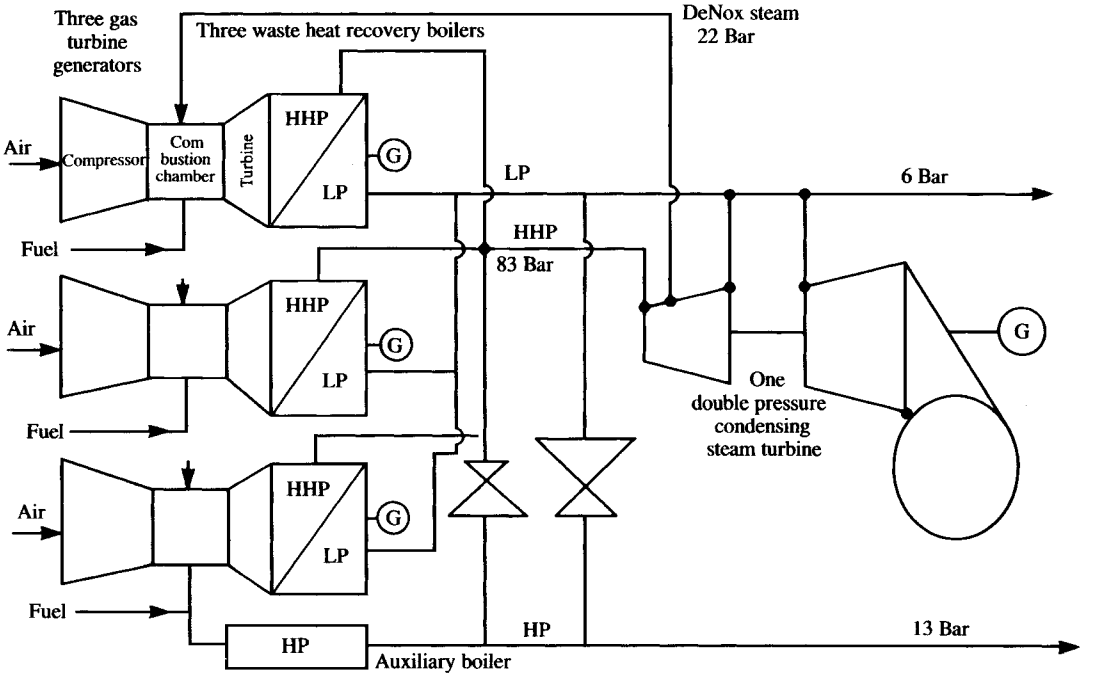

Fig 3.1 Sellafield CHP

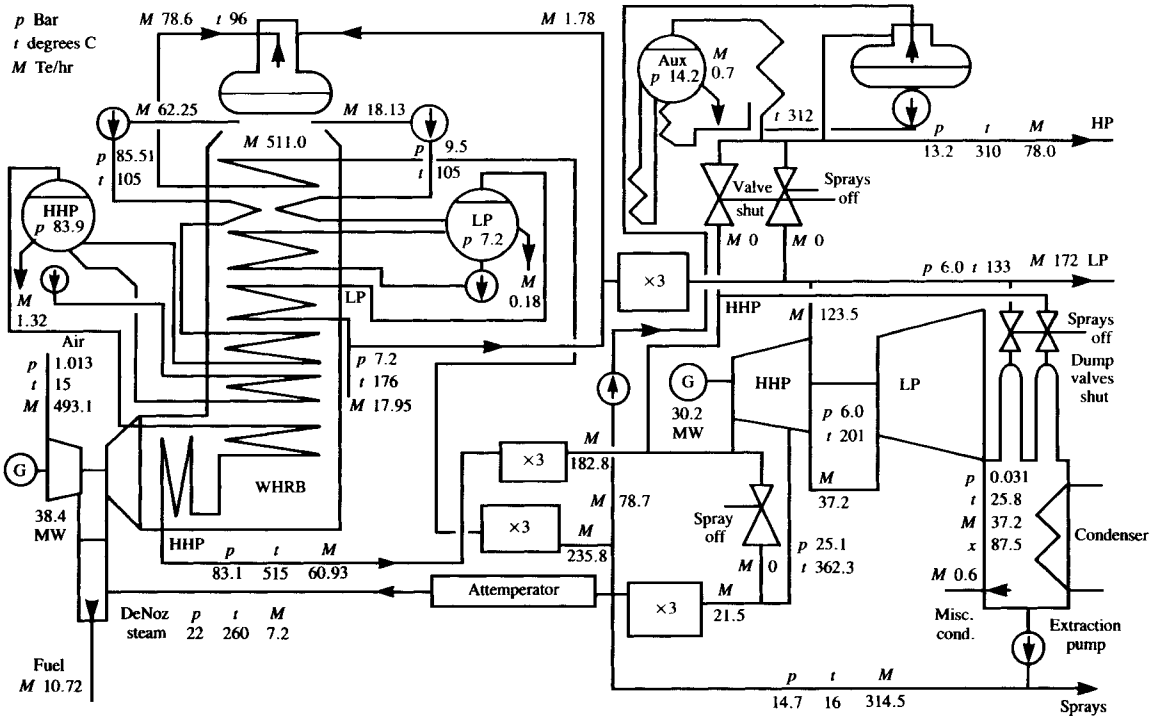

Fig 3.2 Sellafield CHP – winter conditions

exchange. The exhaust gas going to the stack contains both thermomechanical exergy and chemical exergy. In the first place its temperature is higher than ambient, and in the second place its composition is not the same as the atmosphere. In principle, therefore, membrane processes could extract work from the concentration or chemical potential differences. The fuel enthalpy of combustion (**26**), calculated from enthalpies of formation or measured in a steady flow gas calorimeter, does not reflect these latter work potentials or chemical exergies, which are part of the fuel chemical exergy (Chapter 4). See also (**17**), article 3, 'Available energy quantities' by L Rodriguez.

3.2 The gas turbine fuel

The reference or design point fuel is natural gas of the following tabulated analysis and properties, calculated according to the data and methods of ISO 3977:1991(E) via BS 3863:1992. 'Gas turbines procurement'. The specific energy and the calorific value are obsolescent and imprecise terms, replaceable by the gross and net enthalpy and internal energy of combustion, (**32**). The gross enthalpy of combustion applies if water vapour in the combustion products is condensed, whilst the net value applies if, as is more usual, the water remains as vapour (low partial pressure superheated steam). The gross enthalpy of combustion is measured in steady flow gas calorimetry, or calculated from tabulated enthalpies of combustion of reactants as in Table 3.1. A modern computerized gas chromatograph, as fitted by British Gas at Sellafield, can determine the gas analysis on line at seven minute intervals, and calculate immediately the gross and net enthalpies of combustion.

3.3 Chemical exergy of fuel

The chemical exergy of CO and H_2 are calculated in Chapter 4. The ΔG_o of methane, the main constituent of natural gas is also determined. From these results the chemical exergy of natural gas (a calculation involving the invention of an equilibrium fuel cell for each natural gas constituent) is guessed as 1100 $kWsmol^{-1}$ = 68 557 kWs/kg, greatly in excess of the net enthalpy of combustion of 42 997 kJ/kg. The modified definition of fuel chemical exergy in Chapter 4 gets away from the puzzling approximation that its value is close numerically to the net enthalpy of combustion. The latter is an energy flow from practical irreversible combustion. The thermomechanical exergy or work obtainable from such a combustion energy flow (heat) is Carnot limited. Chemical exergy is pure work.

Table 3.1 Natural gas composition and specific energies at 15 °C

a	*b* (*Vol/mol%*)	*c* (*RMM*)	*d* (*bxc/100*)	*e* (*d*/M = *% mass*)	*f* (*GSE*)	*g* (*NSE*)
Methane (CH_4)	85.26	16.04	13.68	73.97	55 545	50 000
Ethane (C_2H_6)	4.43	30.07	1.33	7.19	51 920	47 525
Propane (C_3H_8)	1.04	44.10	0.46	2.49	50 385	46 390
n-butane (nC_4H_{10})	0.37	58.13	0.22	1.19	49 565	45 775
i-butane (iC_4H_{10})	0.18	58.13	0.11	0.60	49 445	45 660
n-pentane (nC_5H_{12})	0.14	72.15	0.10	0.54	49 060	45 400
i-pentane (iC_5H_{12})	0.07	72.15	0.05	0.27	48 970	45 305
C_6 Hydrocarbons	0.08	86.18	0.07	0.38	49 710	46 130
C_7 Hydrocarbons	0.025	100.21	0.025	0.14	55 010	50 967
Carbon-dioxide (CO_2)	0.59	44.01	0.26	1.41		
Water (H_2O)	10–50 ppm	18.04				
Nitrogen (N_2)	7.81	28.013	2.19	11.94		
Others	0.005					

Hydrocarbon dew point – 3 °C
Water dew point – 23 °C
Natural gas RMM 18.495 = M
Flammability limits 5–15% in normal air
C atoms: 85.26 + 8.86 + 3.12 + 2.2 + 1.05 + 0.48 + 0.175 = 101.45
hence H/C = 3.795
H atoms: 341.25 + 26.48 + 8.32 + 5.5 + 2.52 = 383.86
and C/H = 0.264
Fuel GSE = $\Sigma ef/100$ = 41 086 + 3733 + 1255 + 590 + 297 + 265 + 132 + 189 + 77
= 47 624 kJ/kg
[18.495 g = 222.412 1, hence 1 m^3 = 18.495/22.412 = 0.825 kG at 0 °C]
Hence GSE/m^3 = 47 624 × 0.825/1000 × 273/286 at 15 °C = 37.50 MJ/m^3
Fuel NSE = $\Sigma eg/100$ = 36 985 + 3417 + 1155 + 545 + 274 + 245 + 122 + 175 + 71
= 42 989 kJ/kg
Hence NSE/m^3 at 15 °C = 33.85 MJ/m^3

The rational efficiency of an engine, or for that matter of a fuel cell, is the ratio between its exergy output and its chemical exergy input per unit mass or mole of fuel. In perfect reversible conditions (unachievable if the engine fuel is burned; also unachievable because the fuel cell hydrogen fuel is in combined form in nature), the ratio reaches 100 percent. In practical conditions the irreversibilities bring the ratio down quite drastically. While first law efficiencies can exceed 100 percent in the

presence of heat pumps, rational second law efficiencies are always below 100 percent. A heat pump becomes an imperfect machine whose performance is less than ideal, and less than 100 percent efficient.

3.4 The plant flow sheet and energy balance

The detailed flow sheet is shown above in Fig. 3.2. The example of winter plant utilization has been selected for analysis because all plant items are in vigorous use. To assist the fully extended combined cycle plant the auxiliary boiler is steaming; its low exergetic efficiency can be compared unfavourably, when second law analysis is performed, with that of the alternative of extraction from the steam turbine. High make-up shows as excess extraction pump flow above turbine exhaust.

A quantitative energy balance rests on the axiom that energy can neither be created nor destroyed. With an energy balance to hand, an exergy account can be prepared. This shows the losses when the fuel chemical exergy is partially destroyed in combustion, and converted in the heat cycle to a further reduced amount of thermomechanical exergy in electricity and process steam, after internal irreversibilities.

The gas turbine combustion chamber mixes then ignites a fuel/steam/air mixture. The gas tables cope with this situation for the simple case of octane fuel, but for a complex natural gas mixture a computer is needed. Within the turbine the exhaust gas changes in composition slightly, due to the entry of air to the cooled turbine stages. In this chapter, manual calculations, the gas tables, and computers are all deployed. Exergy losses are calculated via entropy growths, as a convenient and educational change of tactics, compared to steam cycle analysis in Chapter 2.

The bias in what is written here is toward thermodynamic considerations, but in general a balance must be struck, involving site considerations, speed of procurement and construction, safety and reliability, controllability, and maintainability, in addition to thermal performance, and its capital cost. Sensitivity to fuel cost and money cost (interest rate) are important economic factors. The latter factors vary strongly and arbitrarily. The best that optimization can achieve may be robust designs, insensitive to economic changes.

The foundation of a gas turbine energy balance is a detailed combustion calculation, and an example follows for the gas turbine of Fig. 3.2, using the natural gas described in Table 3.1.

3.5 Combustion calculation

The compressor of the gas turbine at its design point takes in 'standard air' at 1.01325 bar, 15 °C (288.15 °K), Relative humidity 60 percent. Dry air comprises by vol/mol 21 percent O_2, and 79 percent N_2 at (atmospheric nitrogen includes argon and rare gases 0.93 percent, and has an RMM (relative molecular mass) of 28.15). The analysis by mass is 23.2 percent O_2 and 76.8 percent N_2at.

The relative humidity of 60 percent gives the partial pressure of the water vapour as 60 percent of its saturation pressure at 15 °C, which from the steam tables is 1.705 kN/m^2 and 60 percent = 1.023 kN/m^2 = 0.01023 bar = 100 × 0.01023/1.01325 = 1.01 percent partial pressure.

Hence standard air analysis by vol/mol is as shown in Table 3.2.

Table 3.2

H_2O	=	1.01%
O_2 98.99% × 21	=	20.79%
N_2at 98.99% × 79	=	78.20%

To obtain analysis by mass, calculate the RMM and its components: 20.79×32/100+78.2×28.15/100+1.01×18.04/100=6.6528+22.0133 + 0.1822=28.8483.

Hence standard air analysis by mass is as shown in Table 3.3.

Table 3.3

H_2O	=	0.63%
O_2	=	23.06%
N_2at	=	76.03%

Stoichiometric or zero excess air relationships are calculated in Table 3.4 and are summed up in Table 3.5.

The excess *S*-air figure of 205 percent (305 percent theoretical air) was obtained by interpolating between calculations for guessed figures of 200 and 250 percent to obtain the desired Table 3.5 dry basis oxygen of 15 percent. Since the gas tables are on a dry air basis the atmospheric moisture and deNO_X steam are added in as excess air making 207 percent. The gas tables are insensitive to small changes of carbon to hydrogen ratio. The exhaust gas analyses are, on a wet basis by mass, shown in Table 3.6.

The dry basis oxygen content by volume is 13.54×100/(100–9.70) = 14.99 percent.

Table 3.4 Stoichiometry

Methane 73.97% by mass	
$CH_4 + 2O_2$	$= CO_2 + 2H_2O + N_2$at.
$16.04 + 64$	$= 44.01 + 2 \times 18.015$
$1 + 3.99$	$= 2.744 + 2.246 + 13.155\ (76.03/23.06 \times 3.99)$
$0.7397 + 2.951$	$= 2.03 + 1.661 + 9.730$
Ethane 7.19%	
$2C_2H_6 + 7O_2$	$= 4CO_2 + 6H_2O + N_2$at.
$2 \times 30.07 + 7 \times 32$	$= 4 \times 44.01 + 6 \times 18.015$
$1 + 3.725$	$= 2.927 + 1.797 + 12.28$
$0.072 + 0.2682$	$= 0.2107 + 0.1294 + 0.8840$
Propane 2.49%	
$C_3H_8 + 5O_2$	$= 3CO_2 + 4H_2O + N_2$at.
$44.1 + 5 \times 32$	$= 3 \times 44.01 + 4 \times 18.015$
$1 + 3.628$	$= 2.994 + 1.634 + 11.99$
$0.0249 + 0.0903$	$= 0.0746 + 0.0407 + 0.2990$
Butanes 1.79%	
$2C_4H_{10} + 13O_2$	$= 8CO_2 + 10H_2O + N_2$at.
$2 \times 58.13 + 15 \times 32$	$= 8 \times 44.01 + 10 \times 18.015$
$1 + 3.578$	$= 3.028 + 1.550 + 13.614$
$0.0179 + 0.0640$	$= 0.0542 + 0.0277 + 0.2436$
Pentanes 0.81%	
$C_5H_{12} + 8O_2$	$= 5CO_2 + 6H_2O + N_2$at.
$72.15 + 8 \times 32$	$= 5 \times 44.01 + 6 \times 18.015$
$1 + 3.548$	$= 3.050 + 1.498 + 11.697$
$0.0081 + 0.0287$	$= 0.0247 + 0.0121 + 0.0948$
Carbon-6-hydrocarbons (Analysis unstated, content 0.38%, assume hexane)	
$2C_6H_{14} + 19O_2$	$= 12CO_2 + 14H_2O + N_2$at.
$172.36 + 608$	$= 528.12 + 252.21$
$1 + 3.528$	$= 3.064 + 1.463 + 11.632$
$0.0038 + 0.0134$	$= 0.0116 + 0.0056 + 0.0442$
Carbon-7-hydrocarbons (Analysis unstated, content 0.14%, assume heptane)	
$C_7H_{16} + 11O_2$	$= 7CO_2 + 8H_2O + N_2$at.
$100.21 + 352$	$= 308.07 + 144.12$
$1 + 3.513$	$= 0.307 + 1.438 + 11.582$
$0.0014 + 0.0049$	$= 0.0004 + 0.002 + 0.0162$

Table 3.5 Stoichiometric equations summed up (HC ≡ hydrocarbons) By addition from Table 3.2

$HC+$	CO_2+	N_2at	$+$	O_2	$+$	H_2O	$=$	CO_2	$+$	H_2O	$+$	N_2at	$+$	O_2
0.8678	+ 0.0141	+ 0.1184					=	0.0141	+			0.1184		
Theo. *S*-air 100%		11.3028	+	3.4205	+	0.0937	=	2.4073	+	1.8785	+	11.3028		
Excess *S*-air 205%		23.1707	+	7.0120	+	0.1921	=			0.2858	+	23.1707	+	7.0120
$DeNO_x$ steam = 1.45% of *S*-air						0.6557	=			0.6557				
Sum:														
0.8678	+ 0.0141	+ 34.5919	+	10.4325	+	0.9415	=	2.4214	+	2.8200	+	34.5919	+	7.0120
							=	46.7505						

Table 3.6 Exhaust gas analysis (wet)

CO_2	H_2O	N_2a	O_2	
5.17 [44.01]	6.02 [18.015]	73.84 [28.15]	14.97 [32]	(with RMM 28.94)
3.40%	9.67%	75.91%	13.54%	(% by vol)

Since this exhaust gas analysis is a close approximation to that of the manufacturer it is possible to be confident of any derived figures. Unit mass of fuel consumption demands 45.85 units of *S*-air. With a compressor air output of 493.1 Te/hr this amounts to 10.75 Te fuel/hr, and a turbine exhaust flow of 493.1 + 10.75 + 7.2 = 511.0 Te/hr. Note the omitted detail in this approximate analysis, in which the number of decimal places indicates the use of a calculator, and not accuracy. The turbine inlet flow is less than the exhaust flow because of the use of compressor air for oil burner cooling and turbine disc and blade cooling. Note also that some compressed air is recirculated to the compressor inlet filter for cleaning. Compressed air for bearing cooling is discharged to atmosphere.

3.6 EHRB stack temperature

The flow sheet given to the author does not give a stack temperature, for the winter peak operating condition, so it is estimated below as 83 °C, (Table 3.7) by deducting the (make-up sensitive) steam cycle heat intake from the mass-enthalpy at the gas turbine exhaust, using the Keenan gas and steam tables.

Interpolating in the gas tables for 307 percent theoretical air parameters:

Table 3.7 Gas turbine exhaust conditions

P (*Bar*)	T (°*C*)	M (*Te/hr*)	
1.04	541	511.7	28.94

$h\,400 = 24664.4 + 0.15(24697.1 - 24664.4)$
$= 24664.4 + 4.95$
$= 24669.4$ J/gmol

$\bar{\Phi} = 224.67$

$\bar{h} = 25053.9 + 0.15(25087.5 - 25053.9)$
$= 25053.9 + 5.04$
$= 25058.9$ J/gmol

$\bar{\Phi} = 225.20$

$\bar{h}\,307 = 25058.9 - (25058.9 - 24669.4) \times 107/200$
$= 25058.9 - 6.85$
$= 24850.5$ J/gmol

$\bar{\Phi} = 224.93$

$h\,307 = 24850.5/28.95$
$= 858.4$kJ/kg

$\Phi = 224.93/28.94 = 7.772$

Hence turbine exhaust mass-enthalpy $= 511.7 \times 858.4 \times 10^3 = 439 \times 10^6$ kJ/hr.
At 25 °C 1.0132 bar

$\bar{h}\,400 = 8710.3 + 29.5 \times 0.15 = 8714.7$
$\bar{h}\,200 = 8774.0 + 29.9 \times 0.15 = 8778.5$
$\bar{h}\,307 = 8778.5 - 63.8 \times 107/200 = 8744.4$
$h\,307 = 8744.4/28.94 = 302.2$

Hence exhaust enthalpy referred to 25 °C, 1.0132 bar

$= 858.4 - 302.2 = 556.2$ kJ/kg and corresponding mass enthalpy
$= 511.7 \times 556.2 \times 10^3 = 284.6 \times 10^6$ kJ/hr

Turbine exhaust entropy; the latter parameter is needed later relative to 25 °C 1.0132 bar, at which

exhaust gas $\bar{\Phi}_{400} = 193.9$, $\bar{\Phi}_{200} = 194.0$

hence

$\bar{\Phi}_{307} = 193.95$, $\Phi_{307} = 6.7017$.

Hence

$\Delta s = 7.772 - 6.7017 - 0.287262 \ln 104/101.325 = 2.063$

to which must be added a constant representing the entropy of mixing at the reference point, namely 0.12468, so that

$s = 1.063 + 0.12468 = 1.188$

(the entropy of a single element perfect gas is zero at the reference). Note that the entropies for Gas Tables 1, 3 and 5 are close together, see $\bar{\Phi}$ values immediately above, and extrapolate to Table 3.1 using the procedure on page xvi of Gas Tables. Accordingly 0.12468 is interpolated from Table 3.10.

Calculation of the steam cycle heat intake, Table 3.9, leads to EHRB entropy growth.

The design point is 96 °C; a test value 110 °C; for not quite identical conditions.

3.7 Entropy growth in the EHRB

The entropy reduction in the EHRB gas pass is $s_2 - s_1 = \Phi_2 - \Phi_1 - R\ln(p_2/p_1)$. Gas pass is calculated using the data in Tables 3.7 and 3.8.

Table 3.8 Steam cycle data (assembled to provide input for Table 3.9)

	P	T	M	h	s	$\Delta s/sec$
HHP	83.9	515	60.93	3431.0	6.7438	91.05
HHP blowdown	83.9	298	1.32	2752.0	3.2344	0.69
LP	7.2	176	17.95	2788.4	6.7486	27.03
LP blowdown	7.2	166.1	0.18	2764.7	2.0035	0.03
De-aerator LP	9.5	105	18.13	440.8	1.3629	
De-aerator HHP	85.5	105	62.25	446.5	1.3553	
De-aerator spray	12.0	96	78.6	402.2	1.2615	22.32
Extraction pump	14.7	16	314.50	67.2	0.2390	
Total entropy growth rate = (RH column) = 141.12						

Table 3.9 Steam cycle heat intake from exhaust gas

Heat intake per EHRB
= (3431 – 446.5) 60.93 + (2752 – 446.5) 1.32 + (2788.4 – 440.8) 17.95
+ (2764.7 – 440.8)0.18 + (402.2 – 67.2)78.6
= 181 846 + 3043 + 42 139 + 418 + 26 331 = 254.0×10^6 kJ/hr
Hence:
Mass-enthalpy at stack = $(439 - 254.0)10^6 = 185.0 \times 10^6$ kJ/hr
Specific enthalpy at stack = $(185.0/511.7) \times 10^3 = 361.5$ kJ/kg
Molar enthalpy at stack = $361.5 \times 28.936 = 10\,461$ kJ/kg.mol
then
$\bar{\Phi}400 = 199.2$; $\bar{\Phi}200 = 199.0$
$T400 = 85$ °C; $T200 = 81$ °C
and by interpolation
$\bar{\Phi}307 = 199.1$; $\Phi = 6.88$; $T307 = 82$ °C = Stack temperature

$= 7.773 - 7.04 - 0.287 \ln 1.04/1.032$
$= 0.733 - 0.002$
$= 0.731$ kJ/(kg.K) Δs/sec
$= 0.731 \times 511.7/3.6$
$= 103.9$

which (see below) is less than the steam entropy increase of 141.1. The growth is 37.2 kJ(kg.K)Δs/sec per EHRB.

3.8 Irreversibility between steam and gas cycles

The mean heat intake temperature of the double pressure heat cycles is lower than the mean heat rejection temperature of the gas turbine exhaust, entailing the above calculated excess of the entropy growth of the steam over the entropy reduction of the exhaust gas. The product of the net entropy growth of the previous paragraph and the environment temperature of 283.15 °K, is the irreversibility, which can be interpreted as the additional heat rejected relative to an idealized arrangement with infinite boiler surfaces and an infinite number of steam pressures, leading to a perfect match between the gas and steam temperature profiles. The mismatch is illustrated on a Q/Carnot diagram, Fig. 3.3 which is a graph of η_c to a base of heat addition (constant pressure enthalpy rise). The area between the two η_c plots $\int(\eta_{cg} - \eta_{cs}).dQ = \int T.dS$. (See equation (2).) This way of portraying irreversibility will be of interest when the topic of process integration is discussed in Chapter 7. The gas and steam cycles

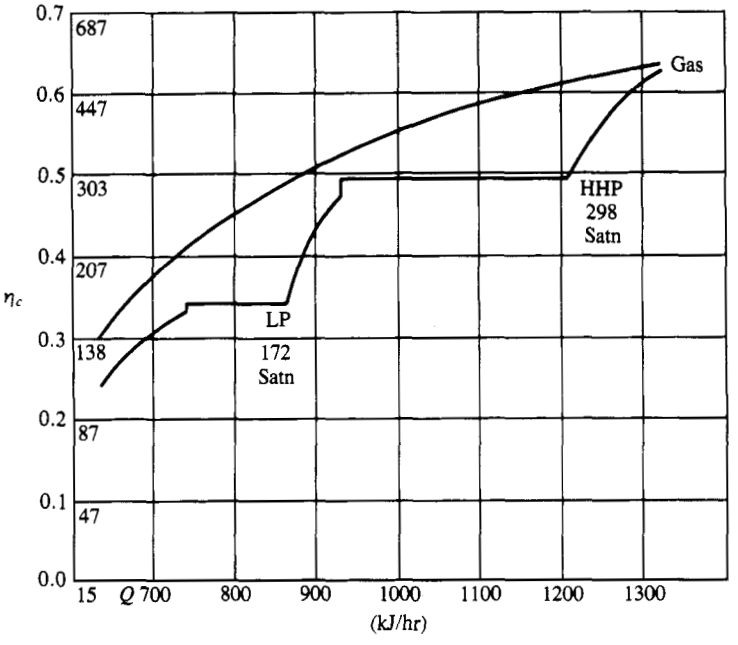

Fig 3.3 Q-Carnot diagram

are linked by a network of heat exchangers (economizers, evaporators, superheaters, or – in newer plants – reheaters). The diagram highlights the existence of four potential pinch points at which heat transfer temperature difference is approaching zero. Small design changes can make any one the actual pinch.

In Fig. 3.3 some kinks in the curves are omitted which would show the tiny LP superheater and the details of the economizers and the de-aerator, with its small steam supply. The kinks for non-steaming economizers are shown. The term 'pinch point' was used in the early 1950s in connection with the Calder Hall nuclear power double pressure plants, at Sellafield, UK.

Note that the Fig. 3.2 non-linear scale means that, at the cool end, a given temperature difference, means disproportionate loss of η_c. Irreversibility is relatively easy to incur. The losses inherent in the use of driving forces or temperature differences for heat exchange, decline swiftly in importance with increasing temperature level above ambient. For the same loading (energy flow), a relatively small high-temperature heat exchanger will destroy the same exergy as a larger low-temperature device. That is fortunate as the materials for high temperatures will tend to be more expensive. The effectiveness of cooling the blades at the hot

end of the gas turbine is not unrelated to the minimal irreversibility associated with heat transfer from combustion gas to cooling air at high temperature.

A plot of temperature, rather than η_c in Fig. 3.3, would have made it clear where the closest pinch occurs. The pinch Δt must, of course, be positive to allow heat transfer from gas to steam/water. In the EHRB, the superheater uses bare tubing in the presence of radiation, whilst other surfaces use finned tubing. The system can of course afford high Δt at high temperature, but in fact the four potential pinches are not grossly different. If, impracticably, the number of operating pressures were infinite, the steam and gas temperatures would match. There would be no pinch points. Large elaborate plants use three operating pressures, and reheat to improve the match. In even larger future plants the use of supercritical steam pressure would offer a major degree of improved matching between steam and gas. The pinch points, so prominent at subcritical pressure, are of design importance, since it is there that the designer can run out of temperature difference, or encounter a need for excessive and costly heat transfer surface. The local irreversibility is a minimum. A balance between cost and efficiency is, as usual, a requirement.

The choice of steam conditions is somewhat more restricted than when a large steam cycle without a superposed gas turbine is being considered. In the latter case there is plenty of furnace gas temperature to work with, and the designer pushes the materials available to him, so as to achieve high thermal efficiency, via high mean heat intake temperature. The mean heat intake temperature is raised by regenerative feed heating, high operating pressure (possibly supercritical), and one or two stages of reheat, all subject to achieving an exhaust wetness of not more than about 12 percent. The latter limitation survives into combined cycle design, but the gas turbine exhaust limits all else. For the operating regime under discussion the steam turbine condition line is not published, so that the line shown in Fig. 3.4 is an estimate for a status in which the condenser end has a wet flow and reduced efficiency relative to the turbine inlet.

The HHP superheat temperature is 515 °C which relates to the gas turbine outlet temperature of 540 °C. The HHP pressure of 83.9 bar is chosen to result in a reasonable exhaust moisture. The HHP saturation temperature of 298 °C is compatible with curve fitting activities on the Q/Carnot, or Q/T diagram. The superheat of the LP steam generator should be about equal to that of the corresponding bleed point on the turbine, so as to avoid a mixing irreversibility at the confluence of the two

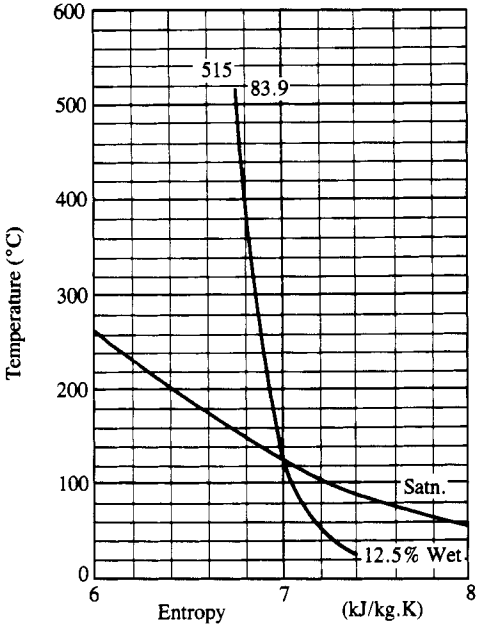

Fig 3.4 Turbine condition line – winter operation

streams. Moreover, it is pointless to degrade an excessive superheat in the de-aerator steam supply. The pre-existing processes being steamed have, of course, determined the LP steam pressure which is, however, compatible with curve matching. The use of regenerative feed heating is incompatible with curve matching at the cold end, and results in raised stack losses. However, there is every point in deoxygenating the boiler feed in what amounts to a single-stage de-aerating feed heater, with most of its heat supply from exhaust gas, but with controlled achievement of saturation temperature in the de-aerator by means of a small flow of LP steam.

The result is a winter heat recovery boiler stack temperature of 83 °C. Such a temperature is a reasonable compromise. There is little exergy in 83 °C stack gas. When fuel oil which contains sulphur is burnt in the gas turbine, the stack temperature is raised by recirculating fan to 140 °C as a defence against corrosion by acid condensate. The boiler design is based on finned tubes, which allow a close approach of gas and steam/water temperatures, and which benefit from the clean exhaust gas, notably with natural gas fuel.

Simple non-steaming economizers are selected. These result in water at less than saturation temperature entering the drum and a kink in the temperature profile.

3.9 Compressor work

The moist 'normal air' is compressed from 15 °C, 1.032 bar to 350 °C, 12.27 bar; a case for Gas Tables interpolation between dry air Table 1, and Table 3 in its 6.7 percent by mass moist air guise Table 3.10.

3.10 Temperature changes in the dual fuel combustion chamber

At the combustion chamber inlet, which is bypassed by blade cooling air and the like, the reactants – namely natural gas, deNO_X steam, mainstream compressed air, and oil burner cooling air – are mixed, with resulting entropy growth. From high initial pressure, the steam and gas

Table 3.10 Compressor parameters

Gas Tables	*Table 1 Dry air, RMM 28.9669*
$h_i = 288.38 + 0.15 \times 1 = 288.53$ kJ/kg	$\Phi_i = 5.6606 + 0.0035 \times 0.15 = 5.6611$
$h_0 = 631.49 + 0.15 \times 1.05 = 631.65$ kJ/kg	$\Phi_0 = 6.4484 + 0.0016 \times 0.15 = 6.4486$
$\Delta h = 343.13$	$\Delta\Phi = 0.7875$
Gas Tables	*Table 3 Moist air, RMM 28.9512*
$h_i = 8415.3 + 0.15 \times 29.5 = 8419.7$	
$h_i = 290.8$ kJ/kg	$\bar{\Phi}_i = 192.85 + 0.1 \times 0.15 = 192.87$
$h_0 = 18\,548.9 + 0.15 \times 31.3 = 18\,553.6$	
$h_0 = 640.85$ kJ/kg	$\bar{\Phi}_0 = 216.10 + 0.05 \times 0.15 = 216.11$
$\Delta h = 350.05$	$\Delta\Phi = (216.11 - 192.87)/28.9512$
	$= 0.8027$
Interpolating	
$\Delta h = 343.13 + 6.92 \times 0.63/6.7$ and	$\Delta\Phi = 0.7875 + 0.0152 \times 0.63/6.7$
$= 343.78$ kJ/kg	$= 0.7889$
Hence, compressor entropy growth	$= 0.7889 - R \ln 12.49/1.0132$ [$R = 0.287$]
	$= 0.7889 - 0.7209$
	$= 0.068$ kJ/kg·K
and compressor work	$= 494.2 \times 10^3 \times 343.78/3600$
	$= 48.61$ MW

This simple underestimate takes no account of cooling air bled from various stages of the compressor, nor of the small auxiliary atomizing air compressor which cools the non-operating oil burner. The flow magnitudes for these purposes are part of the manufacturer's commercial expertise and are not published. Air is also recirculated for cleaning the inlet filter.

are throttled for flow control and mixing purposes, finally reaching a relatively low partial pressure. The cool (26 °C) natural gas lowers the inlet temperature whilst the (260 °C) steam has relatively little effect. The oil burner cooling air has been compressed, then throttled and heated in the burner passages so that it heats the fuel air mixture. The fuel then ignites and the end product, after temperature rise and entropy growth, is heated combustion products, with no significant amount of unburnt fuel. This over-simplified picture masks the transient combustion chemistry, observable by spectroscopists, and the complexity involved in using compressed air to cool the combustion chamber internals and turbine inlet stages. It is, however, convenient for approximate analysis and for arriving at the adiabatic flame temperature at the combustion chamber outlet on the basis of guessing the combustion chamber by pass fraction. The result of the latter calculation has to coincide with the addition of a possible Δt of, say 150 °C, across the stage 1 fixed blading, to the design firing temperature at the entry to the first row of moving blades of 1104 °C. Such Δt increments are tried below. The complex analysis of the natural gas (Table 3.1) makes this calculation a candidate for the computer. The code GASVLE (vapour liquid equilibrium) was used due to A.P. Laughton of the Loughborough Research Station, of British Gas plc. The code calculates thermodynamic properties from equations of state of mixture components, such as methane or steam, and entropy growths due to mixing in any proportions. It also calculates thermodynamic changes due to combustion in the presence of excess air and steam. The code has a reference point of 25 °C, 1.0132 bar, for an unmixed gas.

3.11 Summary of computer calculation (Tables 3.11–3.15)

Data

Air H_2O 0.63 N_2 76.3 O_2 23.06 Molecular Wt 28.738 Flow 493.1 T_i 15 P_i 1.0132 T_o 346.5 P_o 12.49 Fuel as Table 3.1.

The loop calculation from point 6 to point 19 iterates to a chosen outlet temperature of 1250 °C, at the edge of current technology, and calculates a combustion chamber throughput of 76.693 percent to allow for disc, blade, and bearing cooling, the flow magnitudes for which are unstated commercial expertise. If the guessed 1250 °C is too high, the throughput increases. At a more conservative 1213 °C, the throughput is 80.577 percent, and the data are as shown in Table 3.14.

Table 3.11 Compressor calculation Inlet 1, outlet 2 Thermodynamic reference 1 bar 25 °C

Pt	*Calc.*	*Temp (C)*	*Pressure (Bar)*	*Total-H (MJ)*	*Entropy (MJ/Mg)*	*Total-S (MJ/C)*	*Entropy (MJ/Mg·C)*
1	SPHS	15.00	1.0132	−5130.4	−10.404	60.393	0.12248
2	SPHS	346.5	12.49	0.16461E+0.63	33.83	94.864	0.19238

Power = 47 151 kW; Efficiency = 0.8782 (simple underestimate ignoring bled air)

Table 3.12 Mix DeNO$_x$ steam and fuel

FLOW 7.166 Mg FLSH T = 260 P = 22 STEAM

Pt	*Calc.*	*Temp (C)*	*Pressure (bar)*	*Total-H (MJ)*	*Enthalpy (MJ/Mg)*	*Total-S (MJ/C)*	*Entropy (MJ/Mg·C)*
3	SPHS	260	22.0	2643.3	368.87	−2.3415	−32675

UNIT MOL COMP FUEL

H_{20} N_2 O_2 CO_2 C1 C2 C3 NC4 IC4 NC5 IC5 C6 C7

0 7.81 0.0 0.59 85.26 4.4 31.0 4.3 7.1 8.1 4.0 7.0 8.025
(analysis ignores argon)

FLOW Mg 10.72 FLSH T = 26.7 P = 21 FUEL

4	SPHS	26.70	21.0	−181.970	−16.974	−12.1140	−1.1300

USE 3 4 ISHPH = H3 + H4 P = P2
Feed Composition of point 3 used
Composition of point 4 used STEAM AND FUEL

5	VLE	148.5	12.49	2461.3	137.61	−4.075	−0.22783

Table 3.13 Add combustion air

USE 5 2*%1 ISHP H = H5 + H2*%1 P = P5 !MIX STEAM FUEL-AIR = Reactants

20	SPSH	312.66	12.49	0.22871E+06	324.97	97.130	0.24524	!MIX
21	SPHS	1249.96	12.49	0.58956E+06	1488.6	564.82	1.4261	!BURN

When, in an alternative calculation, the computer was told that the throughput was 91.8 percent the data shown in Table 3.15 appeared. This temperature (1106.22) is too close to the firing temperature of 1104 °C. Tables 3.13, 3.14 and 3.15, are a means of interpolation. Each of the three

Table 3.14

USE 5 2*%1 ISHP H = H5 + H2*%1 P = P5 !MIX STEAM FUEL-AIR = Reactants								
10	SPHS	324.27	12.49	0.20993E + 06	323.5	85.297	0.25101	!MIX
11	SPHS	1213.67	12.49	0.59596E + 06	1435.3	575.80	1.3868	!BURN

Table 3.15

Use 5 2*% 1 ISHP H = H5 + H2*%1 P = P5 !MIX STEAM FUEL-AIR = Reactants								
6	SPHS	327.61	12.49	0.15352E + 06	326.52	111.07	0.23624	!MIX
7	SPHS	1106.22	12.49	0.60148E + 06	1279.3	594.27	1.264	!BURN

puts the same amount of fuel into the same total stream (turbine exhaust flow), but the hottest (Table 3.13) will give the greatest turbine output. It is clear that the entry of cooling streams into the main turbine flow will reduce the specific entropy and steepen the condition line, whilst the mass entropy must increase. Moreover, the exhaust conditions in Table 3.7 must be reached. With so many unknowns (compressor and turbine power and airflows for filter cleaning and for turbine cooling) the judgement has to be made that the combustion chamber outlet temperature is in the region of 1200–1250 °C, dictating a temperature drop of 96–146 °C across the heavily cooled inlet fixed stage nozzles. These figures are adequate for the arguments conducted in this book.

3.12 Heat cycle distortion

The business of extracting gas or steam from the combined heat cycle generates losses. The carefully arranged heat cycle is distorted, and loses efficiency. Where an engine exhaust is both hot and unutilized, exergy is being needlessly thrown away. Utilization of the exhaust results in an efficiency gain, as indeed has occurred at Sellafield. However, an engine with an unutilized exhaust is not a carefully contrived heat cycle; rather it is likely to be a machine adapted to economic circumstances dictating simplicity and minimum capital cost arising from low load factor, adverse operating conditions, and the like. The opportunity to use the exhaust exergy is, for good economic reason, ignored.

Accordingly, if a plant such as Sellafield is to be designed to produce

power and process steam, the thermodynamic sense of proportion is that the extractions of steam (and gas) should not be excessive, as perhaps they were in the 1960s power and desalination plant described earlier. The plant should be producing generous amounts of electricity. The thermodynamics of the processes and their economics, together with the same features of the associated internal and public utility electricity networks, are important additional variables. The notion, which influenced the design of the Chapter 2 power and desalination plant, must be eschewed: that the avoidance of heat rejection to the condenser, by bypassing it with a (heat rejecting) process, is a vital objective. Indeed isothermal heat rejection to the environment is the basis of many reversible thermodynamic concepts, which are by definition devoid of losses (no net entropy growth).

At Sellafield the processes are of the throwaway variety: building heating and the movement of radioactive liquids by ejector pumps; processes with an economic return but no thermodynamic return, for example in the form of chemical exergy of the product. A classic throwaway process is a machine shop which shapes artifacts using motive power. The return is commercial, and non-thermodynamic.

3.13 Entropy balance for Sellafield CHP

In Table 3.16 as each of the engine processes occurs, an entropy growth takes place: in the compressor, in mixing the reactants, in burning the reactants, in the turbine, and between the exhaust gas and the steam generator. Finally there is a mixing loss when the warm stack gas encounters the atmosphere, and is infinitely diluted by the air, effectively closing the so-called 'open cycle'. The entropy growths multiplied by the environment temperature, represent heat rejected or chemical/thermo-mechanical exergy destroyed. The exergy destruction mechanisms include temperature degradation, friction and turbulence, mixing of flows of different analyses, and entropy growth during combustion.

3.14 Stack loss calculation

The stack loss calculation cannot be handled as an entropy growth since dilution with an infinite amount of air is involved. It is, however, possible to calculate the loss of thermomechanical exergy. Moreover, the loss of chemical exergy is small, since the analyses of exhaust gas with 307 percent theoretical air and of atmospheric air are little different, and their entropies much the same.

Table 3.16 Entropy balance, with 1250 °C combustion. Basis: one gas turbine of three

Process	*Entropy growth*	*Reference*
Compression	34.471	Table 3.9
Mix steam/fuel	10.385	Table 3.10
Mist steam/fuel/0.76693 air	20.205	Table 3.11
Burn steam/fuel/0.76693 air	466.690	Table 3.12
Expand products + cooling air compression blade cooling	37.20	Table 3.7
EHRB heat transfer		
Steam turbine, HP to bleed 1	3.659	Figs 11, 12, 13; Table 3.7
Bleed 1 (denox) to LP inlet	0.300	Table 3.7
LP inlet to exhaust	1.960	Steam Tables
Stack	8.58	Section 3.14

ξ_T stack
$= h - h_o - t_o(s - s_o)$
$= 415.3 - 291.9 - 288.15(7.040 - 6.664) - 0.287 \ln (1.04/1.0132)$
$= 123.4 - 288.15(0.376 - 0.0075)$
$= 17.4$

$M\xi_T$stack
$= 511.7 \times 17.4/3.6$
$= 2473.3$

Dividing by 288.15 to get a number for Table 3.17 gives 8.58. Note that the same sense of proportion could have been obtained by multiplying the entropy growths in Table 3.16 by 288.15 to convert them into exergy destructions.

As in all heat engines the major loss occurs when the fuel is oxidized at an achievable temperature. For the future, the designers are discussing combustion chamber outlet temperatures (turbine entry temperatures) of up to 1600 °C, allied to much higher compression ratios, so as to minimize this and other losses. The losses involved in mixing enable complete combustion to be obtained compactly and are, therefore, paid for or economically justified.

Turbine and compressor blading are highly developed. Some weight saving and compactness, but not reduced losses, may be achieved using hypersonic gas speeds.

The degradation in heat transfer between gas and steam in the EHRB is comparable to the compressor losses and much more important than the stack loss. It may be that a more complex EHRB with three pressures would have been justified.

Very much more detail would be possible in the entropy balance in which for example the condenser irreversibility has been omitted, having already been calculated in the Chapter 1 power and desalination plants. The turbine exhaust and the condenser involve a series of events, each with its own losses. The exhaust hood operates as a limited diffuser able to slow down the exhaust steam and recover some kinetic energy. The steam, however, needs some velocity for effective heat transfer in the presence of air films which can build up at condenser tube surfaces, dependent on the air in-leakage quantity. After temperature degradation in the air film, the tube metal and the cooling water boundary layer, the bulk of the cooling water is warmed. Then the water is discharged and degraded to inlet temperature and its pump derived kinetic energy dispersed. Given the detailed data, all this could be portrayed, and put in perspective.

The main thrust of the argument, however, is that the sense of proportion derived from exergy analysis is not the same as for energy considerations, albeit the latter underlies the former. For example the stack loss is relatively small in exergy analysis. Both perspectives cannot be correct!

3.15 The auxiliary boiler

The flow sheet of the auxiliary boiler is shown in Fig. 3.5. The boiler needs to be adjusted, depending on whether gas or oil is used. For oil burning the stack temperature is controlled above the dew point using the feed preheater in the drum. The modest spray controlled superheat required is achieved by screening the superheater from radiation and rapid convection using an appropriately arranged natural convection surface. The boiler technical data are given in the three part Table 3.17 (gas firing).

The auxiliary boiler, in the winter flow sheet, provides the supply of HP process steam. One alternative route, namely throttling of HHP steam, is unavailable, since the steam turbine is required to provide maximum electrical output, and needs all the HHP steam. EHRB supplementary firing is also available, but not used on the winter flow sheet under analysis.

From a first law point of view, the natural convection unit is efficient and well adapted to its seasonal duty. The gas tight combustion chamber

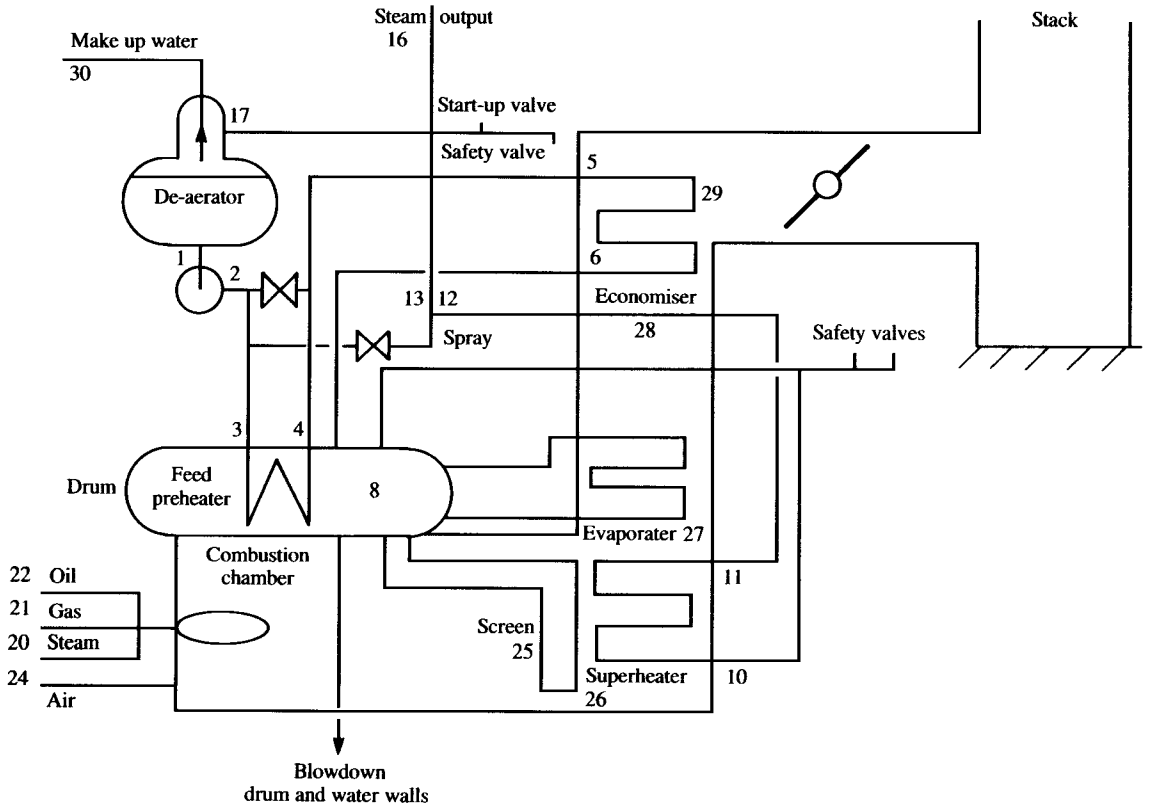

Fig 3.5 Auxiliary boiler – Sellafield CHP

Table 3.17

Feed data

Point	*Units*	*30*	*17*	*1*	*2*	*5*	*6*	*8*
Flow	kg/sec	22.3	3.8	26	26	25	25	–
Pressure	bar g	3	14	0.5	22.1	16.8	16.4	16.3
Temp.	°C	5	312	110	110	110	199	205
Density	kg/m^3	1000	5.9	950.7	951.7	951.5	875.7	858.6
Enthalpy	kJ/kg	21.4	3064.3	462.5	462.5	462.5	866.0	875.7
		Make-up	D/A Stm	Feed	Feed	Econ in	Econ out	Drum

Steam data

Point	*Units*	*10*	*11*	*12*	*13*	*16*
Flow	kg/sec	25.0	25.0	25.0	26.0	22.2
Pressure	bar g	16.2	15.2	15	14	13.2
Temp.	°C	205	365	365	312	312
Density	kg/m^3	8.6	5.6	5.6	6.0	5.6
Enthalpy	kJ/kg	2793.4	3179.4	3179.4	3064.3	3064.3
		Sprhtr in	Sprhtr out	Desup in	Desup out	Main steam

Natural gas fuel, air and flue gas data

Units	*21*	*23*	*24*	*25*	*26*	*27*	*28*	*29*
kg/sec	1.72	26.8	13.4	28.5	28.5	28.5	28.5	28.5
bar g	7.5	0.0 m	28 m	10.6 m	10.4 m	9.2 m	7.8 m	4.4 m
°C	–	15	15	1249	1184	922	476	187
kg/nm^3	–	1.2877	1.2877	1.2436	1.2436	1.2436	1.2436	1.2436
kJ/kg	43 000	15.2	1574.8	1404.5	1123.6	548.5	208.4	
	Fuel	Amb. air	Pri. air	Comb out	Sprhtr in	Evap in	Econ in	Stack

gives zero air leakage with minimum fan power consumption; whilst the stack temperature and energy losses are controlled at a prudent minimum.

From a second law point of view, the low pressure and temperature at which the steam is generated, means that the exergy supply to processes is small, after much degradation. The chemical exergy (work potential) of the fuel is part destroyed, by burning the fuel and releasing its enthalpy of combustion as the energy of a hot gas. The latter is subject to Carnot's limitation, so around half of the fuel exergy has gone. The temperature of the combustion gas is then degraded down to steam/water mean heat intake temperature, with further loss of exergy. Then the process steam has to be adapted to a multiplicity of uses, involving throttling and desuperheating. Alternatives to these time honoured practical processes are in the up-and-coming category. In a subsequent chapter the generation of steam for a distillery, using an electrically driven steam heat pump is discussed. In another chapter, the direct oxidation of fuel in a fuel cell is described. Avoiding Carnot's limitation, the fuel cell, without internal moving parts, produces combined power and heat. Both of these new technologies encounter heavy irreversibilities, which represent significant development problems, and competitive handicaps.

3.16 Efficiency at Sellafield CHP

The first law efficiency of a power plant is the ratio of its power output, in Joules, to its input in net combustion enthalpy in Joules. The second law efficiency is the ratio of its output in Watts of motive power to its input in chemical exergy in Watts. The first law values the process steam as a heat source, rather than a work source. The second law values the process steam according to its thermomechanical exergy.

In paragraph 3.3 the natural gas chemical exergy is guessed as 68 557 kWs/kg. Disregarding momentarily the process steam, the two efficiencies have the same numerical value. Note, however, that only the second law efficiency is a genuine dimensionless ratio (work/work). The first law efficiency is in fact (work/heat). The *raison d'etre* of exergy analysis is to reiterate the distinction between work and heat (energy flow).

The introduction of the process steam is a crunch point, because the steam enthalpy is a much larger number than the thermomechanical exergy. Moreover, the energy is conserved in a process, whereas the exergy is destroyed or partially destroyed.

Both efficiencies regard the engine and associated processes as black boxes. But the exergy method offers break down of losses, as an additional virtue. Note, however, that if the losses are known at the design point, they are not pro rata elsewhere. The losses vary unevenly and their relationships are called structural bonds. The structural bonds are the basis of optimization studies.

Efficiency calculations for conditions of Fig. 3.2 – Winter conditions.

Gas turbine fuel = 10.72 Te/hr = 2.98 kg/sec × 3
Net enthalpy of combustion = 42 989 kJ/kg; $M\Delta h$ = 384.3 MJ/sec
Chemical exergy of fuel = 68 557 = 44 709 kWs/kg; $M\xi_c$ = 604.3 mW
Electrical output = 38.4 × 3 + 30.2 = 145.4 MW
Process steam; LP 172 Te/hr, p 6.0 bar, t 193 °C,
$\xi_t = h - h_o - t_o(s - s_o) = 2834.7 - 63 - 288(6.9335 - 0.2202)$
= 838.3 kWs/kg; $M\xi_t$ = 40.05 MW
Process steam: HP 78 Te/hr, p 13.2 bar, t 310 °C (from Auxiliary Boiler).
$\xi_t = 3064.3 - 63 - 288(7.0250 - 0.2202) = 1041.5$ kWs/kg;
$M\xi_t$ = 22.57 MW
Auxiliary boiler fuel = 1.72 kg/sec = 6.19 Te/hr
$M\Delta h$ = 73.94 MJ/sec and $M\xi_c$ = 117.9 MW
Auxiliary boiler second law efficiency = 22.57/117.9 = 19.14 percent
Gas/Steam Turbine/EHRB 2nd Law Efficiency
= (145.4 + 40.05)/604.3 = 30.69 percent
Overall second law efficiency = (145.4 + 40.05 + 22.57)/(604.3 + 76.9)
= 30.53 percent

There is no way of reconciling the 19.14 percent second law efficiency of the auxiliary boiler with a first law efficiency in the high nineties. The second law takes into account energy degradation/exergy destruction, but the first law does not.

Since the overall efficiency contains the second law boiler efficiency, it too is irreconcilable.

In the next chapter on equilibrium isothermal oxidation, the nature of the chemical exergy of the fuel is elaborated, on the new basis used above.

Chapter 4

Fuel and Equilibrium Fuel Cells

'For in and out, above, about, below,
'Tis nothing but a magic shadow show,
Play'd in a box, whose candle is the Sun,
Round which we Phantom Figures come and go.'
Omar Khayyam

4.1 The near equilibrium photosynthesis of fuel

A non-equilibrium, spontaneous chemical reaction, such as a fire, requires a minimum of apparatus. Fuel and air must be brought together and ignited, for example trees, air, and lightning (local high temperature). The combustion reaction is characterized by $\Delta_c H$, the enthalpy of combustion, and an irreversible entropy growth, following annihilation of Gibbs's potential to leave only Carnot limited energy.

A near-equilibrium, observably isothermal chemical reaction with elaborate apparatus is photosynthesis. This is usually illustrated by the overall equation for the formation of glucose (**37**). Reference (**37**) contains no thermodynamics, and those below are by the author using (**39**).

$$6H_2O(-237.1/69.9) + 6CO_2(-386/117.6) = C_6H_{12}O_6(-910/2\,12) + 6O_2(0/205.1) \quad (1)$$

The characterizing numbers in brackets are the Gibbs work potential and entropy of formation, $(\Delta_f G\,^\circ/S_f)$, at standard conditions.

Work is well conserved, and the endothermic, isothermal enthalpy of reaction $\Delta_r H$ is irrelevant. Isothermal energy at ambient temperature is of zero Carnot efficiency and can do zero work. Bonds, which are at base a matter of forces between electrons and between electrons and atoms, can be reorganized, but only in a work interaction.

From Equation (1), the work absorbed by the endergonic reaction per mol of glucose $\Delta_r G$ °, is + 2828.2 kWs.mol^{-1}. The reversible entropy reduction $\Delta_r S_{rev}$ is + 317.7 JK^{-1} mol^{-1}; and $\Delta_r Q$ is the reversible heat of reaction + 94.7 kJ mol^{-1}. The two-stage dark/light (endothermic and exergonic) reaction, catalysed in the dark (**37**) by enzyme 'rubisco' and in the light by chlorophyll, fixes CO_2, then takes in work from resonant photons and absorbs heat, $T_o\Delta_r S$, from the environment. Work transforms the simple chemical bonds of H_20 and CO_2, into the complex of glucose, with an accompanying reversible entropy change. Via a small temperature difference, and involving limited irreversibility, heats of reaction and of evaporation are absorbed from the air and from scattered light through the leaf membranes, into the numerous chloroplasts within the leaf. These are the tiny double-membrane-surrounded isothermal enclosures, or Van't Hoff Boxes, containing solid chlorophyll catalyst in which the chemical reaction is organized. Separate mechanisms for work and heat are an essential feature of all equilibrium reactions (**38**). The zero current equilibrium fuel cell conforms to that description; the practical current generating fuel cell less so since there is limited loss of work. Like photosynthesis, the practical fuel cell is a reaction with a significant forward rate, involving some loss of Gibb's potential via irreversibility, but not total destruction as in fire.

Since a dissolved solid product is formed in a product biased equilibrium, photosynthesis exhibits a volume reduction. Carbon dioxide, and oppositely oxygen, diffuse into and from the reaction via the leaf stomata (automatic control valves), gas interspaces, and chloroplast wall membranes. Water enters the root hairs propelled by osmotic pressure (water molecule concentration difference; dilute ground water relative to concentrated sap). The root water is pulled up to the chloroplasts in fine filaments, via its tensile strength and by the volume reduction. The difference in mechanical properties between bulk liquid and interfacial liquid is involved, as experienced by pond-surface-skating insects. Interfacial liquid has its protons turned relative to the interface. Note that, because of their contents, the chloroplasts are robust against collapse but not against internal pressure. Indeed there are specialized stomata, which discharge to prevent sap over-pressure. In all equilibrium reactions, the reactants and products have to be conveyed to and from the environment, or from storage, to the reaction enclosure. This is done by circulators and is aided by perm-selective membranes. These separate the desired substance either from both the environmental or reaction space mixture. Osmotic pressure and of significantly more importance, volume reduction comprise the water circulator for photosynthesis. Diffusion in a

concentration gradient – at stomata and at chloroplast wall membranes – circulates the gases. These are partly-irreversible, work-consuming, exergy-converting processes.

DNA-controlled plant growth is based on the formation of kindred sugars, lipids, proteins, and other molecules such as starch, catalyst chlorophyll, and structural cellulose. The plant structure enlarges to support more leaves and hence more chloroplasts: this generates further seasonal growth.

In making its own structural materials in a near equilibrium reaction, nature makes herself immune to the criticism levelled on a first law basis at industrial systems, that their manufacture is disproportionately fuel consuming.

All the fuel or food that has ever been, or will be, oxidized, is derived in this near-equilibrium reaction from solar radiation exergy. The latter exergy, which 'disappears' into chemical bonds, would otherwise have become heat. Hence the vegetation has a cooling effect pro rata to its rate of growth. Evaporation of sap, to produce water vapour transpiration through the stomata, provides a further cooling effect.

In non-equilibrium reaction chemistry, the equation $\Delta G = \Delta(H - TS)$ is consistent because all work potential has been annihilated and all quantities are energy packets. In equilibrium chemistry all terms can be allocated work units (the $T\Delta S$ term is of zero work content at ambient temperature, but not at other temperatures). The latter sentence is, with some expansion, important in fuel cell technology. The fuel cell produces electrical work, reversible heat, and irreversible losses (heat). At high temperatures the reaction heat has a useable thermomechanical exergy content, which is useable to drive heat engines or circulators, or chemical reactions such as the reforming of natural gas for hydrogen production.

Fuel cells are now introduced using second law analysis and separating work from heat. The SI unfortunately allocates the same units to both processes. In an ambient temperature cell, all the work is done by the electrochemical reaction. Outside the cell, circulators supply the reactants and remove the product. In the equilibrium cells calculated below, the circulators generate power.

4.2 Equilibrium fuel cells

Figure 4.1 is the flowsheet of an equilibrium Bacon fuel cell. The Bacon cell is replaceable by the equilibrium alternatives of Fig. 4.1(a) which have cell-specific half reactions, but the same overall reaction of hydrogen oxidation. Catalysts are irrelevant to equilibrium.

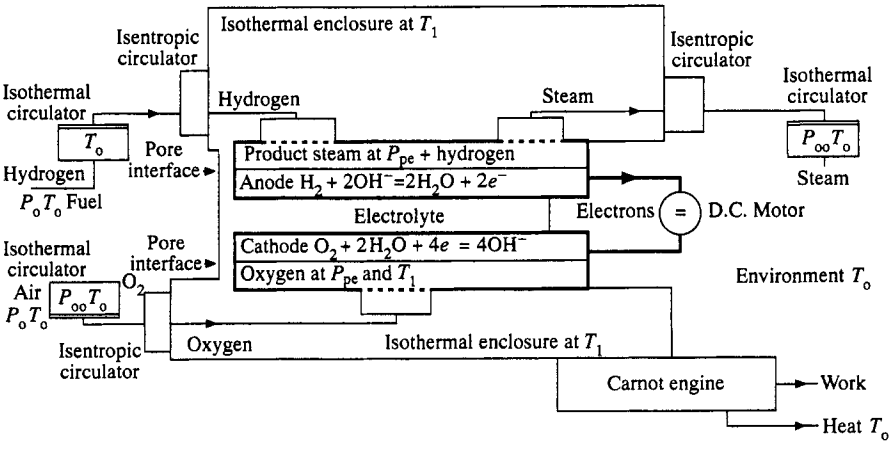

Notes

1 The isothermal and isentropic circulators relate cell to environment.
2 The Carnot engine exploits the thermo-mechanical exergy of the isothermal enclosure.
3 The oxygen, steam and hydrogen are at equilibrium concentrations, or equilibrium partial pressures determined by the equilibrium constants both of the electrode half reactions and of the overall cell reaction. Because steam is very imperfect, fugacity-based equilibrium constants must be used, from the JANAF thermochemical tables, reference (**39**).
4 Dotted lines are perm-selective membranes.
5 Half reactions involving CO_3^- or O_2^- are the basis of high temperature MCFC and SOFC.

Fig 4.1 Equilibrium fuel cell for any pressure and temperature

For an equilibrium fuel cell to operate at any isothermal enclosure pressure and temperature specified by its designer, ancillary equipment is required, Fig. 4.1. A pair of circulators is in series: isothermal followed by isentropic for reactants; isentropic followed by isothermal for products. Perm-selective membranes at both ends of a circulator pair keep one gas only in the circulator pair by preventing access to the pair from the reaction mixture, or the environment mixture, by any other than the selected gas. A circulator pair picks up oxygen from the atmosphere at partial pressure, P_{oo}, via a perm-selective membrane. A second circulator pair picks up manufactured hydrogen fuel by convention at environmental temperature and pressure. A third circulator pair discharges product steam to the environment via perm-selective membranes at standard partial pressure, P_{oo}, corresponding to 40 percent relative humidity. That arrangement allows environment cooling of isothermal circulators at T_o, with zero exergy flow. For an ambient temperature fuel cell, the isentropic circulators are redundant. Experience with such diagrams indicates that it is best not to characterize particular machines as compressors or expanders until the unique set of equilibrium concentrations in the

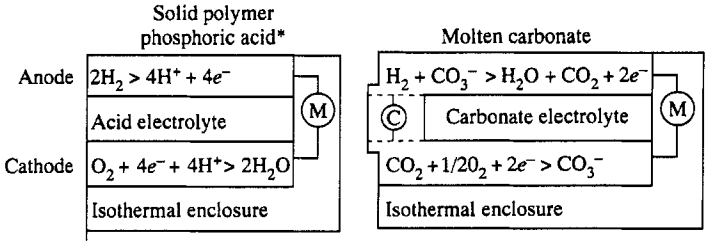

A carbon dioxide recirculator C and membranes are required for the MCFC.

* The mobility of hydrogen ions or protons in aqueous media involves proton exchange between water molecules via the formation of H_3O+, the Hydrated Proton. Hence proton exchange membrane, ref. (**42**) p. 840.

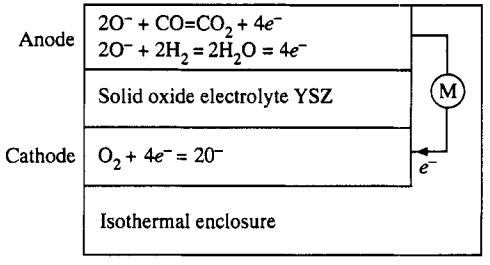

Notes
YSZ is yttrium-stabilized zirconium oxide operating at 1000°C.

When negative ions are involved the products appear at the anode, and vice-versa.

SOFC

Fig 4.1 (a) Alternative fuel cells for Fig. 4.1

isothermal enclosure are calculated. Control of the circulator speeds gives stoichiometric flows. Appropriate circulator pressure ratios, taking account of the selected total pressure and temperature in the isothermal enclosure, provide equilibrium concentrations (partial pressures/ fugacities) therein. The calculation of equilibrium concentrations along the lines of (**38**) or (**42**) is best done using (**39**) which, for highly imperfect steam, tabulates fugacity-based equilibrium constants. Appendix 1 shows the equilibrium reactant concentrations for hydrogen or carbon monoxide oxidation are very low, and product concentrations very high. Circulator pressure ratios are very high, and are impossible for existing machines. Some practical low-temperature SPFC cells can vigorously absorb their own air supply. The chemical reaction is trying to approach equilibrium and a low oxygen concentration, and so provides the required driving force. The product water must somehow disperse to the air. If the selected fuel is carbon monoxide then: pressure = fugacity. The CO ideal gas equilibrium constant is independent of pressure. The hydrogen equilibrium constant is independent of fugacity, which means that the constant and the E_n are functions of pressure. The fuel cell in the

isothermal enclosure of Fig. 4.1, produces an electrical output $-\Delta_r G_t$, which is a function of temperature, but not of fugacity, at equilibrium.

The isothermal enclosure is maintained at its specified temperature by energy interchange with a Carnot engine, of output $-\Delta Ct$, coupled to the environment. For some chemical reactions, a Carnot heat pump is needed, depending on the sign of the reversible entropy change.

At each perm-selective membrane, the concentration of the selected gas on either side of the membrane is the same. Inside the isothermal enclosure, the cathode concentration of oxygen is steady and in equilibrium with the steady fuel and product concentrations in the anode space. There are no irreversible mixing processes.

The combined work (**43**) of the chemical reaction, $-\Delta_r G_t - \Delta Ct$, and the associated reversible entropy change are fixtures. As the gas concentrations in the isothermal enclosure are changed with pressure and temperature, the net circulator power changes. Appendix A looks into numerical aspects of selected operating pressures and temperatures, and the numbers must be seen to comply with the above principles. Advantages claimed for particular practical operating conditions may have their origins in equilibrium theory, or in the theory of irreversible kinetic processes associated with significant reaction rate, for example overvoltages. As irreversibilities and imperfections are introduced, the presentation complicates. For example, an air-breathing cell must expend power on the movement of nitrogen and must discard unused oxygen. A practical fuel cell passes its reformate fuel mixture (hydrogen/steam/carbon monoxide) along the anode surface to an exhaust, which must contain some unburnt fuel. The flowsheet of a practical cell precludes operation at precise equilibrium conditions. An equilibrium fuel cell, controlled by its circulators, is slowed down to an increment away from zero reaction rate and zero current, at which condition it has equilibrium concentrations of reactants and products in the reaction mixture. The practical fuel cell can be open circuited to reduce its current to zero, for the purpose of measuring its emf which is not quite E_n. Control of the anode/cathode gas concentrations to the equilibria of Fig. 4.1 is not achievable, and this is a necessary condition to obtain E_n, which occurs when the equilibrium cell is adjusted to zero current and then open circuited. Additional emfs will exist, dependent on the concentration differences between the practical situation and Fig. 4.1. Exchange currents, (**42**), at the idle electrodes are functions of the surface gas concentrations.

In the practical cell, hydrogen and oxygen concentration gradients along the electrodes lead to voltage gradients and loss-generating, parasitic currents. At 1300K steam dissociates slightly. The resulting low background of oxygen at the anode is not shown in Fig. 4.1(a).

4.3 Hydrogen manufacture from natural gas

The principal source of hydrogen for fuel cell operation is steam reforming of natural gas. A typical sweet natural gas volumetric analysis from Chapter 3 is

methane (CH_4) 85.26 percent
ethane (C_2H_6) 4.43 percent
n-butane (C_4H_{10}) 0.37 percent
i-butane (C_4H_{10}) 0.18 percent
n-pentane (C_5H_{12}) 0.14 percent
i-pentane (C_5H_{12}) 0.07 percent
C_6 hydrocarbons 0.08 percent
C_7 hydrocarbons 0.025 percent
carbon dioxide CO_2 0.59 percent
water H_2O 10–50 ppm
nitrogen N_2 7.81 percent
others 0.005 percent

Ideally, fuel cells should be able to oxydize natural gas hydrocarbons C_aH_b directly (notably methane (**43**)). At present, however, they can deal only with hydrogen and, in some cases, carbon monoxide. Low temperature fuel cell protagonists have been driven to use a fired reformer, and shift reactor, to make hydrogen. An existing industrial natural gas and waste gas fired process that steam reforms natural gas and finally separates the hydrogen by pressure swing adsorption, is described in Chapter 6. Some proprietary fuel cells are complemented by modern and compact versions of the latter process, without hydrogen separation. For compactness, catalytic combustion may be used. Recently, better thermodynamic performance has been achieved (MCFC, SOFC) where the fuel cell anode reversible heat output is suitable for driving a reform reaction, and with greatly reduced pollution (no fire), Chapter 6.

A process which started with large, exergy-rich, photosynthesized molecules, degraded by storage to natural gas, ends with hydrogen. Much of the sun's exergy has been lost! There is much to understand about nature's example in conserving large exergy-rich molecules: optimum use of the sun.

The production of hydrogen using non-equilibrium processes, notably reform/shift at the cell anode, can, for an efficiency calculation, be compared with a hypothetical equilibrium process, Fig. 4.2. In the practical reform process, fuel gas, steam, and carbon monoxide are

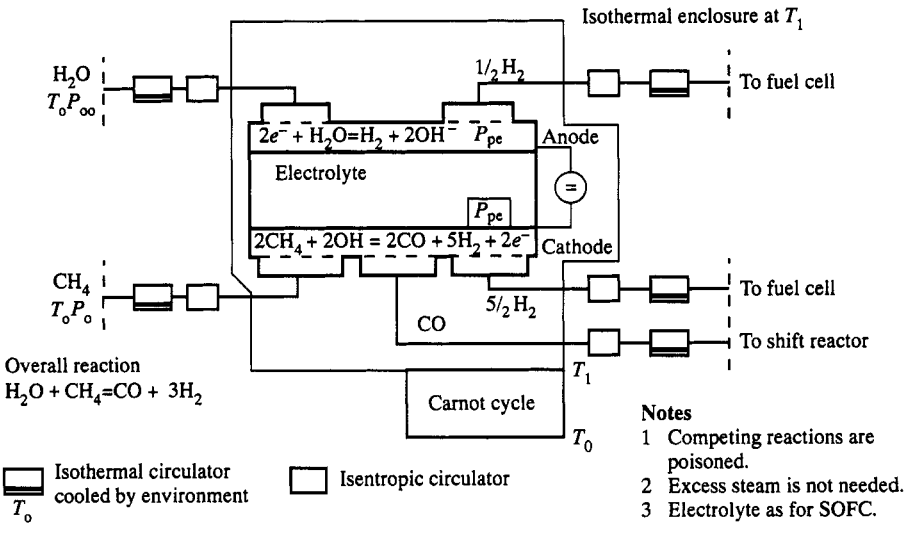

Fig 4.2 Hypothetical methane equilibrium reformer

reacting at the anode; hydrogen and some CO are oxidized by the cell; the shift reaction takes up most of the CO; steam, CO_2, and unused fuel and depleted air are exhausted.

Figure 4.2 applies to the major component of the mixture, methane. A full analysis of the problem would entail separating the oxidizable components of natural gas, and passing them to separate reformers along the lines of Fig. 4.2. This exploratory chapter will pursue the argument for methane only. Moreover, sweet natural gas has been chosen to avoid discussion of desulphurization.

Figure 4.2 proposes an equilibrium isothermal reform of methane using fuel cell technology. The ancillary apparatus enables the process to be carried out at any pressure/fugacity and temperature. The perm-selective membranes at inlet and outlet of each circulator pair are shown. There is circulator work, electrical work, and Carnot cycle work, as in Fig. 4.1. Signs for the work packets need to be established from the thermodynamic data. Integration of Fig. 4.1 with Fig. 4.2 via the circulators is considered later. The steam supply for the reformer and for the shift reactor, will come from the fuel cell (see Appendix B). The equilibrium shift reaction must enter the discussion. There will be no irreversibilities, but chemical exergy may move to and from reacting molecules.

At this point in the argument, a minor dilemma appears. The carbon monoxide could go to a shift reactor, or it could go to a separate fuel cell,

with MCFC or SOFC capability to oxidize CO. The theoretical emf of CO is not quite the same as that of H_2. Accordingly the two fuels cannot be consumed in an equilibrium process in one cell. The selected fuel cell path (Appendix A) is the ideal for comparison with SOFC/MCFC. In the practical electrode reform process, the CO shift reaction dominates CO oxidation (**43**) and that must be seen as a minor adverse feature. The equilibrium shift reaction path is relevant to those low temperature fuel cells unable to support electrode reform, and which may be sensitive to catalyst poisoning by CO.

4.4 The equilibrium shift reaction

Figure 4.3 features circulator pairs isolated by perm-selective membrane, with the isothermal machines cooled by the T_0 environment. The reactants and products are conveyed reversibly to the isothermal enclosure of the reaction, at T_1, the latter temperature maintained by a Carnot cycle. In such an equilibrium process, the circulators, and the Carnot cycle, can be arranged to produce any conditions of operation. These must be matched by the appropriate equilibrium ratios of reactants and products in the isothermal enclosure (**38**), (**42**). In practice the choice of electrode/electrolyte pairs is rather limited and, for theoretical convenience, mythical materials superbium/idyllium are introduced in Fig. 4.3, to allow flexibility of operating conditions.

Equation (2) shows the exergonic equilibrium shift reaction at standard conditions

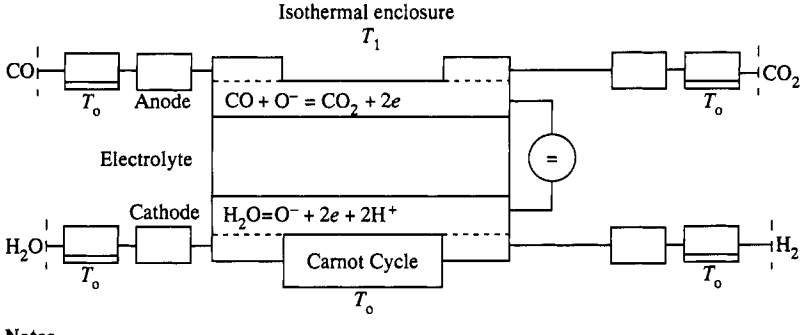

Notes

1 Circulator pair; isothermal followed by isentropic
2 Electrolyte is idyllium; electrodes superbium
An idealized reversible loss free pair.
3 Perm-selective membranes at inlets and outlets of circulator pairs.
4 Overall reaction $CO + H_2O=CO_2 + H_2$.

Fig 4.3 Equilibrium shift reactor

$$CO(-137.17,197.67) + H_2O_G(-228.57,188.53)$$
$$= CO_2(-394.36,213.74) + H_2(0,130.7)$$
$$H_2O_L(-237.13, 69.91)$$
$$\Delta G = -28.52\ \Delta S = -31.76_G$$
$$\Delta G = -20.06\ \Delta S = +76.86_L \qquad (2)$$

The reaction does work (is exergonic) regardless of whether the water is taken in as liquid or gas. The choice exists because water at standard conditions is a liquid with an accompanying vapour pressure. Gaseous conditions would be selected both for an equilibrium example and, in practice, by operation at 500/600 K. Thermodynamic data for the reaction are available by combining pages 626 and 1275–9 of (**39**).

The forward outlook is to calculation of alternative equilibrium systems involving reform, shift, fuel cell (low temperature fuel cells), or reform, hydrogen fuel cell/carbon monoxide fuel cell (SOFC/MCFC). Only the SOFC/MCFC path is studied in this chapter. The initial and final circulators of the path will be coupled to the environment/fuel at standard conditions. The circulators coupling the three reaction systems will change gases from one set of equilibrium conditions to the next. In other words, the processes will be integrated.

4.5 Hydrogen and carbon monoxide production integrated with fuel cell operation

The process is one in which the equilibrium reformer of Fig. 4.2, produces hydrogen and carbon monoxide. The carbon monoxide is separated by a perm-selective membrane and is oxidized in a relatively small high temperature fuel cell. The hydrogen is oxidized in a large cell, along the lines of Fig. 4.1. Operating conditions are made flexible by using idyllium electrolyte and superbium electrodes, from Fig. 4.3. In the background are the realities of current MCFC and SOFC designs, Chapter 6.

The arrangement of Fig. 4.4 for integrated operation may appear complicated, but the reader should think back to nature's photosynthesis organization, in which millions of chloroplasts and thousands of leaves are interconnected on a single tree, with the leaves near the forest floor in a decay-generated high carbon monoxide concentration, and the upper leaves at reduced concentration. The arrangement in Fig. 4.4 is dictated by the need to separate the hydrogen and carbon monoxide outputs of the reformer, and pass them to separate cells for oxidation, where they produce slightly different emfs. The selection of identical operating

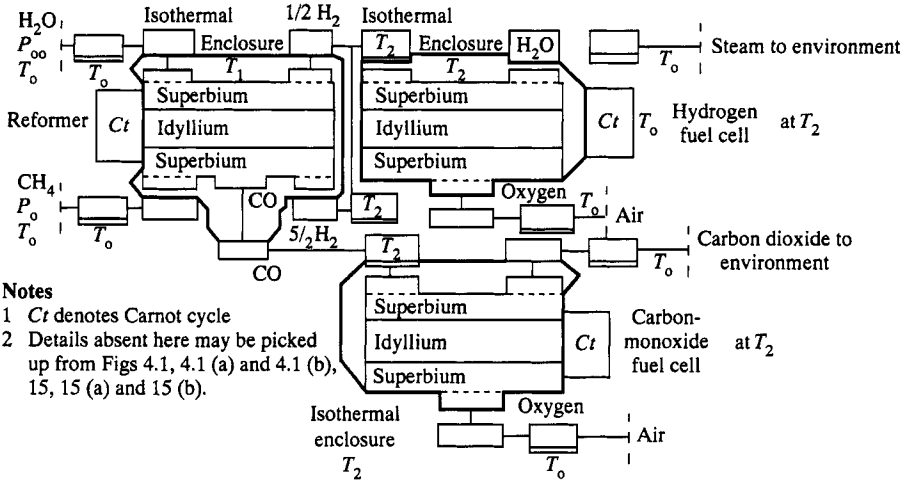

Fig 4.4 Equilibrium methane reform and isothermal oxidation of product by fuel cell

temperatures for the two fuel cells simplifies the circulator set up between reformer and cells. For each of the three processes, it is necessary to select operating temperature and pressure/fugacity. Then $\Delta_r G_t$ the electrical work and ΔCt, the Carnot cycle work, can be calculated for each process using the thermodynamic data from (**39**). Calculation of the components of the three reaction mixtures will lead to the circulator work. Circulators working at T_2 will need to be maintained there by a Carnot cycle. The calculation results of the perfect equilibrium process allows a comparison with real processes – the highlighting of irreversibilities. For the same reasons as given in the discussion of Fig. 4.1, the combined work, $\Delta G_t + \Delta Ct$, of the reformer and of the two fuel cells are fixtures. The circulator powers are dependent on operating pressures and temperatures. Work ultimately comes from rearranged chemical bonds.

4.6 Main conclusions

The calculations in Appendix A confirm that the combined power $-\Delta_r G_t - \Delta Ct$ of an elevated pressure and temperature fuel cell is, on an ideal gas basis, a fixture. The circulator power output, on the other hand, rises to a maximum at ambient (standard) temperature and pressure. On the basis of equilibrium theory, elevated pressure and temperature create a disadvantage. Each fuel cell type has its own irreversibilities and non-equilibrium electrode fugacity distributions, so that the complete picture

for each fuel cell type will emerge when the losses and emf adjustment (due to non-equilibrium electrode gas concentrations) have been seen against the background of equilibrium theory. For example, most, but not all, practical cells gain emf with pressure, but the equilibrium hydrogen cell looses emf. (The phosphoric acid cell can exhibit a fall in the vicinity of its operating point.) See page 74 on E_n.

Since hydrogen is the main fuel, and has a very imperfect product, calculations should use fugacity-based equilibrium constants (**39**). Only by using the latter can the fall in emf with pressure of the equilibrium cell be predicted. Such calculations do not show quite the same understandable results as the ideal gas variety.

The fuel chemical exergy is the output of an equilibrium fuel cell (equilibrium partial fugacities/pressures) having an equilibrium reaction mixture at standard total pressure and temperature. The fuel chemical exergy is calculated for hydrogen and carbon monoxide in paragraphs 8(f) and 8(i).

Appendix B is intended to provide an equilibrium basis for comparison of practical test results from integrated hydrogen/carbon monoxide production and fuel cell systems. The variability of circulator power with temperature and pressure means that there is not a unique basis of comparison. Indeed a basis has to be selected. If one is looking at the SOFC, then the electrolyte dictates 1300K and a usual operating pressure is 10 bar.

Appendix C explains the new basis for the definition of fuel exergy relative to older definitions.

Further detailed conclusions are in the text, under the 'Comment' sections.

Appendix A

4.7 Equilibrium fuel cell calculations

(Theoretical Reactant and Product Concentrations in Equilibrium Fuel Cells.) Note: The calculations involve fugacity, defined in ref (**42**).

(a) Equilibrium hydrogen fuel cell for any pressure and temperature

In the Fig. 4.1 fuel cell at equilibrium, the oxygen reaches the anode as OH ions. The oxygen circulators must supply oxygen to the cathode space of the heterogeneous reaction with the reaction going forward

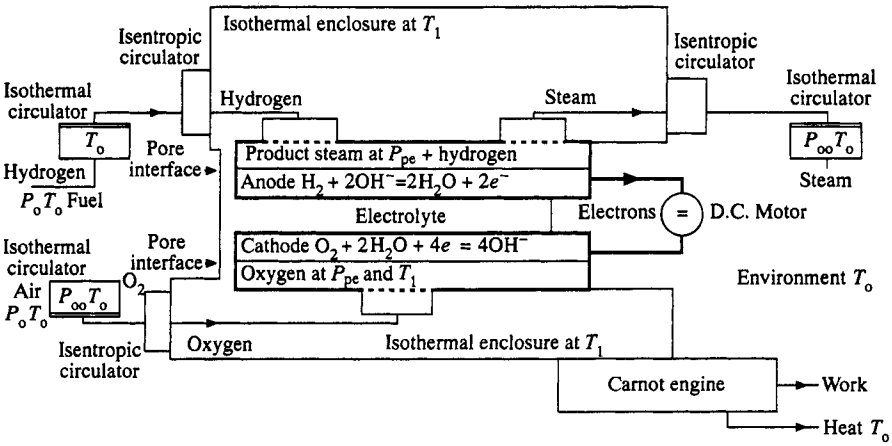

Notes

1 The isothermal and isentropic circulators relate cell to environment.
2 The Carnot engine exploits the thermo-mechanical exergy of the isothermal enclosure.
3 The oxygen, steam and hydrogen are at equilibrium concentrations, or equilibrium partial pressures determined by the equilibrium constants both of the electrode half reactions and of the overall cell reaction. Because steam is very imperfect, fugacity-based equilibrium constants must be used, from the JANAF thermochemical tables, reference (**39**).
4 Dotted lines are perm-selective membranes.
5 Half reactions involving CO_3^- or O_2^- are the basis of high temperature MCFC and SOFC.

Fig 4.1 Equilibrium fuel cell for any pressure and temperature (repeated)

infinitely slowly. The oxygen concentration in the cathode space half reaction, corresponds to a low partial pressure/fugacity. The remaining constituents of the equilibrium reaction mixture are in the anode space. Some concentrations are calculated here, for 1 and 10 bar equilibria, at 298K and at Solid Oxide Fuel Cell temperature 1300K, using (separately) CO and H_2 fuel.

The model calculation which occurs on page 630 of (**38**) is adapted. The symbols are:

z = kmols of fuel in the equilibrium mixture
n = number of moles in the mixture = $z + z/2 + (1 - z)$ corresponding to the equations,
$1CO + \frac{1}{2}O_2 >> zCO + z/2O_2 + (1 - z)\ CO_2$, the CO reaction mixture.
$1H_2 + \frac{1}{2}O_2 >> zH_2 + z/2O_2 + (1 - z)\ H_2O$, the H_2 reaction mixture.
$n = z + z/2 + (1 - z) = (2 + z)/2$

The molar equilibrium mixture analysis comprises

$$\gamma_{CO} = \gamma_{H_2} = 2z/(2 + z)$$
$$\gamma_{O_2} = z/(2 + z)$$

and

$$\gamma_{CO_2} = \gamma_{H_2O} = 2(1-z)/(2+z)$$

(b) 1 bar, 1300K calculation for CO and H_2 (following (38) page 630)

From (**39**) p628,	$0 = CO_2 - O_2 - C$	$\log_{10}k = 9.101$, (equation notation from (**42**))
p626,	$0 = CO - \frac{1}{2}O_2 - C$	$\log_{10}k = 15.919$ and by subtraction,
	$0 = CO_2 - \frac{1}{2}O_2 - CO$	$\log_{10}k = -6.818$; and by subtraction
and from (**39**) p1275,	$0 = H_2O - \frac{1}{2}O_2 - CO$	$\log_{10}k = -7.063$

The analysis of the reaction mixture at equilibrium is independent of reaction direction and the sign of the equilibrium constant. A change of sign makes products into reactants and vice versa, without affecting the equilibrium mixture. ΔG changes sign with circulator reversal. Hence

$$K^{H_2}{}_f = 8.6497E-08 \text{ @ } 1300K$$

and

$$K^{co}{}_p = 1.5205E-7 \text{ @ } 1300K$$
$$K = \{z/(1-z)\}\ (z/(2+z(2+z))^{1/2}$$

which, for the very small z values for these product biassed reactions reduces to

$K = z^{3/2}/1.414$, a simplification allowing analytical rather than iterative solution.

Hence

$$z^{3/2} = 1.414 \times 8.6497E-08 \qquad z^{3/2} = 1.414 \times 1.5205E-07$$
$$z = 2.4626E-05 \qquad z = 3.5870E-05$$

For very small z,

$$\gamma_{fuel} = z$$
$$\gamma_{O_2} = z/2$$
$$\gamma_{product} = \text{remainder.}$$

Hence for 1bar 1300K

$$\gamma_{H_2} = 2.4626 \times 10^{-5} \qquad \gamma_{co} = 3.5870 \times 10^{-7}$$
$$\gamma_{O_2} = 1.2313 \times 10^{-5} \qquad \gamma_{O_2} = 1.7935 \times 10^{-7}$$
$$\gamma_{H_2O} = 0.999997 \qquad \gamma_{CO_2} = 0.99999996$$

(c) 10 bar 1300K calculation for CO and H_2

At 10 bar, 1300K $K = 0.707z^{3/2} \times 10^{1/2} = 2.2355z^{3.2}$ ($P/P_{ref} = 10^{1/2}$) (for H_2O the fugacity coefficient (**39**) is <0.99, so $10^{1/2}$ is a valid approximation).

$\log_{10}K^{H_2}{}_f = -6.063 \quad \log_{10}K^{co}{}_p = -6.818$

Hence

$z^{3/2} = 8.6479E-07/2.2355 \quad z^{3/2} = 1.5205E-07/2.2355$

$z = 5.3065 \times 10^{-5} \quad z = 1.6653 \times 10^{-5}$

$\gamma_{H_2} = 5.3065 \times 10^{-5} \quad \gamma_{co} = 1.6653 \times 10^{-5}$

$\gamma_{O_2} = 2.6533 \times 10^{-5} \quad \gamma_{O_2} = 8.327 \times 10^{-5}$

$\gamma_{H_2O} = 0.999995 \quad \gamma_{CO_2} = 0.999998$

Comment

Pressure has moved the CO equilibrium mixture towards the products, at constant equilibrium constant. But the altered equilibrium constant for hydrogen dominates and moves the equilibrium towards the reactants.

With the change in $\log_{10}K$ from –7.063 to –6.063, between 1 bar and 10 bar, (**39**) pp1275/6, E_n at 1300K declines from 0.911 to 0.782 for hydrogen fuel. In most real cells the change is in the opposite direction. That is partially explicable in terms of irreversible phenomena in the real cells and in terms of electrode non-equilibrium gas concentration, page 74.

The reaction mixtures at standard (ambient) conditions are also calculated.

(d) Standard conditions 298.15K 1 bar calculation for CO and H_2

At standard conditions pressure = fugacity.

$\log_{10}K^{H_2}{}_p = -40.048 \quad \log_{10}K^{CO}{}_p = -45.066$

$K = 8.9536E-41 \quad K = 8.5901E-46$

$z^{3/2} = 1.414 \times 8.9356E-41 \quad z^{3/2} = 1.414 \times 8.5910E-46$

$= 1.266E-40 \quad = 1.2148E-45$

$z = 2.5136E-27 \quad z = 1.1346E-30$

$\gamma_{H_2} = 2.5136E-27 \quad \gamma_{co} = 1.1346E-30$

$\gamma_{O_2} = 1.2568E-27 \quad \gamma_{O_2} = 0.5673E-30$

γ_{H_2O} = almost 100 percent $\quad \gamma_{CO_2}$ = almost 100 percent

Comment

The reactions go virtually to completion, and consume incoming reactants very quickly, so that the equilibrium reactant concentrations are extremely small. The product concentration is near to 100 percent,

and the pressure in the anode space is little different from the sum of all the partial pressures. The cathode oxygen concentration would be difficult to imitate in practical conditions with an air cathode having an exhaust, during attempts to measure the equilibrium emf, E_n, of an open-circuited cell.

(e) Ambient versus high temperature and pressure equilibrium cell output

Separate calculations are made of the output of Fig. 4.1 at standard pressure and temperature and 10 bar, 1300K, (SOFC Conditions), for CO and H_2. Each calculation is independent of a change in cell type, from the Bacon cell at standard conditions, to SOFC at elevated conditions, and depends only on the overall chemical reaction and its equilibrium constant, (Figs 4.1 (a) and (b)).

(f) CO reaction, standard conditions, 298.15K, 1 bar, cell output calculation

The CO reaction involves ideal gases only, and is calculated first.

$$CO\,(-137.16, 197.67) + \tfrac{1}{2}O_2(0, 205.14) = CO_2(-394.38, 213.74).$$

The figures in brackets are (ΔG_f kWsmol^{-1}, S_f JK^{-1} mol^{-1}) from (**3**), for standard conditions.

$$\Delta G_0 = -394.38 + 137.16 = -257.22 \text{ kWsmol}^{-1}\ CO_2;$$
$$\Delta S_{rev} = 213.74 - 197.66 - 102.57 = -86.49 \text{ JKmol}^{-1}.$$

At standard conditions the Carnot cycle, and the isentropic circulators are of zero work input or output. With the reaction mixture analysis obtained, all three circulators are expanders contributing work and absorbing heat from the environment to keep them isothermal. The expanders need to be calculated from $RT\ln P_i/P_f = \Delta G = -\Delta Q = -T(S_i - S_f)$. ($f$ = final, i = initial.)

Table A.1 CO fuel isothermal expanders

	$P_f bar$	$P_i$bar	Relative flow	
CO	1.1346E – 30	1.0	1	
$\frac{1}{2}O_2$	0.5673E – 30	0.204	$\frac{1}{2}$	1 bar 298K
CO_2	0.0003	1.0	1	

CO expander (work output and heat absorbed from environment):

$$\ln P_i/P_f = \ln 0.8814E + 30 = 68.95, \times RT/1000 = 8.315 \times 298 \times 68.95/1000$$
$$= 170.849 \text{ kWs/mol}^{-1}$$

O_2 expander (work output and heat absorbed from environment):

$$\ln P_i/P_f = \tfrac{1}{2}\ln 0.204 \times 0.5673E + 30 = 33.461 \times RT/1000$$
$$= 33.461 \times 8.315 \times 298/1000 = 82.953.$$

CO_2 expander (work output and heat absorbed from the environment):

$$\ln P_i/P_f = \ln 1/0.0003 = \ln 3333 = 8.1116 \times 8.315 \times 298.15/1000 = 20.109.$$

Total expander ΔG = −274.180 kWsmol^{-1}, negative sign since these are outputs. **Hence CO fuel chemical exergy = −257.22 − 274.180 = −531.40 kWs mol^{-1}, and CO fuel reversible heat = − 86.49 × 298.15/1000 = −25.79 kJmol^{-1}.**

Comment

The value calculated for the fuel chemical exergy is not the textbook value, (**38**) and (**41**). See Appendix B. The expanders are a very significant part of the process. However, the pressure ratios of the expanders are very large, and the duty could not be approached in practice by machine designers. Ambient temperature operation is unrealistic, against the background of a need for high reaction rate in practical fuel cells.

(g) CO reaction, elevated conditions, 1300K, 10 bar, cell output calculation

The previous calculation has to be repeated for 10 bar, 1300K.

From section 4.7 (b) $\log_{10}k$, = 6.818, which has a +ve sign for the forward reaction, and at equilibrium is independent of the pressure. Hence

$$\Delta G_t = -RT\ln K = -8.317 \times 1300 \times 2.303 \times 6.818/1000$$
$$= -169.770 \text{ kWsmol}^{-1} \ (\Delta G_o = -257.22 \text{ and } \Delta G_t - \Delta G_o = 87.45)$$

The reversible entropy change of the ideal gas reaction is, at equilibrium, independent of pressure. The effect of temperature on entropy is tabulated in (**3**) (ideal gas). The tabulated value at 1300 K is 283.932(CO_2) − 126.439($\frac{1}{2}O_2$) − 243.431(CO) = 85.938, compared to 86.49 at 298K. The corresponding thermomechanical exergy of the Carnot cycle at 1300 K is

$$\{(T-T_o)/T\} \times T\Delta S = 1002 \times 85.938/1000 = 86.11 \text{ kWsmol}^{-1},$$

which approximately = $(\Delta G_t - \Delta G_o) = 87.45$.

For ideal gases, the equality should be exact; rounding off errors and data inconsistency have contributed to the slight inexactitude. For example if the reaction ΔG is calculated from the ΔG_f data the result is not exactly the same as the result using the tabulated $\log_{10}K$, in $\Delta G = -RT\ln K$.

(h) Circulators (CO reaction 10 bar 1300K)

To complete the CO elevated conditions analysis, the power of the isothermal and the isentropic circulators is required.

For the ambient temperature case the circulators (all isothermal expanders) generated -274.180 kWsmol^{-1}.

Qualitatively, in the elevated conditions case, it is apparent that the reactant isentropic machines are compressors raising the temperature of the reactants from 298K to 1300K, at reaction mixture partial pressure, while the product CO_2 is expanded to lower its temperature from 1300K, 10 bar, to 198K. The enthalpy difference values (**3**) are 31.868, 33.34, and 50.148 kWsmol^{-1}, respectively, giving a power of $+31.868(CO)+16.67(O_2)-50.148(CO_2) = -1.61$, (output).

The isothermal machines have a new duty, in the case of the high pressure and temperature cell, because they no longer connect to the reaction mixture, but to the inlets/outlets of the isentropic machines. The pressure ratios of the six machines are needed, to complete the picture. The pressure ratios of the isentropic machines may be got from

$$T_1/T_2 = P_1V_1/P_2V_2,$$

and the isentropic law

$$P_1V^{\gamma}_1 = P_2V^{\gamma}_2.$$

Hence

$$V_1/V_2 = (P_1/P_2)^{-1/\gamma}$$

and

$$T_1/T_2 = P_1/P_2 \times (P_1/P_2)^{-1/\gamma} = (P_1/P_2)^{(\gamma-1)/\gamma}$$ Therefore
$P_1/P_2 = (T_1/T_2)^{\gamma/(\gamma-1)}$, and
$P_2/P_1 = T_2/T^{\gamma/(\gamma-1)}$

CO isentropic compressor, $P_2/P_1 = (1300/198)^{1.4/0.4} = 173.4$
O_2 isentropic compressor, $P_2/P_1 = 173.4$.
CO_2 isentropic expander, $P_1/P_2 = (1300/298)^{1.31/0.31} = 505.1$

Table A.2 CO fuel isentropic circulators

	$P_f bar$	$P_i bar$	*Relative flow*	
CO	$10 \times 1.6653 \times 10^{-6}$	$P_f/173.4$	1	
$\frac{1}{2}O_2$	$10 \times 0.8327 \times 10^{-6}$	$P_f/173.4$	$\frac{1}{2}$	10 bar 1300K
CO_2	10/505.1	10	1	

The CO isothermal circulator connects from standard conditions to the inlet of the corresponding isentropic and is, therefore, an expander.

The O_2 isothermal circulator connects from atmospheric partial pressure P_{oo} to the corresponding isentropic and is, therefore, an expander.

The CO_2 isothermal circulator connects from the corresponding isentropic outlet to $P_{oo}CO_2(0.0003)$ and is, therefore, an expander.

Table A.3 CO fuel isothermal circulators

	$P_f bar$	$P_i bar$	*Relative flow*	
CO	P_i Table 4	1	1	
$\frac{1}{2}O_2$	P_i Table 4	0.204	$\frac{1}{2}$	10 bar 1300 K
CO_2	0.0003	10/505.1	1	

CO isothermal expander (work output and heat absorbed from environment):

$$\ln P_i/P_f = \ln(1)/(1.6653 \times 10^{-7}/1.734) = \ln 1.0413 \times 10^7 = 16.16$$

and

$$\Delta G = -8.315 \times 298.15 \times 16.16/1000 = -40.06$$

O_2 isothermal expander (work output and heat absorbed from the environment):

$$\tfrac{1}{2} \ln P_i/P_f = \tfrac{1}{2}\ln(0.204)/(0.8327 \times 10^{-7})/1.734 = 7.631$$

and

$$\Delta G = -8.314 \times 298.15 \times 7.631/1000 = -18.92 \text{ (isentropic} = 16.67, \text{ pair total} = -2.25)$$

CO_2 isothermal expander (work output and heat absorbed from the environment):

$\ln P_i/P_f = \ln(10/505.1) \times 3333 = 2.303 - 6.225 + 8.112 = 4.19$

$\Delta G = -8.315 \times 298.15 \times 4.19/1000 = -10.38$

$\Sigma\Delta G = -69.36$ isothermal output.

Adding 1.61 isentropic output, total circulator power = –70.97 (elevated) which, due to the very different reaction mixture fractions between standard and elevated conditions, is less than –274.18 (standard conditions) above. Elevated conditions total Fig. 4.1 output = –70.97 – 169.77 – 86.11 = –326.85 kWsmol^{-1}.

(i) Hydrogen reaction, standard conditions, 298.15K 1bar, cell output calculation

Proceeding to the hydrogen reaction, the equation (with standard conditions data from (**3**) (p1260/1667/1275), is:

$H_{2(G)}(0,130.68) + \frac{1}{2}O_{2(G)}(0,205.147) = H_2O_{(L)}(-237.14,69.95)$.

$\Delta G_o = -237.14$, $\Delta S = -265.877$, $\Delta Q = -79.27$ kJmol^{-1}.

The Carnot cycle and the isentropic circulators are redundant. The hydrogen is expanded isothermally from standard conditions to anode concentration. The oxygen from the atmosphere is expanded isothermally from its partial pressure to cathode concentration. The H_2O is expanded isothermally from water to its standard atmospheric concentration. At standard conditions pressure = fugacity.

Table A.4 H_2 isothermal expanders

	P_f *bar*	P_i *bar*	*Relative flow*	
H_2	2.5136E – 27	1.0	1	
$\frac{1}{2}O_2$	1.2568E – 27	0.204	$\frac{1}{2}$	1 bar 298K
H_2O	0.0088	1.0	1	

H_2 expander (work output and heat absorbed from environment);

$\ln P_i/P_f = \ln 0.3978E + 27 = 61.248. \times RT/1000 = 8.315 \times 298 \times 61.248/1000 = 151.77$ kWsmol^{-1}.

O_2 expander (work output and heat absorbed from environment)

$\ln P_i/P_f = \ln 1.623E + 26 = 60.351. \frac{1}{2} \times RT/1000 = \frac{1}{2} \times 8.315 \times 298 \times 60.351/1000 = 74.77$ H_2O expander work.

This work quantity is in fact the chemical exergy of water, from pp257/8 of (**41**), and is 3.177 kWSmol^{-1}.

Total expander $\Delta G = 229.717$ kWsmol^{-1}.

Hence hydrogen fuel chemical exergy = 237.14 + 229.717 = 466.857 kWsmol^{-1}, with ΔS_{rev} and ΔQ_{rev} from above –265.877 and –79.27, respectively.

Comment

The fuel chemical exergy for hydrogen is again not the text book value, (**38**), (**41**), see Appendix B. The value for hydrogen is less than for CO (531.40). The reversible heat from the exergy reaction is relatively high, compared to CO; 79.27 cf 25.79.

(j) Hydrogen reaction, 1300K 10 bar, cell output calculation

The previous calculation has to be repeated at 10 bar 1300K, with isentropic circulators and Carnot cycle included, as per paragraph 6.

At 10 bar, 1300 K, from (**3**) p1276, $\log K_f = 6.063$
and

$$\Delta G = -RT \ln K = -8.317 \times 1300 \times 2.303 \times 6.063/1000$$
$$= -150.97 \text{ kWsmol}^{-1}.$$
$$\Delta G_o - \Delta G_t = -237.14 + 150.97 = -86.17.$$

The reversible entropy change from pp1276/1260/1667 (**3**) is 224.858 – 174.288 – 126.439 = – 75.869JKmol^{-1}, which becomes a Carnot output of $-75.869 \times 1002/1000 = -76.02$, compared to $\Delta G_o - \Delta G_t = -86.17$.

Comment

The reduced equilibrium constant at increased pressure reduces the electrical output as does the increased pressure. The reversible entropy is slightly reduced, but at 1300K represents a significant Carnot output of 76. This does not precisely equate with the decline in electrical output, as in the CO perfect gas case.

(k) Circulators (hydrogen reaction 10 bar 1300K)

The calculation follows the CO example of para 7. The reactant isentropic circulators are again acting as compressors from 298K to 1300K, whilst the product steam is isentropically expanded from 1300K to 298K. The enthalpy (kJ.mol^{-1}) differences are 29.918 (H_2), 16.672 ($\frac{1}{2}O_2$), 82.881 (H_2O), p1276 (**3**)), giving powers of –82.881 + 16.672 + 29.918 = –36.291 kJ mol^{-1}, total. The isentropic pressure ratios are:

H_2 isentropic compressor, $P_2/P_1 = (1300/298)^{1.41/0.41} = 158.497$
O_2 isentropic compressor, $P_2/P_1 = (1300/298)^{1.4/0.4} = 173.398$
H_2O isentropic expander, $P_1/P_2 = (10/0.02) = 500$ from Mollier chart.

Table A.5 H_2 isentropic circulators

	$P_f bar$	$P_i bar$	*Relative flow*	
H_2	$10 \times 5.3065 \times 10^{-5}$	$P_f/158.5$	1	
$\frac{1}{2}O_2$	$10 \times 2.6533 \times 10^{-5}$	$P_f/173.4$	$\frac{1}{2}$	10 bar 1300k
H_2O	10/500	10	1	

The hydrogen isothermal circulator connects from standard conditions to the inlet of the corresponding isentropic and is therefore an expander.

The oxygen isothermal circulator connects from atmospheric partial pressure $P_{oo} = 0.204$ bar to the inlet of the corresponding isentropic and is, therefore, an expander.

The steam isothermal circulator connects from 10/500 = 0.02 to $P_{oo} = 0.0088$ and is, therefore, an expander.

Table A.6 H_2 isothermal circulators

	$P_f bar$	$P_i bar$	*Relative flow*	
H_2	P_i Table 5	1	1	
$\frac{1}{2}O_2$	P_i Table 5	0.204	$\frac{1}{2}$	10 bar 1300K
H_2O	0.0088	0.02	1	

H_2 isothermal expander (work output and heat absorbed from the environment):

$$\ln P_i/P_f = \ln (1)/(10 \times 5.3605 \times 10^{-5}/158.5)$$
$$= \ln (1)/(3.382 \times 10^{-6})$$
$$= \ln(2.957 \times 10^5) = 12.597$$
$$\Delta G = -8.314 \times 298.15 \times 12.597/1000 = -31.225$$ (O_2 isothermal expander work output and heat absorbed from the environment):
$$\tfrac{1}{2} \ln P_i/P_f = \tfrac{1}{2} \ln (0.204)/(10 \times 2.6533 \times 10^{-5}/173.4)$$
$$= \tfrac{1}{2} \ln 1.333 \times 10^5$$
$$= 11.8$$
$$\Delta G = -\tfrac{1}{2} \times 8.314 \times 298.15 \times 11.8/1000 = 29.25/2 = -14.63$$ (H_2O isothermal expander ΔG from extrapolated Mollier chart).
$$= -2.3\, \Sigma \Delta G_{\text{isothermal}} = -(31.225 + 14.63 + 2.3) = -48.155$$

and adding $\Delta G_{\text{isentropic}} = -36.291$, the total circulator power is -84.446 kWs mol^{-1}.

The total Fig. 4.1 output = electrical -150.97, Carnot -76.02, circulator $-84.446 = -311.436$ kWsmol^{-1}, which is less than the ambient temperature result, largely because of reduced circulator power.

Comment

Table A.7 Summary of reaction parameters

Item		ΔG	ΔCt	ΔG + ΔCt	*Circs*
CO 1bar	298K $\log_{10}K - 45.066$	−257.220	0	−257.22	−274.180
1bar	1300K $\log_{10}K - 6.818$	−169.708	Not	Calculated	
10bar	1300K $\log_{10}K - 6.818$	−169.770	−86.11	−255.88	−70.97
H_2 1bar	298K $\log_{10}K - 40.048$	−237.14	0	−237.14	−229.717
1bar	1300K $\log_{10}K - 7.063$	−175.807	Not	Calculated	
10bar	1300K $\log_{10}K - 6.063$	−150.97	−76.02	−226.99	−84.446

An obtrusive difference between CO and H_2 fuel in Table 7 is that at 1300K the CO equilibrium constant does not change with pressure, but with hydrogen, $\log_{10}K$ changes from −7.063 to −6,063 as the pressure goes from 1bar to 10bar. With CO the combined power is independent of operating conditions. With hydrogen the combined power is a weak function of pressure.

The circulator power is determined by the calculated analysis of the equilibrium reaction mixture, which for fuel cell reactions, comprises largely product and a very low fraction of reactants. The isothermal circulators are all expanders, for the hydrogen and for the carbon monoxide reactions examined, and their power dominates the circulator total. The reactant isentropic circulators are compressors, and the product isentropic circulator is an expander, in each case examined. The isentropic total power is relatively small, since the pressure ratios are relatively modest. At SOFC operating conditions the circulator power for both fuels is modest.

In the literature of practical cells the auxiliary power is not an obtrusive feature. Where the cell is integrated with a gas turbine the latter supplies the pressurized air, as a minor task, and utilizes unused fuel and hot exhaust.

Practical fuel cells with atmospheric or lightly pressurized air fed to the cathode, are a long way from the carefully contrived equilibrium oxygen concentration. Their output is, therefore, determined by the anode fuel supply and fuel losses, rather than a controlled balance between fuel and oxygen. In the end their reaction rate is limited by non-equilibrium concentration polarization, and their electrical output reduced by voltage losses at electrode surfaces, overpotentials, and by ohmic potential differences.

4.8 Methane, equilibrium isothermal oxidation

A practical technology for the oxidation of methane and the higher hydrocarbons in natural gas, para 3 above, is not available (**43**). The overall reaction would be

$$CH_4[-50.768,186.251]_G + 2O_2[0,205.147]_G$$
$$= CO_2[-394.389,213.795]_G + 2H_2O[-237.141,69.95]_L.$$

Terms in brackets are $[\Delta G_f, S_f]$ at 298.15K, 1bar.

$\Delta G_o = -817.903$ $\Delta S_{rev} = -242.849$, which can be compared to,
$3H_2\ \Delta G_o = -711.42$ $\Delta S_{rev} = -797.631$ para 8i,
$+CO$ $\Delta G_o = -257.22$ $\Delta S_{rev} = -86.49$ para 8f,
$3H_2 + CO$ $\Delta G_o = -968.64$ $\Delta S_{rev} = -884.121$, the output of a reformer.

The alternative reform reaction is

$$CH_4[-50.768,186.251] + H_2O[-237.141,69.95]$$
$$= 4CO[-137.16,197.67] + 3H_2[0,130.68]$$
$$\Delta G_o = 150.749$$
$$\Delta S_{rev} = 326.509 \text{ and } \Sigma\Delta G = -968.64 + 150.749$$
$$= -817.891(-817.903)\text{kWs mol}^{-1}$$

The same electrical work is available, at standard conditions, if:

(a) methane isothermal oxidation is employed, as is available;
(b) methane/steam reform is used, and the resulting hydrogen and carbon monoxide are oxidized (both oxidations being equilibrium processes).

The entropy changes do not influence the work (exergy) account. They are at T_o and represent zero exergy change. The entropy changes of the two routes are different, because only the reform route needs water to be added.

A full calculation would put numbers on the circulator powers via an equilibrium analysis of the reaction mixtures, but that is outside the scope of this already lengthy chapter.

The real anode reform process as currently employed, is a non-equilibrium reaction, which throws the reactants together without separating work from heat, so that there is an irreversible entropy growth. A reversible alternative is shown in Fig. 4.2 above, the practicability of which is uninvestigated.

Comment

The direct use of methane is a technologically difficult, but beckoning objective. The associated entropy change, and Carnot cycle, are small and with higher hydrocarbons, in natural gas, could disappear. An electrical work only system, would represent greatly improved economics ((**43**), Paper 7).

Appendix B

4.9 Equilibrium hydrogen production and fuel cell operation; calculations

For ease of exploratory calculation, all three cells are selected for operation at 10 bar. If T_1 is selected the same as T_2, then isentropic compressors between reformer and cells are eliminated, together with associated calculations. If $T_1 = T_2 = 1300$K, then advantage can be taken of calculations in Appendix A for the fuel cells. Using reversible processes, there is no disadvantage in taking all cell steam down to the environment, and back up to reformer conditions. Moreover, calculations already done in Appendix A can be re-used. In selecting operating conditions, the fractions of constituents in equilibrium mixtures are being determined, and with them circulated powers. Moreover, the maximum work occurs in ambient temperature reactions, so that the burden of the reform reaction on the fuel cells has been reduced.

The reform reaction is

$CH_4(267.714, 52.626) + H_2O(224.858, -150.893) = CO(243.431, -226.509) + 3H_2(174.288, 0)$.

The data for (S_f and $\Delta_f G$) are from (**3**) pages 600, 1276, 626, and 1212, respectively, for 10 bar, 1300K. Reactants and products are gases.

$\Delta_r S = +273.723$
$\Delta_r Q = T$
$\Delta_r S = 1300/1000 \times 273.723 = 355.84$

and

$\Delta_r G$ is $-128.242 = -RT\ln k$.

Hence

$$\ln k = 128.242 \times 1000/8.314 \times 1300$$
$$= 11.885 \text{ and } \log_{10} k = 5.161.$$

The reaction has an electrical output $\Delta_r G$ but needs relatively large heat pump input. The reversible Carnot heat pump work ΔCt associated with $\Delta_r S$ is

$$\eta_c . T.\Delta_r S = (\Delta T/T).T\Delta_r S = (1300 - 298)/1300 \times (355.84) = 274.27$$

and the net combined work (**43**) paper 4, is $-274.27 + 128.42 = -145.85$ kWs/.mol^{-1}. That amount of work has to be found from the fuel cells and the circulators, and will not be available as electrical power output. The practical fuel cells of today, with electrode reform, use a more irreversible, more non-equilibrium reaction, and so suffer a heavier penalty; the difference will figure in a performance calculation. The hydrogen fuel cell is well endowed with heat output, at SOFC/MCFC temperature, and can support the burden. It remains to determine the circulator work, via a calculation of the reaction mixture components in the reformer. The corresponding fuel cell calculations are in this Appendix. The isothermal circulators from reformer to the two fuel cells have to work between the reformer mixture equilibrium and the cell mixture equilibria.

4.10 The methane reform equilibrium mixture composition

The model calculation on p630 on (**38**) is again used, with full iterative solution rather than the short cut as in Appendix A.

$k_f^{CH_4} = 6.9024\text{E-}06$ for $CH_4 + H_2O > < CO + 3H_2$

The mass conservation equation, reactants to equilibrium mixture, is

$$1CH_4 + 1H_2O >> zCH_4 + zH_2O + (1 - z)CO + 3(1 - z)H_2$$

with z = amount of CH_4 in kmols present in mixture.

The total number of moles in the mixture is

$$n = z + z + (1 - z) + 3(1 - z) = 4 - 2z$$

and the molar analysis is

$$\gamma_{CH_4} = z/(4 - 2z) = \gamma_{H_2O},\ \gamma_{CO} = (1 - z)/(4 - 2z),\ \gamma_{H_2} = 3(1 - z)/(4 - 2z).$$

The equilibrium constant takes the form;

$$k = [(p/p_{ref})/(4-2z)]^{1+3-1-1} x[(1-z).(3-3z)^3/z^2$$
$$= (p/p_{ref})^2 \times [(1-z)(3-3z)^3]/(4-2z)^2 = 6.9024\text{E}-06,$$
$$100 \times [27(1-z)^4/4(2-z)^2] = 6.9024\text{E}-06$$

which reduces to

$$(2-z)^2/(1-z)^4 = 9.779 \times 10^{-8}$$

and by iteration, the approximate value of z is

$$z = 0.9899.$$
$$\gamma_{CH_4} = 0.490 = \gamma_{H_2O}, \quad \gamma_{CO} = 4.9995\text{E}-03 \quad \gamma_{H_2} = 0.015$$

Comment

The reaction equilibrium is reactant biassed, and at first sight unattractive. The reformer would, however, work next to a fuel cell anode, hungry for hydrogen, making an overall effective process. The perspective is that high temperature has reduced ΔG_t the electrical output. The reduction has reappeared as ΔCt, and reduced the Carnot heat pump input. Without pressure, the factor of 100 would be missing from the equation for z above, but the mixture analysis turns out to be insensitive to the pressure, and the move toward the products small.

4.11 Circulator powers

The circulator pairs for CH_4 and H_2O and the interconnecting isothermals remain to be calculated.

Reactant circulator pairs

The isentropic enthalpy differences 1300/298K from (**3**) p600 and p1275/6 are 61.302 $kWsmol^{-1}$ for methane and ([82.941 – 82.881] × 4.9/10) + 82.881 = 82.910 $kWsmol^{-1}$ for steam.

The isentropic pressure ratios are:

CH_4 isentropic compressor, $P_2/P_1 = (1300/298)^{1.31/0.31} = 505.078$
H_2O isentropic compressor, $P_2/P_1 = 4.9/0.009$ from Mollier chart,
$= 544.444$

Table B.8 Isentropic circulators

	$P_f$bar	$P_i$bar	*Relative flow*	
CH_4	4.90	9.071E-03	1	
H_2O	4.90	9.000E-03	1	Reformer reactants

The methane isothermal circulator draws natural gas from atmospheric pressure, with methane at a partial pressure of 85.26 percent and delivers to the isentropic inlet. It is, therefore, an expander.

The steam isothermal expander draws from the 298 K 1bar environment at a partial pressure P_{oo} of 0.0204 bar, and delivers to the isentropic inlet at 9.000E-03 and is therefore an expander.

Table B.9 Isothermal circulators

	$P_f$bar	$P_i$bar	*Relative flow*	
CH_4	9.071E-03	0.8526	1	
H_2O	9.000E-03	0.0204	1	Reformer reactants at 298K

CH_4 isothermal expander (work output and heat absorbed from environment):

$\ln P_i/P_f = \ln 0.8256/9.071E\text{-}03 = 4.5110$, and $\Delta G = 8.314 \times 298.15 \times 4.511/1000 = 11.181$ kJmol^{-1}.

H_2O isothermal expander, from extrapolated Mollier chart $\Delta G = 2.1$ kWsmol^{-1}.

CH_4 circulator pair, input = 61.42 – 11.18 = 50.14 kWsmol^{-1}.

H_2O circulator pair, input = 82.91 – 2.4 = 80.51 kWsmol^{-1}.

4.12 Hydrogen and carbon-monoxide isothermal circulation from reformer to fuel cells

Table B.10 Isothermal expanders

	$P_f$bar	$P_i$bar	*Relative flow*	
CO	1.6653E-04	4.9995E-02	1	
H_2	5.3065E-04	0.15	6	Reformer products at 1300K

CO expander (work output and heat absorbed at 1300 K).

$\ln P_i/P_f = \ln(4.9995\text{E-}02/1.6653\text{E-}04) = 5.704$ and
$\Delta G = 8.314 \times 1300 \times 5.704/1000 = 61.65$ kWsmol^{-1}.

The work content (thermomechanical exergy) of the 1300K heat absorbed is $\eta_c \Delta Q = (1002/1300) \times 61.65 = 47.51$, kJmol^{-1} input via the heat pump shaft.

H_2 expander (work output and heat absorbed at 1300 K).

$\ln P_i/P_f = \ln(0.15/5.3065\text{E-}04) = 5.6443$

and

$\Delta G = 3 \times 8.314 \times 1300 \times 5.6443/1000 = 183.014$

The work content(thermomechanical exergy) of the 1300K heat absorbed is $\eta_c \Delta Q = (1002/1300) \times 366.028 = 141.062$ kWsmol^{-1}, input by the heat pump shaft. **The fuel exergy from paragraphs (h) and (l) is 3 H_2 + 1 CO = $-3 \times 466.857 - 531.4 = -1931.971$ kWsmol^{-1}.**

4.13 Exergy account of integrated reformer and fuel cells

Comment

In Table 11 below, the exergy account of the integrated process, the exergy yield is –1303.815 kWsmol^{-1}. The difference of 462.852 is between two reversible or equilibrium processes, and represents work or exergy stored in chemical bonds.

The steam product should be returned to the plant inlet, but it is easier, for calculation purposes, to take it down to the environment and back up again.

An alternative calculation might have used a practical reformer temperature of 1100 K. No practical electrolyte is yet available for such a temperature, however.

The maximum theoretical efficiency of the integrated process is 1304/1767 = 73.8 percent. A real process with irreversible entropy growths would be of substantially lower efficiency. The next step is analysis of, as yet unavailable, test results.

Table B.11 Exergy account of integrated reformer and fuel cells

Item	*Exergy*	*Totals*
Reformer steam circulator pair	$-80.57\ kWsmol^{-1}$	$\Sigma -1766.667$
Reformer methane circulator pair	−50.14	$\Sigma +462.852$
Reformer	−128.42	−1303.815
Reformer Carnot cycle	+274.27	
Reformer hydrogen isothermal circulator	−183.014	
and Carnot cycle	+141.062	
Reformer carbon monoxide		
isothermal circulator	−61.65	
and Carnot cycle	+47.51	
Carbon monoxide fuel cell	−169.770	
Carbon monoxide fuel cell Carnot cycle	−86.11	
Carbon monoxide fuel cell CO_2		
circulator pair	−70.97	
Hydrogen fuel cell × 3	−452.91	
Hydrogen fuel cell Carnot cycle × 3	−228.06	
Hydrogen fuel cell steam circulator pair × 3	−255.053	

Appendix C

4.14 Fuel chemical exergy

References (**38**) and (**41**) are valued possessions of the author, and have been much used in writing this paper. A difficulty inevitably puts them in the crossfire.

In (**38**) the chemical exergy of fuel (C_aH_b) is introduced via Fig. 13.4, page 601, and in (**41**) the same concept is introduced for CO via Fig. 2.12, page 46. These figures (q.v.) share a common feature, namely that they impose upon the Van't Hoff equilibrium box, or isothermal enclosure, a non-equilibrium reaction mixture analysis. In (**38**) the fuel is at P_o and T_o and the reactants and products are at their environmental concentrations, whilst in (**41**) the fuel reactants and products are at P_o and T_o.

In Fig. 4.1 the reaction mixture must be at its equilibrium concentrations, which are calculated, in Appendix A, to be mostly product and very little reactant indeed.

An equilibrium reaction in the figures of (**38**) and (**41**) would impose on the enclosure, the calculated equilibrium mixture analysis. The regimes in the two figures could not be maintained.

Accordingly the fuel chemical exergy is obtainable, only from the author's Fig. 4.1 in this paper, with enclosure at P_o and T_o and an equilibrium reaction mixture as per paragraph 4.8(d) of this chapter. Importantly the chemical exergy is obtainable only by isothermal oxidation at T_o. In the case of hydrogen or hydrogenous fuels, the pressure must also be P_o. However, in the ideal gas case the reaction yield is independent of pressure.

Since the theoretical circulater yield is high in paragraphs 8(f) and 8(i), which in fact calculate the fuel (CO and H_2) chemical exergy, the departure from tabulated values is substantial. The fact of being obtainable, only at T_o, is crucial.

Comment

The efficiency of a fuel cell, is a ratio of real output, to fuel chemical exergy as defined here. Such an efficiency is depressed when the exergy needed for hydrogen production is accounted for. The calculation of the chemical exergy of a natural gas mixture is not attempted, because it involves postulating a set of fuel cells to consume separately each of the constituents. A guesstimate is used in Chapter 3.

Chapter 5

Whisky Distillation by Heat Pump

Sing first that green remote Cockaigne
Where whiskey rivers run,
And every gorgeous number may
Be laid by any one;
W H Auden

5.1 Whisky distillation

The empirical art of whisky distillation is underlain (**49**) by the following chemical sequence:

$$(C_6H_{10}O_5)_n \xrightarrow[\text{malt enzyme}]{H_2O} C_{12}H_{22}O_{11} \xrightarrow[\text{yeast enzyme}]{H_2O} 2(C_6H_{12}O_6) \xrightarrow{\text{zymase}} 8CH_3CH_2OH + 4CO_2$$

starch — sucrose — glucose — ethyl alcohol — carbon dioxide

The starch in malted grain is hydrolyzed (mashed) to a sucrose solution called 'wort'. Fermentation of the wort with yeast leads via glucose to a water alcohol 'wash' which is double distilled, first in a wash still, then in a spirit still. This is done for purification and to increase the concentration by volume of alcohol from 7 percent (wash) to 22 percent (low wines) and an eventual 70 percent (spirit).

There is doubt about the n in the formula for starch, and its thermodynamic properties are not tabulated in (**42**), although the subsequent sugars and the alcohol are so tabulated. The grain sprouting or malting process generates the enzyme (organic catalyst) for the hydrolysis process, and the yeast supplies the enzymes for fermentation. The distillation requires steam, traditionally from a boiler. In this case, however, the alternative is used: a simple steam-based prototype heat pump to supply the wash still steam. Electricity with a hydroelectric component is fairly stable in price, but fuel oil for the boiler fluctuates

four to one in price, so that at minimum oil price the boiler is competitive.

The pure exergy in the electricity supply is grafted on to a low temperature energy flow, with some exergy losses in the simple heat pump.

Alternatively, the fuel exergy is degraded in the boiler to steam at about 2 bar, T_{sat} 133.5 °C. Before the practical losses begin, the Carnot efficiency is only 108.5/406.65 = 26.7 percent. Yet still the boiler can compete!

5.2 Steam heat pumps

Since the steam power plant regenerative cycle is very highly evolved and developed, an inversion of that cycle suggests itself as an efficient heat pump. The inverse of a bled steam turbine is a fed steam compressor. The inverse of a feed heater train is a multi-stage flash cooler adapted from the desalination equipment of Chapter 2. The requirement is to produce saturated steam for a quasi-continuous batch process, so that the reheaters and superheaters of the power plant are irrelevant. A saturated steam cycle with an infinite number of feed heaters has equality of efficiency with a Carnot cycle working between the same temperature limits. An infinite number of cooling stages should confer perfection (reversibility) on the hypothetical heat pump. The temperature entropy diagram and flow sheet of a notional but practical high-performance four-stage regenerative steam heat pump are shown in Fig. 5.1.

Starting with the ideal infinite version, the cycle is represented by the continuous path DCBA. The heat source is a large flow of river or sea water, on the tube-side of a heat exchanger. Water sprayed on the shell side generates an atmosphere of dry saturated steam at the compressor intake. The line AD is equal in length to BC so that the cycle generates no entropy. AD does not imply that the intake steam is wet, but that its flow magnitude is such that AD = BC. At each compression stage the steam is spray desuperheated. The finite process is isentropic compression XY, followed by desuperheat YZ. The infinite process has to be imagined! The practical process has five desuperheat sprays which cool mixed compressor and flash cooler steam feeds. If the fifth spray is omitted, the end product will be slightly superheated dry steam.

Note that the specific volume of steam at ambient temperature is very high, there being a factor of 19 between 20 °C and 80 °C, so the compressor would be large and expensive (as are the low pressure ends of power plant turbines) if the source temperature is chosen low. Hence in

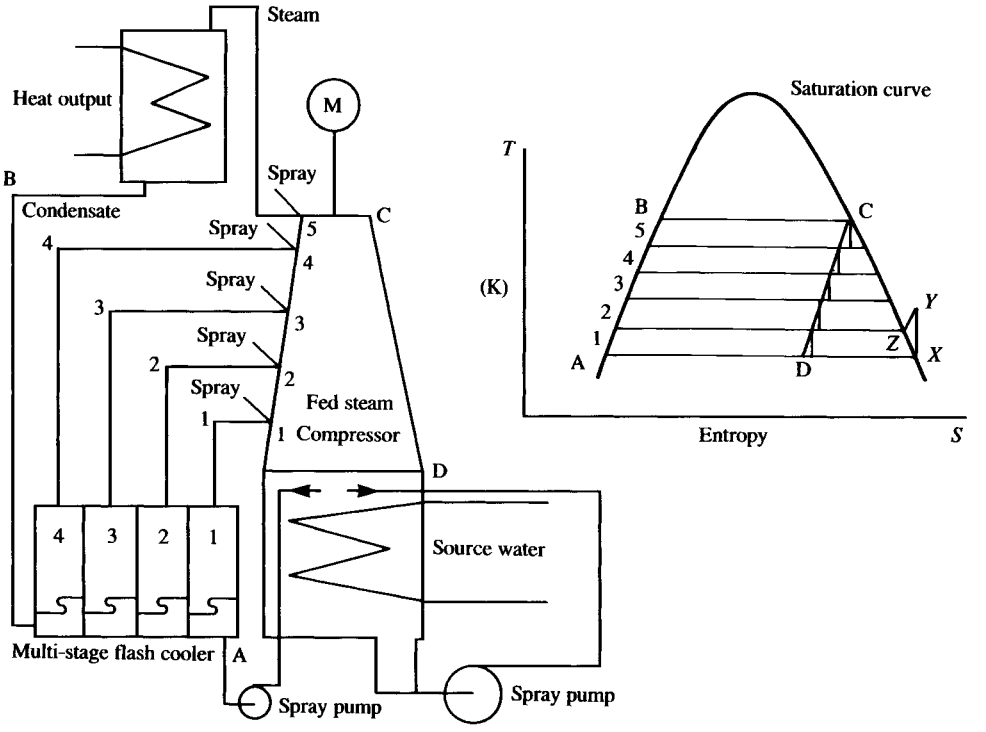

Fig 5.1 Hypothetical steam heat pump
(NB: The temperature entropy diagram cannot show the flash cooler irreversibilities. The compressor is shown as isentropic for simplicity.)

practical applications there is a need to select a high source temperature if possible, and to be judicious in selecting compressor type. Note that the fed steam principle reduces the throughput of the low pressure end and, therefore, the compressor size. See Fig. 5.1.

Each stage of the four-stage cooler features orifice-controlled flow into a flashing flow region, followed by a hydraulic jump to a non-flashing regime (a practical process used in multi-stage flash desalination plants.

In a real compressor XY would slope upward to the right (entropy growth).

Not every real compressor would be compatible with sprays, in which event they could be omitted in favour of an outlet desuperheater. The power plant cycle and this heat pump share the advantage of having only one major loss generating machine.

The product of such a heat pump is valued for its exergy (temperature), and must go on to a utilization process. From this there may be a condensate return at a useful temperature to be put into the cooler at the temperature-matched stage and make its contribution to the fed steam.

5.3 Whisky distillery

In whisky distillation (Fig. 5.2) the product is valued, *inter alia*, for increased ethanol concentration (chemical potential), and must as part of the process be condensed and sub-cooled. The cooling water temperature of the wash still condenser determines the input conditions of the heat pump compressor, whilst the heated condenser cooling water is flashed to provide most of the compressor steam.

The wash still flow sheet shows the practical application of a steam heat pump, in simplest possible prototype form, to the successful first stage distillation of whisky. The installation was a pioneering demonstration sponsored by the Electricity Council Research Centre at Capenhurst, UK, and was installed by International Distillers and Vintners Ltd at their Auchroisk (pronounced Athrusk) Distillery, Aberdeenshire, Scotland.

IDV Ltd have approved this article on their plant.

5.4 Wet compression in a screw compressor

Uniquely, a screw compressor benefits mechanically from water spray injection at its inlet, via even temperature distribution and minimized differential expansion, leading to smooth running. The steam coils of the

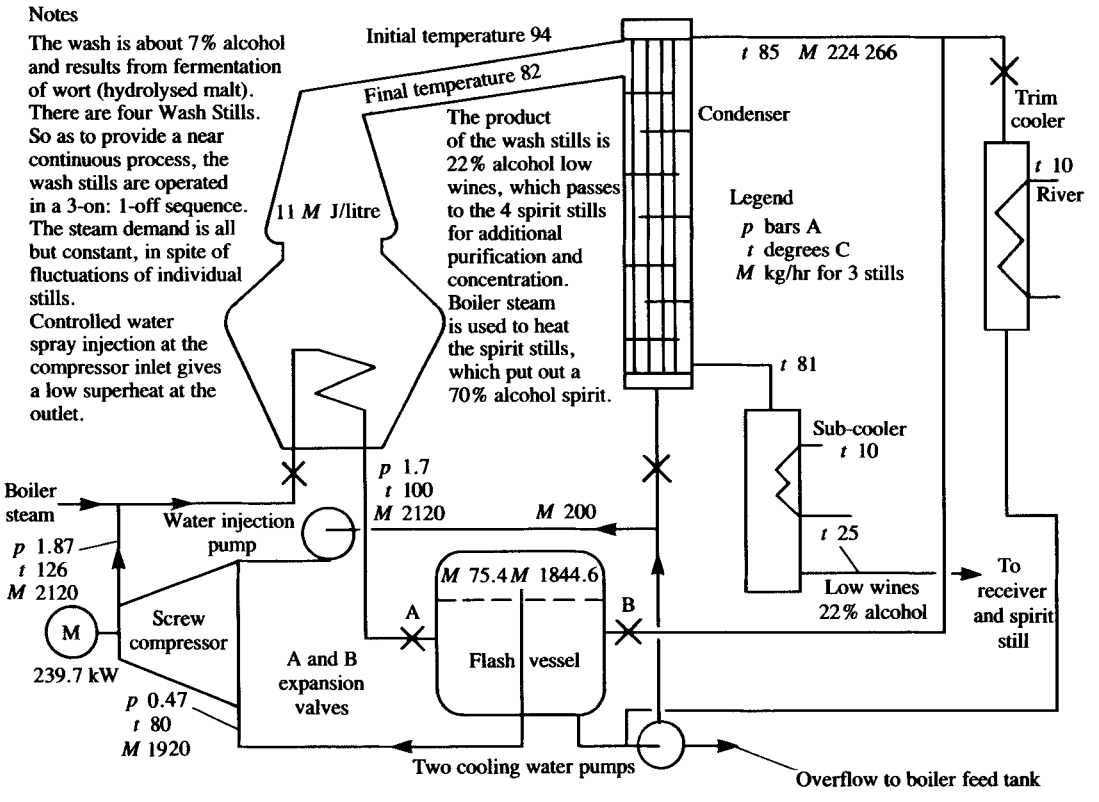

Fig 5.2 Wash-still and heat pump

wash stills enjoy a steady supply of dry, but only slightly superheated steam, which is dependent on control of the spray quantity. Degradation of excessive superheat, which would result from compressing dry steam, is avoided. The spray causes a useful reduction of specific volume at the compressor inlet. The design of spray nozzles is empirical and the interactions between droplets and vapour under compression are complex, with surface tension and slip certainly involved.

5.5 Wash still sequence and steam pressure

The best-achievable continuity and intensity of production is achieved by a one-off/three-on wash still sequence, which results in a near-study steam demand, despite waxing and waning of individual stills between filling, operation, and discharge. In place of traditional pan heaters, new copper heating coils allowed operation with steam pressure reduced from the traditional 3 to 2 bar. This reduced the saturation temperature (by 13 °C) and also in the compressor power consumption. At the start of distillation, coincident with foaming at high-level sight glasses on the wash stills, the product is unsatisfactory (foreshots). These are redistilled in later runs. They are usefully concentrated, and not to be discarded. (Conservation of chemical exergy ξ_c.)

5.6 Condensers and trim cooler

The traditional river-cooled condensers which combined condensation and sub-cooling were replaced by prototype condensers with separate, river water cooled, sub-coolers. These new uninsulated condensers, copper constructed and of baffled shell and tube design, allow recirculation of cooling water with a controlled temperature rise across the condenser, of 5 °C (80 °C inlet, 85 °C outlet). The upward-sloping uninsulated vapour delivery pipe from the uninsulated wash still is as before. Changes to such a pipe would be resisted, as the flavour of the product could be influenced by altered reflux condensation. The new condensers themselves, which had to be of the traditional tall thin shape, were accepted when a three month tryout with a single new condenser confirmed that the flavour of the product had been conserved to the satisfaction of tasters.

The trim cooler is a control device for off-sequence operation, (one, two, and four wash stills). If the cooling water rises above 80 °C the trim cooler valve opens.

5.7 The flash vessel and its irreversibilities

The flash vessel reduces the cooling water temperature by 5 °C and provides flash steam to the compressor inlet. It also accepts condensate at about 100 °C from the wash still heating coils, which is flashed down to a common 80 °C, mixed with flashing condenser cooling water. This 20 °C drop is a significant degradation relative to the compressor temperature rise of 45 °C. Reference to Fig. 5.1, immediately suggests a separate additional multi-stage flash cooler for the wash still heating coil condensate. However, the relative flows of flash steam (see Fig. 5.2) make no economic sense of such a proposal. The screw compressor could, if there were a need, be adapted to provide bleeds or accept feeds, according to its manufacturer James Howden Ltd.

5.8 System performance

A Carnot engine inverted to become a heat pump has a first law performance denoted by $T_1/(T_1 - T_0)$, known as the coefficient of performance, which relates the heat output to the work input. In exergy analysis the end point is a comparison between the practical coefficient of performance and the theoretical value for a Carnot pump working across the same temperature difference; a genuine ratio (100 percent for a perfect heat pump) which relates the work input to the exergy in the compressor output. An accompanying feature is a breakdown of the irreversible losses, accounting for the shortfall of the practical pump. The comparison can be made even more adverse by reducing the temperature rise of the Carnot pump to a level which would be achieved if infinite heat transfer surfaces were used in heat exchangers. Both types of calculation are revealing for textbook purposes. The practical installation has to be a balance. Efficiency must be pursued only to a point far short of infinite numbers of small stages (and components) at which additional capital costs do not outweigh the performance gains. Also, as this installation makes clear, there should be robustness in the face of fuel or power price fluctuations. The real difficulty is to arrive at the practical optimum, when subject to ongoing economic turbulence.

The wash in the wash still and its vapours have thermodynamic properties, which vary as the initial charge becomes spent (Figs 5.3 and 5.4). The enriched vapours entering the condenser from the 7 percent wash decline (94 °C isotherm, 1 bar diagram) from an initial 43 percent to a final 1 percent. The wash still steam flow is adjusted manually during, and set at the end of, the initial foaming period. Thereafter it

needs no adjustment, as the wash becomes spent. The compressor outlet pressure is greater than ideal because of the throttling for independent wash still control; plus the temperature difference across the boundary layers and walls of the condenser tubes; plus the 5 °K flash temperature drop in the cooling water. The designers accepted the wash still manual control regime, and minimized the remaining temperature differences. Hence they minimized the power consumption of their heat pump, subject to the flavour constraints imposed by the nature of the product.

5.9 Performance calculation

Table 5.1 is a thermomechanical exergy account of the distiller and its heat pump.

The 51.87 kW at the end of Table 5.1 comprises: the individual throttling losses at the three wash stills, which are set by hand after foaming subsides at the outset of distillation; the degradation in the still coils and their boundary layers; and the degradation in the condenser tube walls and boundary layers.

Table 5.1

$t_0 = 10$ °C t_{sat}, $h_0 = 42$, $s_0 = 0.151$
$\xi_t = (h - h_0) - t_0(s - s_0)$

	p	t	M	$h - h_0$	$s - s_0$	ξ_t	$M\xi_t$
Flash steam outlet	0.47	80	1 920	2440.2	7.4612	327.6	628 992
Compressor spray	0.47	80	200	294.9	0.9243	33.2	6 640
Compressor wet steam	0.47	80	2 120	2237.8	6.8445	299.8	635 576
Compressor outlet	1.9	125	2 120	2675.7	7.0271	686.0	1 454 320
Wash still condensate	1.7	100	2 120	377.04	1.1599	49.75	105 470
Cooling water (warm)	0.58	85	224 266	313.90	0.9833	35.49	7 959 200
Cooling water (cool)	0.47	80	224 266	294.91	0.9243	33.2	7 445 631

Compressor shaft power = (1 454 320 – 635 576)/3600 = 227.4 kW
Compressor motor power = 227.4/0.95 = 239.7 kW = 82.7% rated power
Compressor irreversibility = 283.15(7.0271 – 6.8845) × 2120/3600 = 23.78 kW
Cooling water flash irreversibility = (7 959 200 – 7 445 631)/3600 = 142 kW, which includes the circulating pump power of about 20 kW
Wash still condensate flash irreversibility = 2120(49.75 – 33.2)/3600 = 9.75 kW
Remaining irreversibilities = 227.4 – (9.75 + 142 + 23.78) = 51.87 kW

5.10 Design alternatives

The main design variable of the three is the condenser. This has a large irreversibility, which can be examined to see if exergy savings are possible.

A useful – but not infallible – guide, which has been followed above, is to look at the largest irreversibility first (**52**).

The new condenser was specified to be of the same tall thin external shape as the traditional device, for conservation of flavour. Therefore, it differs greatly from steam turbine condensers which are the most frequently occurring examples of the art. In the latter, discussed briefly in Chapter 3, the horizontal tube bundle is entered peripherally in inward radial cross flow via generous empty channels which allow steam penetration without pressure loss. In terms of specific volume the steam almost disappears upon condensing. Permanent gases remaining as a film at the tube surfaces are a major heat transfer problem in the large evacuated (leaky) container. The distillery condenser, on the other hand, is slightly pressurized and condenses a steam/alcohol vapour mixture, necessarily without a gas ejector because of the thin-walled, vacuum vulnerable, stills.

Operating experience with the new condensers has revealed an uncalibrated improvement in performance when the owners removed the baffles from one condenser. All four new condensers have an unexplained enhanced rate of corrosion.

Condenser optimization is an extensive problem, beyond the scope of this book, and with many degrees of freedom. Also in this case there are special constraints of flavour and confinement of the product for Customs and Excise purposes. The success in removing the baffles, which might have affected flavour, is an indication that the steam turbine condenser example would bear further examination, if a new distillery with a new product, with a unique new flavour, were to be mooted. The tube bundle could be shorter and fatter and with tube bundle vapour channels; the tube diameter could be varied; a multiplicity of pressure drops on the water side could be trimmed; and any special features of mixed vapour condensation examined. The design of the up-sloping vapour pipe from the wash still could be assessed to see if it could undertake some diffuser/pressure recovery duty while maintaining flavour. The fate of the initial air atmosphere above the charge of wash in the still is an unknown which needs some clarification. The possible production of non-condensable gases by the recently fermented wash could be checked, since even small amounts of gas concentrated at

condensing heat transfer surfaces represent significant degradation. On the other hand, for the wash to boil/bubble freely and continuously, it must contain dissolved/entrained/chemical sources of gas to promote bubble nucleation.

5.11 Flash calculations

Wash still condensate flash enthalpy drop = 82.13 kJ/kg
Enthalpy of evaporation (**19**) at 80 °C = 2308.8 kJ/kg
Hence flash steam production = 2120 × 82.13/2308.8 = 75.4 kg/hr
Cooling water flash enthalpy drop = 18.99 kJ/kg

Hence

Flash steam production = 224 266 × 18.99/2308.8 = 1844.6 kg/hr
Total flash steam to compressor = 75.4 + 1844.6 = 1920 kg/hr

5.12 Performance of heat pump without accounting for chemical exergy

From Table 5.1 and the adjacent text, the compressor shaft horsepower is 227.4 kW, of which 23.78 kW is dissipated as losses. The compressor efficiency is 203.62/227.4 = 89.5 percent. Note that the performance of the heat pump should not be based on the motor power, since the motor losses do not enter the steam.

The heat intake of the pump is

$$T_0\Delta s = 353.15 \times 2120 \times (6.8845 - 0.9243)/3600$$
$$= 1240 \text{ kJ/sec}$$

Hence

Coefficient of performance = (227.4 + 1240)/227.4 = 6.45

Note also that in order to arrive at this figure the conversion – in accordance with the S.I. definition 1 Watt = 1 Joule/sec – has to be used, the unidirectional character of which was noted in Chapter 2. There is no way in which the Joule can be reconverted to 1 Watt.second of shaft work.

The heat pump, on the other hand, is a potentially reversible apparatus which will give any amount of heat in exchange for work, dependent on the temperature range through which it operates and its irreversibilities. The Joule unit is unhelpful if, for example, it is used for fuel exergy. For the latter, the Watt.second is used in this book.

The temperature range of this pump is 80–118.5 °C, disregarding the

small superheat at the compressor outlet. A reversed Carnot Cycle for this range would have a coefficient of performance of 391.65/38.5 = 10.17.

The efficiency of the heat pump is, therefore, (6.45/10.17) × 100 = 63.42 percent, a number which shows the pump performance more realistically than its coefficient of performance. Relative to the Carnot Cycle the practical pump has no expander or, relative to the infinitely staged ABCD of Figure 5.1, it has a vestigial flash cooler. Its performance is bound to have a shortfall.

5.13 Exergetic process efficiency

An alternative sense of proportion begins to emerge if account is taken of the wash still performance, namely the separation of the wash into the relatively concentrated low wines, 20 percent by mass, and a depleted low alcohol residue. Any such separation means that changes in chemical potential have occurred, that work has been done, exactly as in desalination in Chapter 2. The work, moreover, has been done indirectly by the shaft of the heat pump motor, and directly by the shaft imparted exergy of its steam output. As in desalination the magnitude of the exergy conserved is likely to be small compared to the exergy destroyed. Moreover, the plant data in the references is of the time-averaged process. To make the work visible at the plant would require rather accurate time-dependent data for one of the wash batches, and partial pressures for vapours in the still, which are not available. Nevertheless, the performance of the heat pump is marginally better than stated above.

Numbers can be put to distillation processes using the temperature composition diagrams introduced in (**49**) and the exergy composition diagrams introduced in (**53**). Figure 5.3 is from (**53**) and is an approximate exergy composition diagram for the water–ethanol system. The whisky distillation process includes more than water and ethanol, and the low concentration impurities are of critical importance to flavour; but much may be learnt from the approximate diagram, starting from a position of unfamiliarity.

The areas to the right of the dew point line, and to the left of the 12 °C mixture chemical exergy line, are of no interest. The set of curves may be thought of as a contour map of the thermomechanical exergy relative to 1 bar, 12 °C, of pure water on the upper horizontal axis, pure alcohol, saturation temperature 78.5 °C, on the bottom horizontal axis, liquid mixtures in the narrow space between the bubble point line and the chemical exergy line, and vaporous mixtures in the remaining area up to

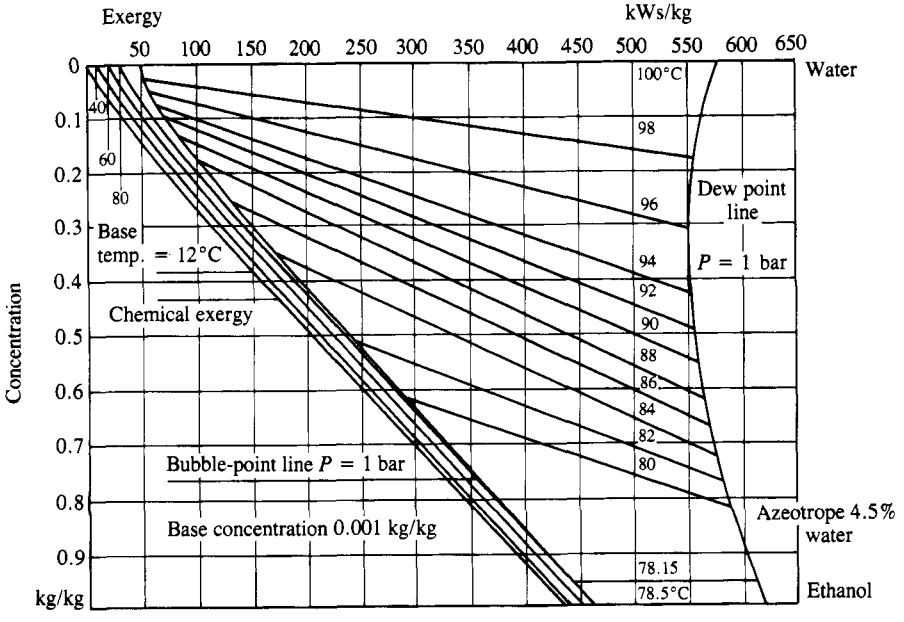

Fig 5.3 Exergy concentration diagram for water/ethanol at 1 bar

the dew point line at which exergies are a maximum. The base or dead state is 0.001kg/kg, which is too small to show on the diagram. In accordance with equation (12), Chapter 1, the total exergy is the sum of the thermo mechanical exergy and the chemical exergy. The molecular interactions which give rise to the chemical exergy of ethanol–water liquid mixtures are described in Section 7 of (**42**). Note that ethanol is not being thought of as a fuel to be oxidized, but exactly as steam is thought of in the steam tables. Hence its thermomechanical exergy, for example, is unrelated in magnitude to its fuel chemical exergy.

The thermomechanical exergy function is $(h - h_o) - T_o(s - s_o)$, and with numerical data from the steam tables, a point on the water horizontal axis can be checked, in addition to the zero at the top left corner. The dew point line value (dry saturated steam) is (2675.5 – 50.54) – 285.15(7.3594 – 0.1779) = 577.2 kWs/kg which checks with the German value. Strictly speaking h_o and s_o should have been evaluated at an ethanol concentration of 0.001kg/kg. The error is within the accuracy of the diagram.

The line labelled 78.15 °C represents the azeotropic (zero vapour enrichment) mixture of 4.5 percent water and ethanol (**42**). A water–ethanol mixture is deemed to have a bubble point rather than a boiling point. Below the azeotrope the bubble contains ethanol enriched mixed

vapour. The wash still achieves an increase in concentration from 7 percent to 20 percent ethanol by mass (**51**). (See (**42**) Fig. 7.1 for the non-linear relationship between mass and volume concentrations.) As the wash depletes, its bubble point must approach the boiling point of water, 100 °C on the 1 bar diagram, realistically 116.3 °C in the evolved 1.75 bar distiller. The mixed vapours have available to them the main condensing surfaces cooled by water at 80–85 °C and the cooler, air-exposed, naked surfaces of the still, overhead pipe, and condenser. This empirical complexity represents non-equilibrium and limits somewhat the applicability of the equilibrium Fig. 5.3.

On the 1 bar Fig. 5.3 the 94 °C isotherm initiates at a wash concentration of 7 percent, and gives a dew of 43 percent concentration. As the wash depletes, the dew concentration declines, and the dew point rises. This part of the process can also be followed on the simpler and better-known temperature concentration diagram, Fig. 5.4, again for 1 bar.

The actual 'low wines' concentration of 20 percent discloses a mixing of the dews as a function of the batch distillation time, an irreversible process which dissipates separative work. From 7 percent wash to 20 percent low wines represents, on the Fig. 5.3 bubble point line, an exergy increase of about 50 kWs/kg of mixture. The depleted wash has zero exergy on this diagram. It is at the selected dead state. The depletion

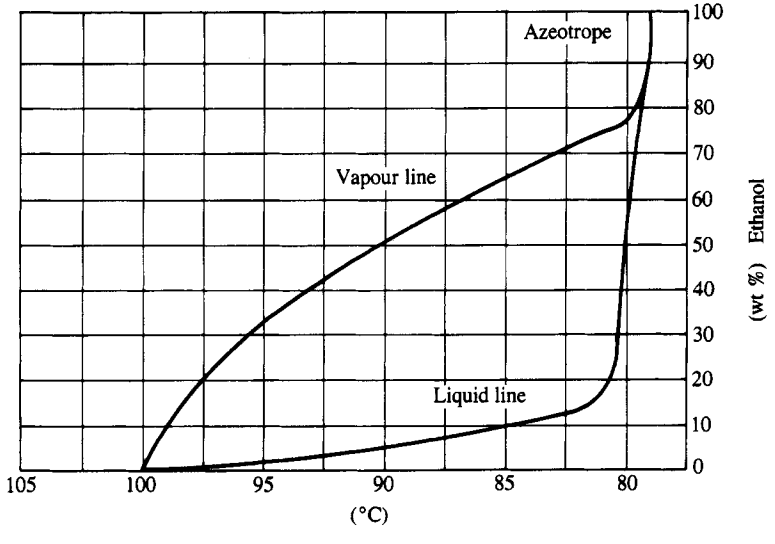

Fig 5.4 Temperature concentration diagram for water/ethanol

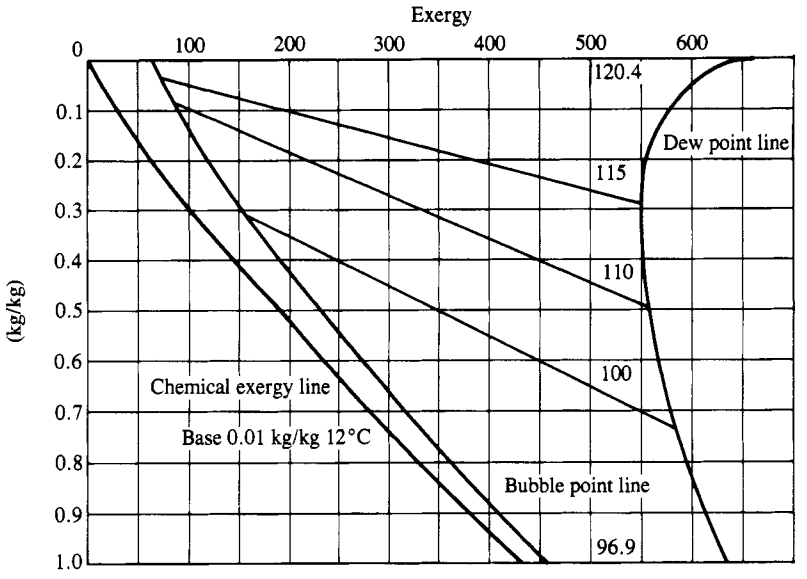

Fig 5.5 Exergy concentration skeleton diagram for water/ethanol at 1 bar

is worth about 16 kWs/kg. These changes represent conserved heat pump output, a little of which is lost in sub-cooling. At the wash still about 4900 litres of low wines are produced from a 14 500 litre batch of wash in 5.25 hours to leave a residue of 9 600 litres of near water. Treating the litres as kg, for a first approximation, the low wines amount to $4900 \times 50/3600 = 68$ kWh and the spent wash $9600 \times 16/3600 = 43$ kWh. In the 5.25 hours the heat pump compressor shaft at 227.4 kW absorbs 1194 kWh of which 111 kWh are conserved as chemical exergy. The dissipated power of the compressor shaft can be reduced by $111/5.25 = 21$ kW to 206.4 kW. The coefficient of performance becomes $(206.4 + 1240)/206.4 = 7.01$ and the efficiency $7.01/10.17 = 68.9$ percent.

On the 1 bar Fig. 5.3 the cooling water temperature of 80 °C always leaves some small driving force for condensing heat transfer available relative to the dew point, but the process is slightly pressurized at 11psiG or 1.75 bar. For steam, a pressure rise of 0.75 bar, there is a saturation temperature rise from 99.6 to 116.3 °C. Hence the driving forces for condensing heat transfer are much more generous than indicated on Fig. 5.3. ξ_t values in Fig. 5.3 have been checked out using the software GAS.VLE already used in Chapter 3 for gas turbine combustion. A skeleton diagram for 2 bars is given as Fig. 5.5 from the same software. For practical work the requirement is either access to the software or a

set of tables at intervals of 0.1 bar. The diagrams in Figs 5.3, 5.4 and 5.5 suffer from the limitations of computerized drawing, as well as any data inaccuracies. They are good enough to get the drift of the argument.

Note that the process of fuel ethanol production (**54**) from biomass is a near relative of potable ethanol distillation, but unconstrained by considerations of flavour. In such a process there could be merit in separation of differently concentrated steams of distillate, so avoiding mixing losses and minimizing the separative work of subsequent stages. The usual balancing act is required, which will compromise between an infinity of stages, and over-simple brutality.

5.14 Process perspective

The complete story starts with the breakdown of starch during mashing, to yield wort and an animal food residue called 'draff'. Fermentation of the wort yields the wash, which is double distilled to give the final spirit. This series of reactions and separative steps, which commence with the unknown of starch, represent changes in Gibb's potentials of formation and chemical potential, in which the boiler/heat-pump partnership is involved, via batch preheating for improved reaction rate during hydrolysis and fermentation, and via heating of the spirit stills. The actual changes of ΔG_f, (**42**), are starch/sucrose unknown, sucrose/glucose 633 kWs/kg, glucose/ethanol + carbon dioxide 166.16 kWs/kg. A story is also missing for the multiplication of the yeast during fermentation.

Each mol of ethanol produced is accompanied by a theoretical work output of a minimum, neglecting the hydrolysis of starch, of $800/3600 \times 8 = 0.0275$ kWh which could be electricity to drive the heat pump. In 5.25 hrs 4900/5 kg of pure alcohol are produced by the wash still, a power production of $980 \times 0.0275/46.03 \times 10^{-3} \times 5.25 = 111$ kW, a substantial contribution to the heat pump drive. In the absence of suitable fuel cells, none of this power is realized. This status may be compared with the chemistry of the human body which, in return for food, exactly as consumed by the distillery, will provide superbly controlled motive power, warmth, and the manifold chemicals needed for food processing, self-repair, and replacement. All these are achieved by isothermal processes in a blood-bath at 37 °C, controlled at that temperature by heat and vapour transfer to the air.

Chapter 6

Practical Fuel Cell Systems for Hydrogen, Power, and Heat Production

'Forget six counties overhung with smoke,
Forget the snorting steam and piston stroke,'
William Morris

6.1 Introduction

William Morris dreamed of, and fuel cell pioneers foresaw, conversion of fuel to electricity, without Carnot's limitation, without rotating plant, without heat, and without pollution. A recommended starting point for the reader seeking the realization of the dream is (**55**) the Grove Anniversary Symposium Series, London, published every two years since 1989 in the *Journal of Power Sources*. Sir William Grove, the inventor of the fuel cell, recorded his conceptions in 1839. His key notion was the need to achieve a 'notable surface of action' between his hydrogen and oxygen reactants, his dipped platinum strip electrodes, and his liquid electrolyte by convoluting the meniscus at which the action occurs via an extended surface. An obstacle to the analysis of practical fuel cells is the absence of a generally accepted equilibrium theory of the reformer/cell system, as attempted in Chapter 4, and the non-availability of test results designed to be interpreted against the background of such a theory. Meanwhile, mere descriptions and theoretical generalities must suffice.

The Japanese phosphoric acid fuel cell (**56**) which is a main example in this chapter, is a modern descendent of Groves' ideas. It uses gas-fired, steam-reformed, hydrogen fuel, platinum alloy catalyst loaded porous carbon electrodes, and pressurized phosphoric acid electrolyte at around 200 °C. The pressure, the temperature, and the catalyst are aids to increased reaction rate. Modest conditions for small units such as this one are 4 bar, 190 °C; and advanced conditions for large units 8 bar, 205 °C.

Groves' dipped strip electrodes have, in most modern cells, matured into horizontal flat sheets with porous substrates giving an extended contact area. The cell mechanical arrangement is a horizontal sandwich, and groups of series-connected cells are called 'cell stack assemblies'. For a large power output, multiple cell stack assemblies are needed. The useable fuel is hydrogen, which must be freed from its natural combined forms (water or hydrocarbons). Carbon and hydrocarbon gases are on the sidelines awaiting higher reaction rates, cheaper catalysts, and better economics.

As noted in Chapter 4, the direct isothermal oxidation of methane and the higher hydrocarbons in natural gas could eliminate hydrogen production and lead to cell half-reactions and overall reaction, with minimum entropy change and near-zero heat production: an ultimate target for economy and efficiency (**43**).

Industrial hydrogen comes from steam reforming of hydrocarbons, mainly natural gas (**57**), or could in the future come, for example, from solar cell electrolysis of water. In the latter case the fuel cell releases stored solar radiation. Bacon (**58**) whose fuel cell kept the concept alive through much of the twentieth century, regarded his hydrogen-fuelled, oxygen-breathing device as a storage system. He employed a cell stack of vertical sandwiches comprising bi-porous, sintered powder, nickel electrodes and a circulated caustic potash solution as an electrolyte at 200 °C, and up to 45 bar, without the need for platinum catalyst. Bacon's electrodes were bi-porous double layer, so that the circulating, condenser-dried hydrogen fuel could, from the coarse side, meet the surface tension of the confining electrolyte at the convoluted meniscus, at the fine/coarse interface. Bacon protected his cathodes from oxidation by means of a p-type semi-conducting oxide film, prepared by impregnating them with a solution of mixed nitrates of lithium and nickel. After drying and firing at 700 °C the film was ready. Re-optimization of Bacon's heavy, earth-bound cells at reduced pressure by Pratt and Whitney provided the means to power the Apollo moon landings. The modified reaction-rate-determining parameters, were electrolyte concentration, up from 30–70 percent, electrolyte temperature up from 200 °C–260 °C, as part compensations for operating pressure down from 45 bar–3.4 bar; all worth recounting to illustrate design compromises. Too high a temperature would initiate solidification of the porous nickel, or cause component corrosion.

By general consent, the phosphoric acid cell operating at about 200 °C, will be the first of the many competing systems to achieve modest commercialization (**55**) (**56**) (**59**). For that system the Japanese 'Moonlight' programme (**56**) (became 'New Sunlight' in 1997) shows development of

robust 1m × 1m square 'glassy' carbon sheets (separators) and ribbed porous carbon substrates with a range of pore sizes, by a variety of competing manufacturing routes. These indicate future fuel cell technology and cell stack dimensions. The ribbed substrates are an aid to increased electrolyte content and extended cell life, via extended electrolyte dry out time. Some general arrangements of American phosphoric acid cell sandwiches are illustrated in (**60**), including cross-flow ribs.

Platinum alloy catalysts of reduced cost/increased effectiveness are being evolved, in Japan (**56**) and elsewhere.

All the components of the Japanese fuel processing train are under development, by competing manufacturers (**56**).

A first sight appraisal of carbon against nickel indicates poorer electrical conductivity (higher ohmic heat generation), better corrosion resistance, and high-temperature capability, again highlighting the subject of design compromise. Bacon avoided platinum – the phosphoric acid system needs it, and would benefit economically from a cell arrangement leading to inexpensive platinum recovery.

An objective of this chapter was to use a Japanese working system to demonstrate qualitatively the nature of the irreversible losses in fuel preparation and in the cell itself which, even in the absence of a Carnot limitation, hinder the realization of economic fuel cells. Unfortunately, due to unsuitable test results, this objective could not be achieved. All the system components are relevant, from fuel desulphurizer to direct current inverter. In terms of volume and mass the cell stack is a small part of the system (**56**) (**60**) (**61**).

A summary of as yet unmentioned relevant features of the phosphoric acid fuel cell is as follows. The electrolyte is static; uncirculated. When exposed to air as the cell oxidant, it does not interact with (i.e. rejects) the atmospheric carbon dioxide; similarly with the larger carbon dioxide content of reformed/shifted natural gas fuel.

A useful coolant is air, an electrical insulator which, relative to water, leads to reduced damage in the event of electrolyte containment leakage. If steam production is required, water can hardly be avoided. The reaction product is discharged as steam. Destructions of fuel exergy in the cell processes add somewhat to the reversible entropy growth of the electrochemical reaction, and lead to coolant streams at around 200 °C, a temperature high enough, in the example given in this chapter, to motivate an absorption refrigerator/air conditioner. Note that improvements in internal performance reduce the exergy destruction and the necessary coolant flow. An electrically driven heat pump could add to the heat output if required.

6.2 Theoretical considerations

In Chapter 4 the fuel chemical exergy was derived from consideration of equilibrium processes in Fig. 4.1 and its Van't Hoff box, or isothermal enclosure. In practice, increased cell reaction rate must be pursued, by catalyst, and via increased pressure and temperature. This requires an engine or a process to use the resultant high-temperature heat. References on electrochemistry, such as (**42**) and (**14**) deal mainly with fixed, consumable electrode galvanic (spontaneously reacting) cells. The fuel cell is in the same family, but uses a steady flow of gaseous reactants, which are included in the thermodynamic treatment of Chapter 4. The steady flow of reactants is maintained by expanders and compressors, adjusted to the equilibrium concentrations in the coupled anode and cathode reaction spaces. The reversible cell must be equipped with rotating plant. Its emf is $\Delta G_t/2F$. To operate at elevated pressure and temperature, it must deliver its heat output to an engine or chemical process, such as a reformer. Mature consideration of real cells with substantial internal heat generation, indicates that the cell losses are the more useable in the engine, the higher their temperature of release. In other words the entropy growth arising from losses in the cell is reduced as the cell operating temperature rises. The optimum hydrogen production/cell/engine/process combination is perhaps emerging, see Fig. 6.2.

The practice is current (**55**) (**56**) and (**61**) of assessing fuel cell performance on the basis of the lower/higher heating value (net/gross enthalpy of combustion). This non-thermodynamic commercial compromise will be justified if it sells the fuel cell, but inevitably creates confusion, now and in the future, which can be unscrambled only by exergy analysis. Since the enthalpy of combustion (gross or net) carries Carnot's limitation, it is inapplicable to near-equilibrium fuel cells. This book uses exergy analysis exclusively.

6.3 Description of NTT Japan small fuel cell for combined power and heat

The general scheme is shown in Fig. 6.1 (**61**) (**62**). The fuel cell needs a large system of fuel treatment auxiliaries, which give rise to irreversibilities, additional to those incurred in the fuel cell stack. Sulphur must be removed from the fuel gas, because it poisons the reformer catalyst. (The Japanese have several types of desulphurizer under development and do not say which one is used by NTT.)

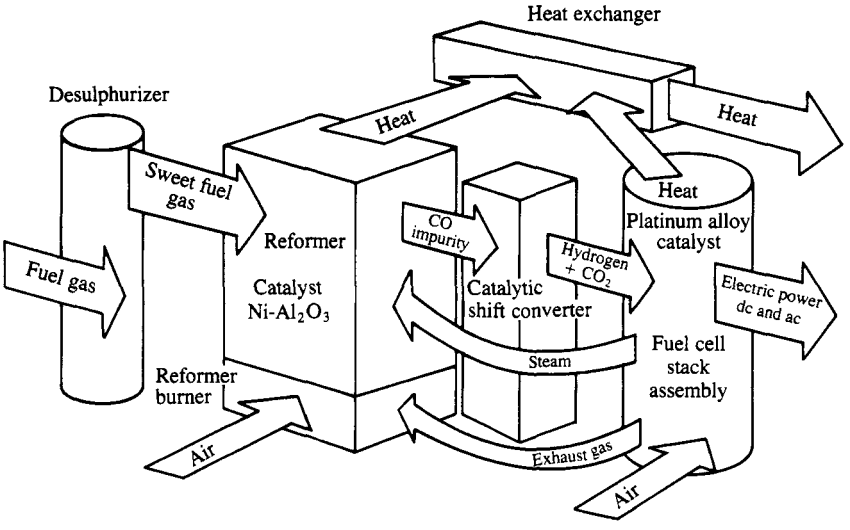

Fig 6.1 Scheme of NTT Japan phosphoric acid fuel cell – 50 kWe

The catalytic reformer is driven by anode exhaust gas. From hydrocarbons and steam it yields carbon monoxide and hydrogen. Note that hydrogen is contributed by the steam, as well as by the methane, see Table 6.1 for standard conditions. Details of the industrial reaction with excess steam are given in Chapter 7. For some fuel cells CO is a fuel, (MCFC and SOFC), and for others, such as this example, it is a catalyst poison and is removed in a catalytic (iron oxide?) water gas shift converter ($CO + H_2O = CO_2 + H_2$), requiring an unshown steam supply. The fuel cell oxidizes much of the hydrogen and rejects the CO_2. The resulting lean anode exhaust gas is combustible with air, and is used to heat the reformer and its excess steam. In high-temperature fuel cells, (SOFC/MCFC), reforming can be achieved using anode heat from the electrochemical reaction, a relatively efficient process compared to the use of fuel in the reformer. Rejected heat from the reformer and from the cathode exhaust are channelled to a heat exchanger, which in turn powers an absorption air conditioner. Direct current from the fuel cell stack is used to power communication equipment, while the remaining

Table 6.1 Methane/steam stoichiometric reforming

CH_4+	$H_2O=$	$CO+$	$3H_2+$	+206.1 kJ/mol, $\Delta_r H$
−74.81	−241.82	−110.53	0	ΔH_f kJ/kmol

motorized plant gets an alternating current supply from an inverter. This lays the foundations of an energy balance for the system – an essential preliminary to an exergy account. It is clear that there is a need to distinguish near-equilibrium reactions (cell electrochemistry) from non-equilibrium reactions, combustion, reform reactions, shift reaction, and desulphurization. The distinction between equilibrium and non-equilibrium reactions is the qualitative foundation of the exergy account, and a guide to performance improvement (reduced irreversibility).

6.4 NTT fuel cell performance and losses

Reference (**56**) states that, 'The test showed the maximum total efficiency of the fuel cells to be 70 percent (electricity 40 percent, heat 30 percent)'. Results in that publication are based on the HHV. To be understood, the asserted performance would have to be enlarged into an energy balance, showing the detailed fate of the 30 percent heat, which is then valued for its thermomechanical exergy content. In many analyses the work and the heat are added directly – a practice which ignores both the thermodynamic and the economic value of electricity. Lack of data will preclude exergy analysis. The gas analysis is unstated, so to get at the order of things, the natural gas of the gas turbine of Chapter 3 can be used (the desulphurizer would be redundant). Electrolyte conditions of 4 bar 190 °C, appropriate to the smaller Japanese units, will be assumed. An environment temperature of 25 °C is reasonable. From Table 3.1:

HHV is 47 624 kJ/kg	(37.5 MJ/m^3)
LHV is 42 989 kJ/kg	(33.85 MJ/m^3).
The fuel chemical exergy estimated in Chapter 3 is	(68.6 MWs/m^3).

Figure 6.2 shows further details of the plant, leading to a better qualitative picture of the breakdown of the losses. The figure also shows the versatility of the reformer, which for continuity of power supply can cope with two auxiliary fuels stored on the premises. Following the gas fuel route, the details of the desulphurizer are not known, but any separation process involves exergy destruction. The reformer is required to carry out an irreversible endothermic process which, if supplied with the stoichiometric steam quantity, would not go near to completion. To supply the necessary two or three times the stoichiometric steam requires additional fuel/heat, which is fortunately available unconsumed from the anodes of the cell stack. Water cooling of the cells provides the reformer steam supply. This takes up, with some exergy destruction, the cell losses and heat of reaction. The cell losses are mainly power dissipation in ohmic

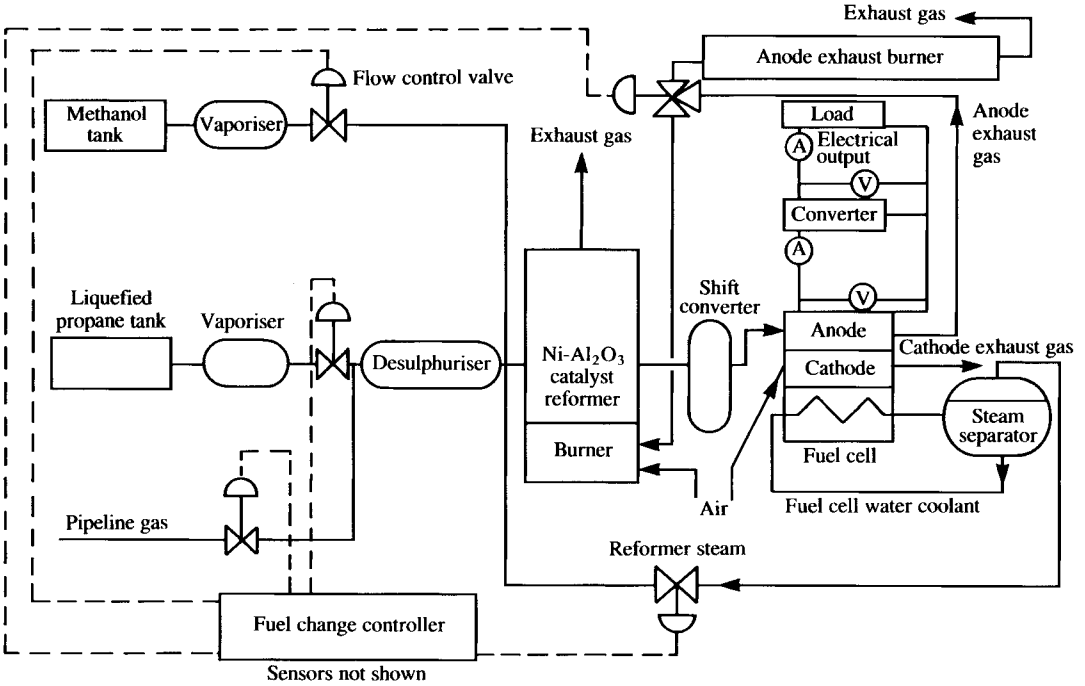

Fig 6.2 Detailed flowsheet, NTT Japan phosphoric acid fuel cell

resistances, of electrolyte and electrodes, electrode over potentials, and in the phenomenon of concentration polarization (**42**) within the electrolyte. The operating point of the cell is selected as the maximum current which can be drawn, before concentration polarization begins to cut the current back. The cell stack exports exergy in the steam from its coolant and in its anode and cathode exhausts. Note, however, that the entire steam supply is taken up for fuel processing. Finally, surplus heat from the reformer, and from the cell stack, are taken to a heat exchanger for onward passage to the absorption refrigerator. The cell succeeds in its objectives as a communications power and heat supply, and in carrying the burden of using a fuel, which must be released from its natural combined state.

The following are unaccounted consumers/suppliers of heat, power, and materials: the desulphurizer, the exothermic water gas shift converter, power for air circulation to the reformer burner and cathodes of the cell stack, power for cell stack water circulation and feed, power for the instrumentation and control system, and power for circulation of the heat carrier to the refrigerator. The anode exhaust may need circulation power. Proper account must be taken of the thermochemistry (see discussion of the reformer above).

The pure exergy destroyed during power consumption (Watt-seconds of work potential destroyed to become Joules of low grade energy flow) will appear as heat in the various streams, or leak to the atmosphere. Exergy analysis cannot proceed without a quantitative energy balance, and a material balance.

Within the air-breathing fuel cell the relationship between the operating cell emf of about 0.7V and the reversible cell emf of about 1.23V is not as simple and (**14**) as, for example, references; (**42**) calculate for laboratory equipment. Steady flow gives rise to unoxidized fuel and unconsumed oxygen via composition and emf gradients at the electrode surfaces in the anode fuel mixture stream and in the cathode air flow, with associated parasitic currents in the electrodes and electrolyte. Reference (**43**) opens up this subject. Equilibrium fuel cells are immune to such considerations.

6.5 A modern SOFC fuel cell integrated with a gas turbine

This section refers to the Grove Symposium of September 1997 (unpublished at the time of writing). Solid Oxide Fuel Cells have evolved to the stage where their integration with gas turbines, and later with combined gas/steam cycles as in Chapter 3, can be contemplated. Figure 6.3 is the author's distillation of a Westinghouse flowsheet slide, shown at the 1997

symposium. Note that the term 'topping cycle' is inapplicable. The turbine inlet temperature of the gas turbine at 1200 °C is higher than the fuel cell operating temperature of 1000 °C. The benefit of the fuel cell, however, arises from the superiority of its isothermal oxidation process relative to Carnot limited combustion. The fuel cell has a performance equivalent to an engine with an unachievably high mean heat intake temperature. The fuel cell unburnt fuel and unconsumed oxygen are swallowed by the gas turbine combustion chamber, without addition of further fuel. The gas turbine compressor output is fed to the central tubular, re-entrant, recuperator tube of the all-ceramic Westinghouse Sure Cell™ (**55e**) fuel cell. Similar layouts are being developed by Rolls–Royce/Allison using planar, as distinct from tubular fuel cells (**55e**). The competition is afoot to develop mass-produced, low cost, high-endurance, fuel cell stack designs for gas turbine and, later, large unit size combined cycle, integration.

At 1000 °C reform/shift at the anode is so effective that it creates a local cold spot, and separate reformers are needed pending resolution of this temperature distribution problem. Cooler cell operation, perhaps as low as 600 °C is proposed by various materials developers, using new proton conducting solids. Going below the compressor outlet temperature would be awkward. Such reduced temperature would spread out the reform/shift and ameliorate the temperature distribution problem. In addition, a very important economic characteristic would be

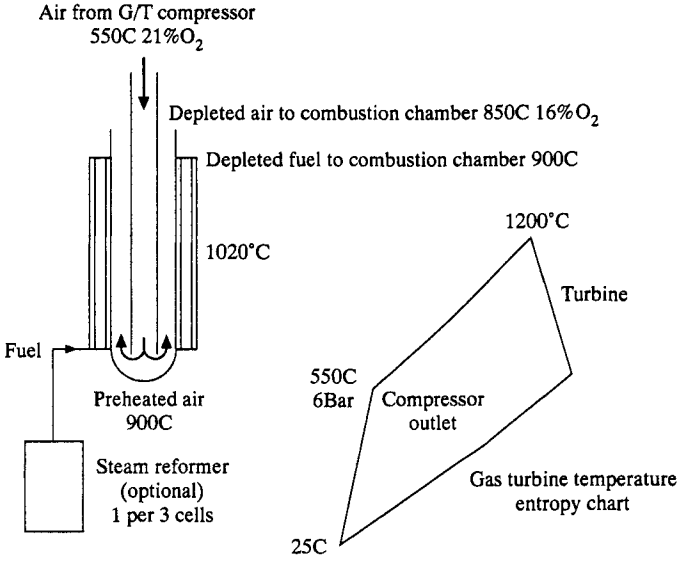

Fig 6.3 Integration of Westhinghouse Sure Cell™

influenced, namely the cell endurance and emf deterioration with time. A shakedown is needed in which, as a minimum target, gas turbine hot gas path parts renewal and fuel cell stack replacement can be orchestrated.

6.6 Effect of modified chemical exergy definition

An enlarged value for the fuel chemical exergy means lower calculated efficiency. Alternatively, it means that the opportunity to exploit fuels is a bigger one. Alternatively again, in photosynthesis or in practical fuel cells, the chemical reaction is struggling to move towards an equilibrium with a very low concentration of reactants. Such a reaction may well suck its reactants from source, unaided by a circulator. Clearly photosynthesis does this with atmospheric carbon dioxide. Some atmospheric pressure fuel cells do the same.

6.7 Further outlook

The perspective of the 1997 Grove Symposium was that the SPFC (**76**) is the prime candidate for vehicle propulsion, with large-scale capital investment in mass-production commencing, for example, Daimler-Benz/Ballard in Canada and Toyota in Japan. The fuel production infrastructure is an open competitive question. The vehicle may have a methanol fuel input to a 300 °C methanol reformer fired by anode hydrogen. An industrial methanol infrastructure would be needed – a significant pollution problem detracting from the clean car.

The photo-voltaic powered electrolysis solution to hydrogen production is immature (expensive) and the nuclear-powered alternative is stalled at the time of writing. Electrolysing in an inverted fuel cell could be attractive. Cheaper, more productive, photovoltaic, mass-produced alternatives are an industrial objective.

Nibbling at the edge of the vehicle market are the MCFC and the lower temperature versions of the SOFC, with direct anode reform. These competitors are immature, but promise natural gas utilization: a different fuel infrastructure.

All cell types will compete in the market for stationary power production in small unit sizes, distributed power production (notably at hospitals), and in military applications.

The competitive outcome can only be awaited, with evident dilemma for investors in a beckoning market.

Chapter 7

Remarks on Process Integration

'We are not here to sell a parcel of boilers and vats,
but the potentiality of growing rich,
beyond the dreams of avarice'.
Samuel Johnson 1781

7.1 Introduction

In this chapter, the process of steam reforming of natural gas is further studied, after its introduction in Chapter 4 on fuel cells. The practical example is a large-scale industrial reformer, operational since 1972, feeding a complex which includes methanol production and hydrogen separation using a pressure swing adsorption plant. The design of the reformer heat exchange network and integrated power plant, commencing 1968, somewhat anticipated the formerly named pinch technology (**64**) with which, however, it is sufficiently compatible to facilitate a modest dip into that extensive subject. The assertion that pinch technology/chemical pinch analysis/process integration, is 'exergy analysis with a difference' is appraised (**67**).

7.2 Remarks on process integration

In Chapter 4 some theoretical process integration is carried out between equilibrium chemical reactions, using isentropic and isothermal circulators, together with Carnot cycles. Such components are not particularly practical. However, there is an indication of what has to be done in practice.

Process integration (**64**) is a name for the business of minimizing exergy destruction, and investment, when dealing with complex non-equilibrium industrial chemical processes. Alternatively, from a first law

angle it is a way of saving heat and capital expenditure. The processes, namely reactors (new molecules) and separators (increased concentrations), have to be optimized, integrated with each other, with power plants, with heat pumps, and (importantly) using heat exchanger networks. The arrangement of the latter has to be selected, with economy of effort, from a sea of alternatives. Some aims are to ignore unavoidable losses, to couple thermodynamics and economics, and to generate target system performances. Note that chemical exergy changes in reactors and separators are not dealt with in (**64**).

The basic problem can be grasped by considering the reforming of natural gas to produce hydrogen for the phosphoric acid fuel cell as outlined in Chapter 6. The practical process employs thermodynamically irreversible (non-equilibrium) reactions and components. Economies are achieved by using an integrating network of heat exchangers. Incoming gas is hydrodesulphurized by injection of hydrogen and passing the heated 400 °C mixture over a catalyst to convert organic sulphur compounds to hydrocarbons and H_2S. The latter is absorbed in zinc oxide to form water and by-product zinc sulphide.

The next process, the steam reformer, which is a heat exchanger/reactor, needs an exit temperature of approximately 850 °C, from an endothermic reaction, so the 400 °C desulphurized natural gas plus excess steam, has to be heated to, and maintained at, reaction temperature. Both the hot flue gas and the hot reaction products then have to be dealt with, see Fig. 5.5. The flue gas passes to a heat exchanger, to motivate the working fluid of the absorption air conditioner. The reaction products must be cooled for the catalytic water gas shift reaction, for example by giving up heat, in a heat exchanger, to the reactants entering the reformer. Both the incoming anode fuel stream and the cathode air stream must be adjusted to fuel cell conditions, involving heat exchange. A heat exchange network is quickly growing which has no doubt been optimized by the Japanese in relation to their fuel cell. Fuel cells and their fuel trains are relatively recent arrivals in process integration studies, hence a degree of heightened interest.

In general (**63**) the elements of a heat exchanger network are *interchangers*, which exchange heat between process streams selected for their matched characteristics, or *heaters/coolers*, which exchange heat between process streams and heat source or sink streams associated with, for example, a power plant. The heat exchangers are intended to conserve thermomechanical exergy, but in the process some of the exergy is lost. The loss has to be minimized.

7.3 Examples of combined power and process already covered

In Chapter 2, regenerative Rankine cycle power and multi-stage flash desalination were linked, distorting and creating losses in the regenerative Rankine cycle. It was concluded that the increased chemical exergy of the fresh water output was as vital a part of the analysis as the electricity output. In Chapter 3, a gas turbine and steam turbine have been integrated using a heat exchanger network, which exhibits a so-called *utility pinch*. The plant is bled steam coupled to very simple unintegrated processes which destroy all the exergy in their input, for an economic return. In Chapter 5, a heat pump has been integrated into the operation of a whisky still, and again the highlight is on the fact that the heat pump can be correctly analysed, only if the increased chemical exergy of the concentrated spirit is considered as a heat pump motivated process output. These notions have to survive in the consideration of larger multi-process operations.

7.4 Pinch technology

In recent history since the early 1970s there has grown, from a nucleation point in chemical plant engineering, the technique called 'pinch technology' (**63**) (**64**), which started with the integration of processes using heat exchanger networks and grew to include heat engines and heat pumps, the designs of which have to be adapted to the process pinch. Pinch technology pre-supposes the optimization of individual processes, and deals with the destruction of thermomechanical exergy, within the integrating heat exchanger network (**66**). As the name implies, the 'pinch point' is seen as a crucial concept, central to designing practical and economical heat exchanger networks.

In chemical plants thermomechanical exergy is converted to chemical exergy, while some exergy is destroyed. Accordingly there must be a thermomechanical exergy source: a power plant, a process furnace, or both. It is necessary in this chapter to expand the Chapter 2 treatment of the Rankine regenerative condensing power plant via Fig. 7.1; a system which would have sufficed in place of the combined cycle plant of Chapter 3 in earlier times, to motivate its processes. The plant is more modern than that of Chapter 2. The steam conditions might be 120 bar, 540 °C, in contrast to 61 bar, 485 °C.

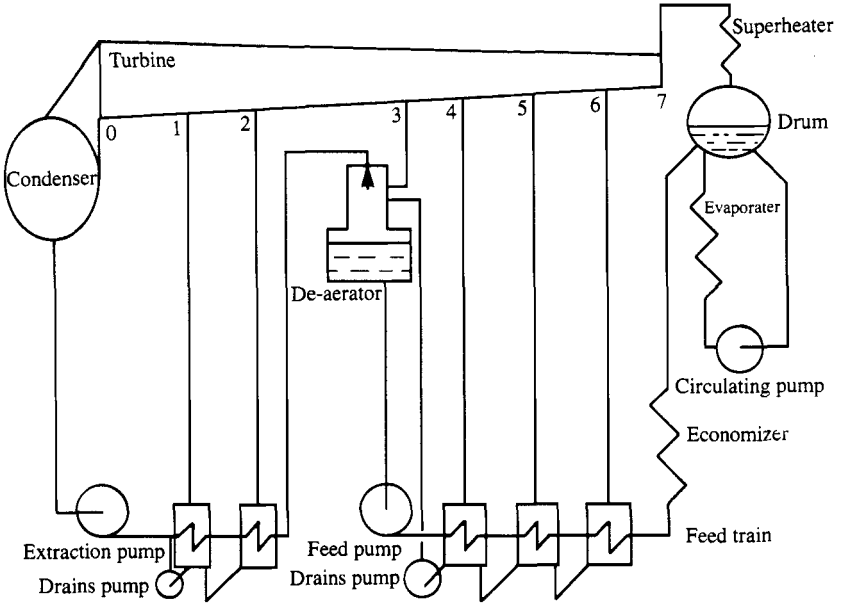

Fig 7.1 Rankine cycle power plant in chemical factory

7.5 Rankine cycle plant in a chemical factory

The boiler could have a standard steam generator furnace or feed on the heat from a high-temperature process, as in the practical example used later in this chapter. The Rankine, regenerative-bled, steam feed heating cycle, by virtue of bled steam heating, has a raised mean heat intake temperature from the fuel; a reduced external irreversibility (Chapter 2); and an increased efficiency. The bleeds can be extended to processes, with some cycle distortion and losses, as in Chapter 2. At the design point there is an optimum: at which steam directions and blade angles coincide; at which the casing fits the flows; and at which the radial equilibrium of the steam is well balanced by the leaned and twisted blading; and at which the full condensate flow is attracting proportionate bled steam to the feed heaters. A condensing turbine squeezes the last iota of exergy from its exhaust. The cycle efficiency is metallurgically limited by low mean heat intake temperature.

To provide for process needs, the turbine can be terminated at, say, bleed 2 or 3 to provide back pressure steam. The condenser may still be needed to dump the back pressure steam in an emergency. Note that the energy in bled steam or back pressure steam is indestructible. Accordingly, even when

the steam is used as a reactant and, with accompanying irreversibilities, contributes exergy to new molecules, or motivates the increase of a concentration, there must be a heat rejection device which substitutes for the turbine condenser. For example the desalination plant in Chapter 2 has its own independent condenser, somewhat larger in capacity than the displaced part of the steam turbine condenser, because of the relatively poor thermodynamics of multi-stage flash distillation compared to engines. (MSF exergetic efficiency < 4 percent, heat engine about 70%.)

There is no particular power plant thermal performance merit in back pressure operation. It is solely a means of tailoring the power plant exergy source to the demand of the process exergy consumer. (See Fig. 7.5 and associated discussion below.)

The thermal performance of most chemical processes is likely to be poorer than that of an engine, although the MSF example above is extreme, so with the best of tailoring the combined exergetic efficiency of an engine and a process will be below that of an engine alone, see Chapter 2. It is by good process integration that exergetic efficiency will be maximized, and avoidable losses minimized.

In a back pressure cycle the main condensate, returned for example at close to the saturation temperature of 120 °C corresponding to the back pressure, is regeneratively bled-steam heated in steps to just short of drum saturation, the final step being in the economizer. If ambient temperature make-up is used, then low pressure bled steam is not available for step-wise regenerative heating with minimum irreversibility.

The steam bleeds are available as reactants (make-up must be available), to operate endothermic processes, to drive pumps, and so on. Also available to interact with the processes are the stage by stage heated condensate, live steam, combustion air, and flue gas. Note, however, that unless otherwise specified, the turbine design point and optimum performance will be when operating the feed train only. Additional extractions of process steam or condensate will cause losses by moving the turbine away from its design point. If the bleeds to process are known in advance the design point can be adjusted to take account of them. The existence of bled steam feed heating usually dictates an air preheater in the steam generator, so as to achieve an economically low stack temperature. Process feeds at ambient temperature are an alternative means of reducing the stack temperature.

In the case of a condensing machine, as in Chapter 2, the condenser exhaust must not be reduced too far relative to the design point, or the flow in the lowest pressure stages will become chaotic and the low pressure cylinder will overheat.

7.6 Auxiliary drives

As an exercise in looking at auxiliary drives (**71**) the motivation of the feed pump of Fig. 7.1 can be considered (in the absence of processes to which adaptation may be required), no drive being shown. In power plant practice various forms of steam drive and electric drive may be found. The issue is affected by:

a) thermodynamics;
b) start capability after total power failure (black start);
c) variable speed capability, and feed regulation;
d) capital costs.

The solutions adopted have varied as technologies have waxed and waned. Figure 3.4 serves to illustrate the drive turbine internal thermodynamics when a nozzle controlled main turbine is used. That should be the case in a variable load industrial plant, which needs to minimize its internal losses, and optimize its economics. Due to water droplet effects, the expansion of wet steam is somewhat less efficient than dry steam, so pump drive turbines are slightly more efficient in the dry field.

On the other hand, a turbine with its own condenser can be fed with live steam during a start up sequence, once cooling water is available. It is important to repeat that a turbine exhausting to the condenser carries no penalty on that account. There is trivial exergy in its exhaust; nothing to be destroyed. The scantlings and cost of a low-pressure auxiliary turbine will be much heavier than those of a high-pressure machine, and interactions with the casing size of the main turbine are unlikely to take place, for manufacturing reasons. The designer can choose between high flow, low pressure ratio drive turbines, and the converse.

Drives which fully use, and do not perturb, the regenerative Rankine cycle are either direct from the turbine shaft or via an electric motor. However, feed pump steam drives arranged between bleeds, say 6 and 4 in Fig. 7.1, are acceptably small perturbations. In order to understand the working of such a scheme it is necessary to include the feed heaters and to remember that the turbine safety system avoids thermal and hydraulic shocks and so prevents back flow in the bled steam pipes. The drive turbine exhaust must be condensed in heater 4, reducing but not stopping the number 4 bleed. A larger drive could span from 6 to 3 and condense in two (4 and 3) heaters, which presents a more complicated layout problem than an electric drive, and be assessed for behaviour at turbine trip, and restart.

Steam drives are amenable to variable speed control, which eases the stress on feed regulators at part load. Black start capability is a complex issue, affected by emergency diesel capability and the whole plant start sequence. Suffice it to say that if black start capability is required, then early in the sequence steam pressure needs to be raised and a steam feed pump initially valved to live steam, may have a part to play.

When electrical drive is used with modern electronic equipment, speed control can be provided. Of course, the drive power is subject to mechanical to electrical conversion in the generator, and electrical to mechanical conversion in the motor, as well as passing through at least one transformer. The capability to start the feed pump from the grid as an early move in a start up sequence may be important. Electrical drives connected up by mere cables rather than insulated pipes are a layout preference. The thermodynamic, capital, and fuel-cost arguments between the various options are marginal. No great savings can be expected from the choice of feed pump drive system, which is not to say that marginal savings should not be pursued. One way to tackle the problem is to start with an electric feed pump drive, and try to establish a case for changing.

The use of externally generated power for drives, is hedged about with contractual considerations beyond the scope of this book. The central power plant may well be more efficient than an industrial installation, but the negotiation of a related low price may be difficult. Peak demand is a sensitive monetary topic.

7.7 Combined cycles and simple gas turbines

In the event that the power plant is of the combined cycle type, looked at in Chapter 3, then the steam turbine has no need of a feed train, other than a part steam/part flue gas heated de-aerator. The bled steam arrangements can be tailored to the processes, in the absence of the constraints of feed heaters (back flow remains forbidden), but within the limitations of the turbine cylinder arrangement. Any desires for part load operation which varies the bleed pressures, needs assessment. A relatively low stop valve pressure is available in the example given in Chapter 3, but as combined cycle optimization becomes more sophisticated, gas turbine exhausts are warming up, and the opportunity for higher steam pressure in conjunction with reheat is improving. Moreover, the first large industrial gas turbine with reheat has entered the market, leading to even hotter exhaust and higher steam pressure.

High excess air gas turbine exhausts will support combustion, and need consideration if very high process temperatures are needed. A simple gas turbine exhaust may fit the needs of a process, the steam cycle having been displaced by an alternative exergy converter, namely a chemical reaction.

With a combined cycle there are no feed heaters to condense steam exhausting from a feed pump drive, so only an electric or a condensing steam drive can be contemplated, subject to an appropriate bleed being available. Electric drives are used in Chapter 3.

7.8 Integration of feed train and turbine

The feed train of Fig. 7.1 can be considered as a water heating process integrated with a steam turbine. The turbine steam under expansion, is tapped to provide increments of (mainly) latent heat to a stream of ambient temperature condensate. The Q-Carnot diagram for such a system was drawn by Seippel in 1950, and has been adapted to S.I. units, in Fig. 7.2.

In principle the change in chemical exergy when the concentration of dissolved air is reduced in the de-aerator should be taken into account, but in Chapter 2 the effect is shown to be trivial. The water heating curve should, in fact, have a small upward temperature jump after the de-aerator, corresponding to the compression in the feed pump. It is worth noting that the feed pump could be divided into two stages, one after the de-aerator, the other after the final feed heater. The result would be increased pump power, since the water density declines with temperature. However, there is a compensation, in that less bled steam is required to produce the same final feed temperature. It can be shown that the compensation is almost exact!

Figure 7.2 shows, as an exaggerated cross-hatched area, the destruction of thermomechanical exergy during heat transfer through the temperature difference between heating steam, and heated water in the Fig. 7.1 feed train. The cross-hatched area is a carefully contrived economic minimum loss, which is small compared to the gain arising from increased mean heat intake temperature.

In the design of the feed heater train, the heat addition per stage is not roughly equal as shown. In fact the rise of Carnot efficiency should be constant; the highest temperature heater being the largest. The irreversibility per stage is approximately equalized. The closest approach of the heater drains to the feed temperature is called the 'terminal difference' and, due to similarity of construction, will be nearly the same in each heater. The de-aerator, being a direct contact heater, needs some

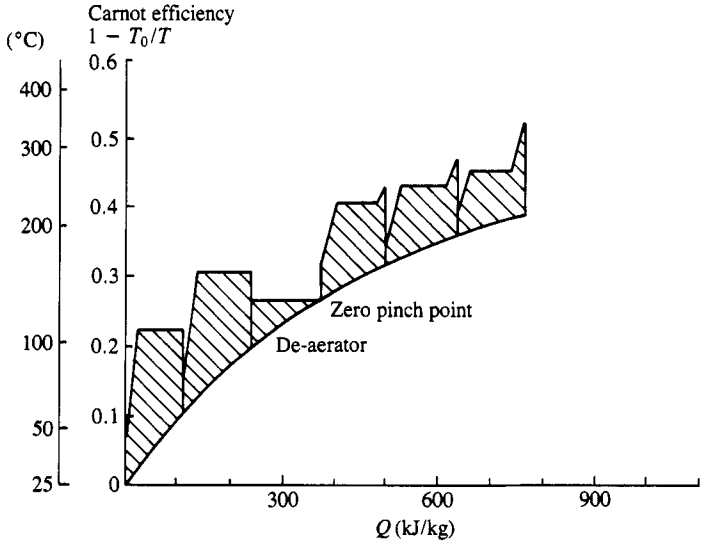

Notes: The bled steam profiles are exaggerated on the vertical scale for improved illustration.

The superheat declines with pressure. In each feed heater except the top and second bottom there is a contribution of flash steam from cascaded drains.

The feed flow after the de-aerator increases because of drains pumping.

The details of the flash steam and the change of feed flow are too small to be shown on the diagram, but would be picked up in material, energy, and exergy accounts.

When drawn to scale, and in accordance with the detail, the cross hatched area represents irreversibility or exergy destruction, when temperature difference is used to transfer heat.

Fig 7.2 *Q*-Carnot diagram for feed heating system

special consideration, and raises the feed to saturation. The de-aerator outlet is the site of a zero pinch point. Due to its low irreversibility the de-aerator deserves a high thermal load.

It is easy to see, with this form of feed train presentation, that as the number of stages tends to infinity, the internal irreversibility tends to zero, whilst the final feed temperature increases towards drum saturation temperature, and the external irreversibility shrinks. In practice the number of bleeds could not exceed the number of turbine stages, and is limited by turbine casing arrangement and economic considerations to a lot less.

7.9 Marginal economics

Seippels' economic principle (**74**) is that a balanced design is one in which no feature leading to improved performance is pursued to an

exaggerated extent. He defines ΔA, the reduction in specific fuel consumption, ΔP the corresponding increase in price, and $p\Delta N$ the product of the price p per kW installed, and ΔN the gain in power (or process output) due to the improvement. The marginal efficiency quotient is then

$$\Delta A/(\Delta P - p\Delta N)$$

This economic criterion can, in principle, coordinate all the features of an installation, and is as true today as in 1950, but it is not easy to apply in all circumstances.

7.10 Heat exchanger networks

Although the feed heating scheme of Fig. 7.1 is a heat exchanger network, it is a special case, in which there is a perfect match between the heat supplied by the cooled stream and the demand of the heated stream. In the general case considered in pinch technology, it has been found helpful to add the enthalpy/temperature characteristics of all the heated (cold) and all the cooled (hot) streams into a pair of composite curves, which have the feature that the energy flow needs of the composite cold stream exceed the supply by the composite hot stream. Moreover, the two temperature profiles do not match.

The process temperature span may exceed that of an associated power plant. The top temperature, that of flue gas, is likely to be common to process furnaces and engine combustion chambers, but processes may be refrigerated, for example air separation, and process reactants may reach much higher temperatures than engine working fluids. The exergy supply is usually from the burning of fuel. The process integrating heat exchanger network contributes to the minimization of thermomechanical exergy destruction and, therefore, of fuel consumption. Within the processes, outside the heat exchanger network, there occurs interchange to and fro between thermomechanical exergy and chemical exergy. The latter is from concentration changes in the separators, and from molecular changes in the reactors. Figure 7.3 shows a pair of composite curves, as usually portrayed for introductory purposes, see (**64**) and (**68**). The Carnot efficiency can be plotted on the vertical axis, as in Fig. 7.2. A temperature plot points the mind at heat exchanger driving forces (temperature differences), whereas the Carnot efficiency draws attention to irreversibility.

If the reaction $CO + 1/2\ O_2 = CO_2$ is taken as an example, then even in the temperature range where all three molecules are perfect gases, the product, having less molecules than the reactants, will have an

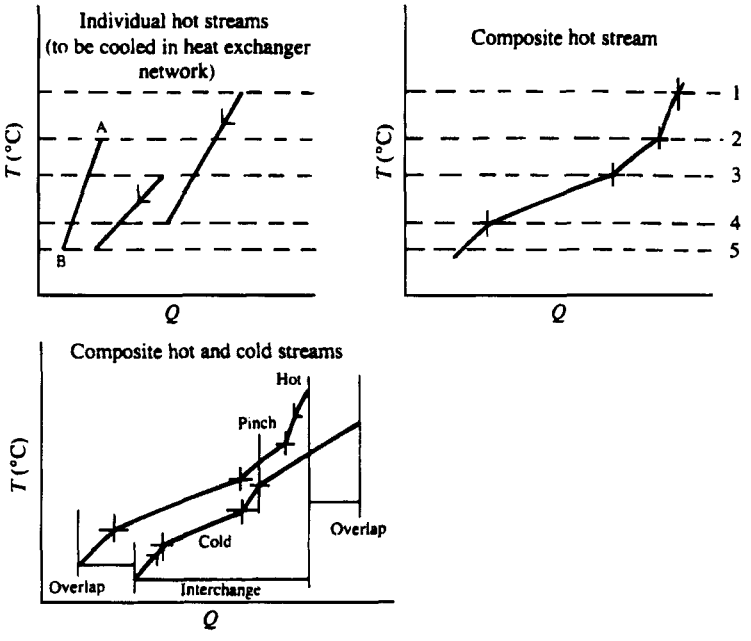

Notes. Hot streams have to be cooled, cold streams have to be heated.
The individual hot stream AB has a process requirement to be cooled from T_2 to T_5 and lose $M\Delta h = \Delta Q$.
The three overlapping streams add graphically to become the composite hot stream.
The above pinch energy balance must be completed, by supplying hot utility to match the right hand overlap. The below pinch energy balance must be completed by supplying cold utility to match the left hand overlap.

Fig 7.3 Build-up of composite curves

enthalpy/temperature cooling characteristic which will not be parallel to the heating characteristic of the reactants. Moreover, the reaction is an exothermic combustion reaction, so that the product temperature is much higher than that of the reactants. There is no way in which the two unmodified streams can tidily interchange heat with each other through an economically small temperature difference. The situation will, of course, be ameliorated by using air rather than oxygen, and by cooling the combustion products, for power production. In general, however, before composite curves are drawn, one can expect a disparate set of hot and cold streams and, therefore, a pinch. If the boiling or condensation of sub-critical fluids is involved, as in Fig. 7.2, then awkward fits are inevitable with the characteristic of flue gas for example. Effectively insoluble curve fitting problems make the development of arguments

difficult along heat engines lines, for an ideal reversible case comprising infinite numbers of components. Such arguments encounter the difficulty that the processes and the heat exchanger network change as irreversibilities and side streams are modified or disappear. The relationship between the real and the ideal becomes distant and tortuous. Rather, a best compromise has to be put together, which accepts the unavoidable and does the best achievable. Mis-matched curves and pinch points have to be lived with – they are unavoidable. The same applies to the hot and cold overlaps between composite hot and cold streams.

(How tidy the human body looks, with consciousness, control, and motive power generation by isothermal, near equilibrium processes, akin to fuel cells, conducted at near ambient temperature and humidity! (**69**))

Linnhoff (**64**) highlights the important conclusions to be drawn from Fig. 7.3. The upward divergence from the pinch point of the composite hot and cold curves dictates the above pinch overlap; a need for a high-temperature heat supply, or hot utility. Below the pinch point the overlap represents heat rejection.

The pinch point itself is a neutral point; the dividing point between two self-contained zones, each with an independent energy balance, *and* an independent exergy account.

The two composite curves can be moved horizontally to and fro carrying their enthalpy changes with them. (An illuminated surface or window, and each plot on a separate sheet, is good education!) When the curves touch at the pinch point, that is a limiting condition at which local heat transfer needs infinite area and investment. As the curves are moved further apart, conditions become practical and a design compromise between investment and performance is necessary. At the selected compromise, the upper and lower overlaps are a practical minimum, determining the utilization of external high temperature heat, and heat rejection capacity (hot and cold utility). Heat interchange is a practical maximum.

The temperature difference for heat transfer is a minimum at the pinch point. Away from the pinch Δt is in surplus; slope mis-matches are of reduced importance.

At this point the second law obtrudes, and it is necessary to reiterate that at high temperature there is smaller irreversibility associated with a given Δt. Smaller heat exchangers are economic at high temperature. A chemical engineer's preliminary rough rule of thumb for heat exchangers allocates Δts as follows: gas to gas 50–100 °C; feed heaters 30–50 °C; superheaters 40–70 °C; boilers 25–40 °C. The second law allows some variation of these numbers with temperature level.

7.11 Appropriate placement rules

In (**70**) and (**71**) Linnhoff *et al.* define their appropriate placement principles: how to integrate the coupled processes with engines, feed pumps, and distillation columns, strategically placed in relation to the pinch point. At this stage of development of the discussion, the conclusions are given, namely that engines should be above or below the pinch, and heat pumps across the pinch. A distillation column should not cross the pinch. The appropriate placement principle is reviewed later in second law terms, which keep the sense of proportion that everything is imperfect, and draw attention to the separate above – and below – pinch exergy accounts. On the other hand Townsend and Linnhoff's treatment (**70**) uses a first law notion that marginal power production can achieve a limited amount of heat to power conversion at 100 percent or 0 percent efficiency depending on placement. The reader will have a choice.

7.12 Power and process examples

A look at the simple examples earlier in this book, through process integration spectacles, should be good preliminary education. The power and desalination plant of Chapter 2 is first for review; pinch analysis was not in use when it was designed. However, modern plants of the same variety are distinguished only by larger unit sizes, somewhat higher steam conditions possibly with reheat, and more advanced anti-scalant and anti-corrosion chemistry. It turns out that this plant is the *reductio ad absurdum* of the process integration business. The process itself, Chapter 2, is a highly sophisticated heat exchanger cum flash chamber network, which cascades brine latent heat through a series of small flash temperature drops, in the temperature range below 120 °C in which brine anti-scalants and, therefore, brine cooled condensers operate successfully. The pure flash steam is condensed as the plant product. The process is integrated using a single steam turbine bleed via a single heat exchanger, the brine heater, rather than via a heat exchanger network. The pinch point of primary interest lies in this heat exchanger, and is displayed in Fig. 7.4.

A steam generator of those days had an excess air of about 30 percent, for which, using the natural gas of Chapter 3, and extrapolating the gas turbine combustion calculations to 30 percent excess air, the adiabatic combustion temperature is about 1857 °C (ignoring dissociation). The stack temperature can be taken as 160 °C, somewhat above the final feed

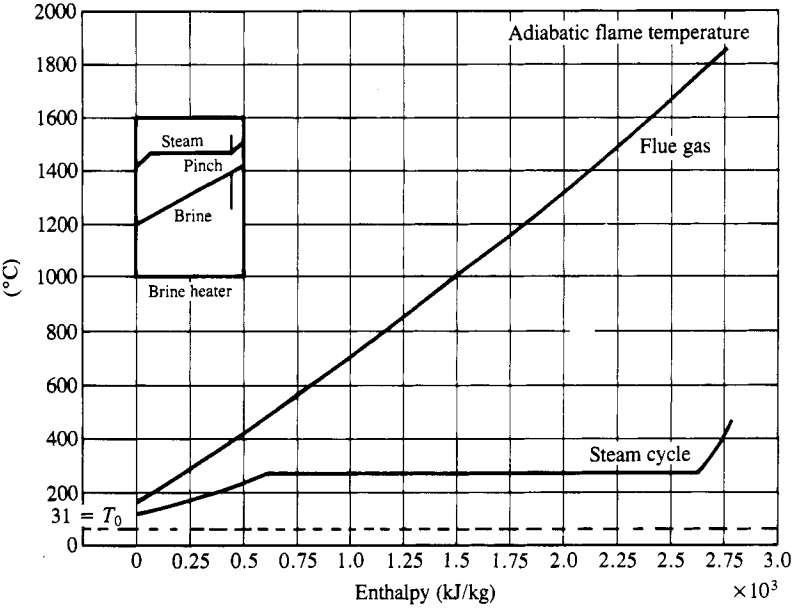

Fig 7.4 Pinch point diagram, power and designificant

temperature of 140 °C, Fig. 2.2. The flue gas profile and the steam generator heat intake profile are displayed in Fig. 7.4. The events in the feed heating system are as in Fig. 7.2 above, truncated at the de-aerator. The pinch in the brine heater (not to scale), is shown inset in Fig. 7.4.

The rules given by Linnhoff above are obeyed. The distiller is below the pinch. That part of the heat cycle with which the distiller interacts is above the pinch, but the interaction with the heat cycle is rather heavy. The design compromise is difficult. The water demand is seasonally constant but the electricity demand peaks by a factor of four in summer. In winter at low electrical load the LP cylinder just avoids overheating and operates inefficiently. Modern technology offers two solutions, both of which cut out thermal integration and substitute electrical integration. The power plant becomes a standard electricity-only installation, be it combined cycle or steam cycle. It feeds power in the first alternative to the compressor (heat pump) of a low temperature vapour compression distiller. The latter operates in a benign scaling regime, needs no recirculation pump, and can use cheaper materials and cheaper construction than multi-stage flash. The second alternative is a reverse osmosis plant. Both alternatives, unproved in large sizes, offer at

least five-fold improved internal efficiency and improved power plant performance in the absence of a costly extraction governor.

Figure 7.4 is a reminder of what happens to the fuel exergy in the steam cycle. The latter is pure work potential, which is partly destroyed by combustion, resulting in Carnot limited energy in hot flue gas, so hot as not to be directly useable in an engine. The vigorous radiation (which precludes the adiabatic flame temperature being achieved), lowers the steam generator heat transfer surface and capital cost. The flue gas energy has to be further degraded to lower temperature steam energy which is useable in a steam turbine cycle with good internal efficiency. Note that any real combustion heat source must be hotter than the steam engine it supplies, distinct from the idealized single temperature heat sources which supply Carnot engines. The gas turbine combustion flame is also excessively hot and is cooled to useable temperature by excess air (Chapter 3).

7.13 Condensing and back pressure operation

It is reiterated finally that condensing heat cycles are not inefficient, albeit they may be difficult to adapt to some pinch situations. The ambient temperature heat they reject contains no exergy. The exergy they extract from the steam goes out on the electrical network. If a turbine is bled or operates against a back pressure the exergy supply is largely unaffected, but is distributed partly by wire and partly by pipe. There is no change in efficiency, unless as in Chapter 2 the (low) process efficiency is included in the overall plant performance. The preceding three sentences can be illustrated using Fig. 7.5. A reversible Rankine cycle has a final feed

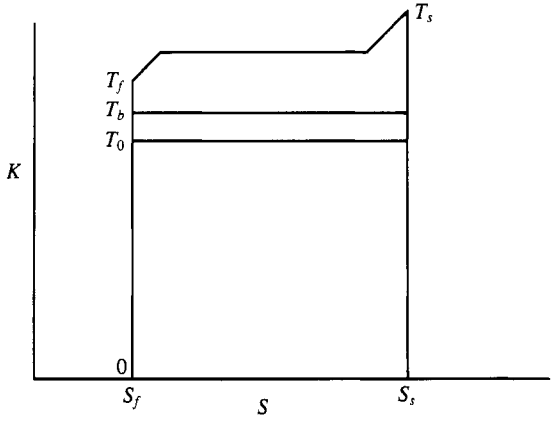

Fig 7.5 Rankine cycle temperature entropy diagram

temperature T_f at the top of its infinite heater train, and a superheater outlet temperature T_s. The cycle may operate in condensing mode down to environment temperature, T_o, or to T_b in back pressure conditions. The heat input to the cycle is the difference of the superheat and final feed enthalpies $H_s - H_f$. In condensing operation the heat rejected is $T_o(S_s - s_f)$. The shaft work is then the difference of the heat input and heat rejected. The difference term may be re-arranged as $H_s - T_oS_s - (h_f - T_os_f)$, being the difference in thermomechanical exergy between final feed and superheater outlet. Since the cycle is reversible it takes in exergy and converts it without loss to shaft work. The turbine exhaust contains zero exergy. It rejects useless heat, that is heat at the environment temperature.

In back pressure operation the turbine exhaust contains thermomechanical exergy $(T_b - T_o)(S_s - s_f)$, which is delivered to process and gets converted or destroyed. The same exergy would have been shaft work in condensing operation. The back pressure exhaust heat is an indestructible energy flow, and so passes through the process undiminished. Some of it (the exergy content) can finish up within in new molecules as chemical exergy if the process is a reactor, or as the chemical exergy of an increased concentration, if the process is a separator. The remainder must be rejected to the environment.

A difficulty which can occur with back pressure installations, arises when as in (**72**), the large mechanical drives are driven by condensing turbines. The ambient temperature condensate from such a machine, should be reheated to near back pressure saturation temperature, using bled steam from a bleed or bleeds on the drive turbine. If that refinement is omitted for simplicity, it will be at the cost of reduced drive turbine efficiency. In (**72**) the problem was ameliorated in a refit, by going over, as far as maybe, to electric drives.

7.14 Appropriate placement relative to heat exchanger networks

Heat engines within a broad temperature range, and heat pumps within a narrow temperature range, can provide a multiplicity of heat sources and sinks: hot flue gas, hot air, live steam, bled steam, compressed steam, hot and cold condensate. From these can be selected candidate sources to supply the above pinch region energy deficit and complete its *energy* balance, or candidate sinks to remove the below pinch energy surplus from the streams which make up the composite hot. In the latter case the utility cooling (sink) streams must ideally be matched in slope to the hot

streams and be within an economic temperature difference. In that way *exergy* destruction in the below-pinch independent region will be minimized. Above the pinch the utility heating streams can be similarly dealt with. There is no scale on Fig. 7.1; the temperature level of the pinch is critical to the detailed tactics. A heat pump can withdraw heat from below the pinch (cooling duty) and supply it above the pinch (heating duty). There is no sense in sinks above the pinch, or in sources below. A diesel engine or gas turbine is a likely candidate to exhaust into an above-pinch region. In the practical example later, a steam cycle withdraws heat from the below-pinch region under a high-temperature pinch.

Any appropriate placement problem can be resolved simply by avoiding putting sources amongst the sinks, or the opposite. Note that the arithmetic of minimization of internal losses by temperature degradation in a heat exchanger network reveals nothing of any associated changes in external irreversibility. The latter has to be accounted for independently. This topic recurs in the practical example below. If a heat cycle gets distorted, as in the desalination example, that also has to be detected and remedied outside pinch technology, but within the broad discipline of exergy analysis.

In the absence of a heat engine, as in the distillery of Chapter 5, a heat pump of the kind discussed at the start of that chapter could provide, in a limited temperature range, multiple levels of sources and sinks, and so absorb heat at several temperatures from the below-pinch zone, and deliver it at several temperatures to the above-pinch zone. An ordinary heat pump with a single throttle expander would be at a disadvantage, (see Chapter 5). In the presence of a heat engine, there is stiff competition for the heat pump which operates with the penalties of double handling: mechanical to electrical conversion, and vice versa; followed by irreversibilities in converting shaft work to working fluid exergy. The temperature range of the engine is very much wider, than the heat pump. However, the heat pump can have an advantage in cases where direct and heavy use of the engine working fluids excessively distorts the engine cycle. Vapour compression distillation of sea water takes advantage of the latter notions, Chapter 2.

7.15 Practical example of process integration

With stand-alone, or lightly integrated power plant reviewed, and process integration with power plant very briefly introduced in a way which diverged slightly from that of Linnhoff, the practical example,

introduced in section 7.1, is the chosen way forward. It is used to demonstrate the constraints of heat exchanger network integrated processes and power plants. In this example, the process is the source of high-temperature heat for the heat cycle.

Figures 7.6 and 7.7 are the flow sheets of an industrial scale natural gas reforming station with integral power plant and heat exchanger network. The double-ended reformer could in a current design be replaced by a single-ended, top-suspended, bayonet tube arrangement with downward firing and simpler thermal expansion problems. Reference (**56**) shows a Japanese reformer with bayonet tube technology and pressurized two-stage catalytic combustion. A reformer uses the high temperature endothermic reaction below with a large excess of steam.

$$CH_4(g) + H_2O(g) \underset{\text{Catalyst}}{\overset{\text{heat}}{\gtrless}} CO(g) + 3H_2(g)$$

and pro rata for higher hydrocarbons

Two reactions which form soot, need to be avoided (**57**) namely

$CO + CO = CO_2 + C$ (Boudouard disproportionation), and
$CH_r = C + 2H_2$ (Methane decomposition)

The reformer tubes are natural gas heated. A modern treatment of the combustion reaction is given in (**38**). Practical combustion calculations in some detail are in Chapter 3, albeit for high excess air.

The plant reactants are steam and natural gas, with a small feed of hydrogen for desulphurization. The main fuel is natural gas with miscellaneous by-product fuels from other processes. The outputs are new molecules (chemical exergy) from the reformer, plus motive power (thermomechanical exergy) from the non-regenerative back pressure Rankine heat cycle. Also provided for the entire complex are back-pressure steam, high-pressure steam, and steam at intermediate pressures – the steam flows all having a thermomechanical exergy content. The heat cycle is energized by the flue gas and 'make gas' emerging from the reformer, with a superheat contribution from the control heater.

The feed train in the bottom right corner of Fig. 7.6 is clarified in Fig. 7.7. It is to be noted that the feed heating (de-aeration apart) is not by bled steam, but non-regeneratively used 'make gas'. That decision was taken in the interest of simplifying an already complex plant. The less irreversible alternative of feed heating with bled steam to 240 °C, just short of 285 °C saturation, would lead to a rearrangement of the flow sheet, before the flow sheet has been fully explored. Discussion is deferred.

Table 7.1 shows the parameters at points 1 to 14 on the flow sheet of

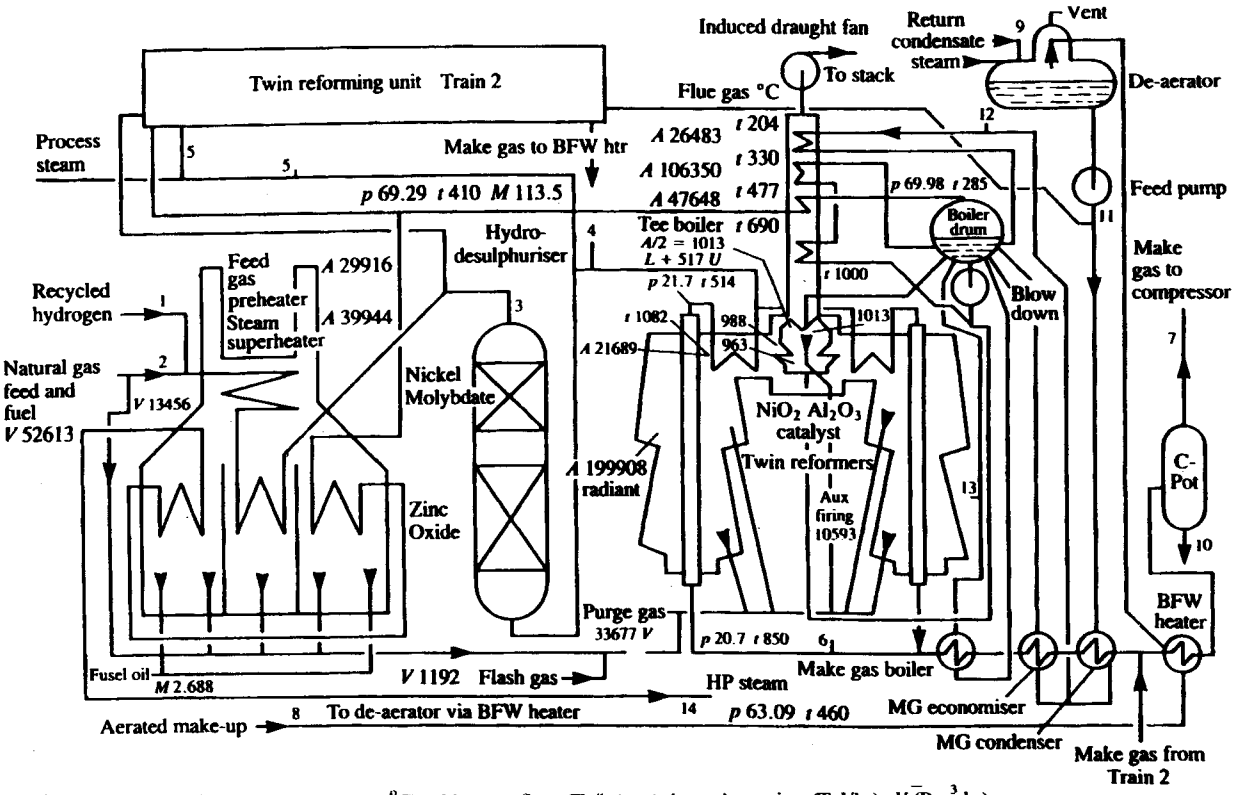

p: absolute pressure (bar); t: temperature (°C); M: mass flow (Te/hr); A: heat absorption (TeJ/hr); V (Rm^3 hr)

Fig 7.6 Industrial scale natural gas reformer system. An explanation of the numbered parameters in this figure will be found in Table 7.1

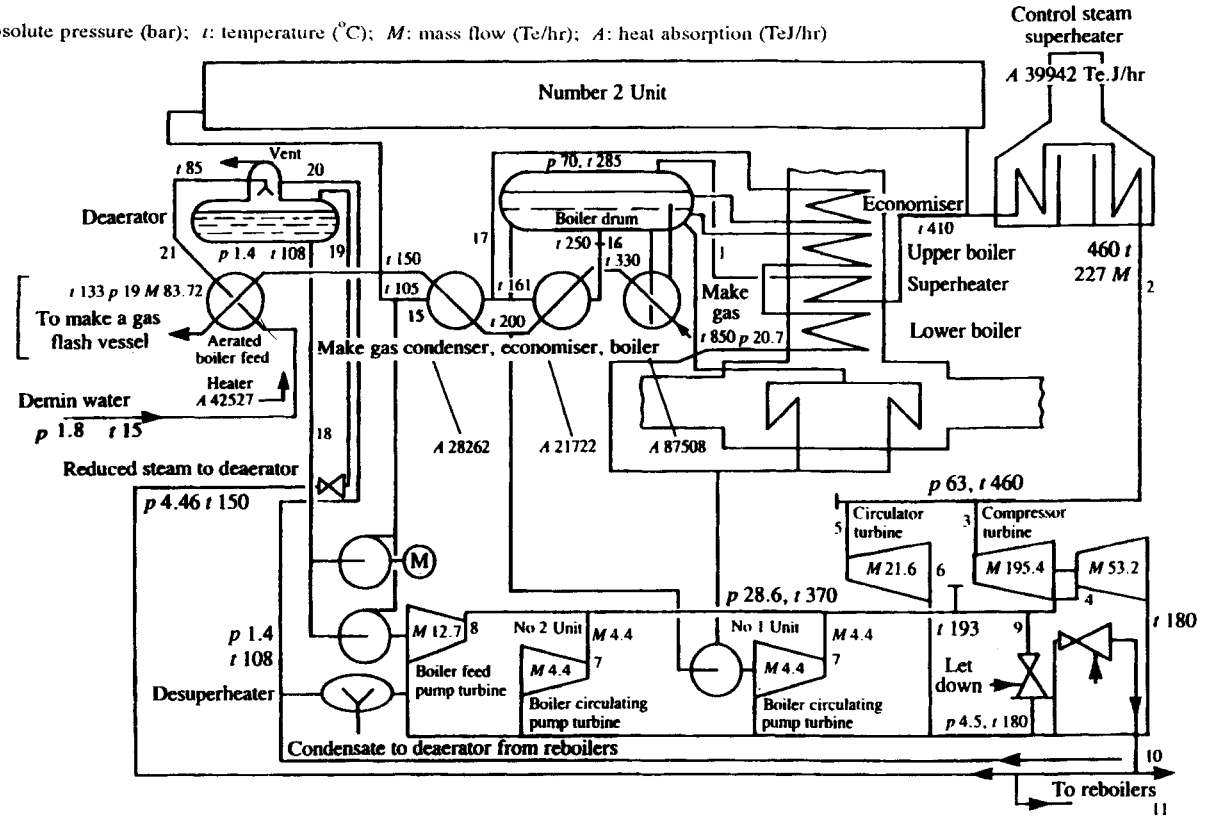

Fig 7.7 Steam system for natural reformers. An explanation of the numbered parameters in this figure will be found in Table 7.2

Table 7.1 Parameters for Fig. 7.6, points 1–14

		H_2	CO	CO_2	N_2	CH_4	C_2H_6	C_3H_8	*Dry gas*	H_2O
1	kg mol/hr	85.93			0.63	4.29			90.85	90.85
	mole %	94.6			0.70	4.70			100.0	
2	kg mol/hr			1.55	39.07	1512.7	55.34	19.6	1627.8	1627.8
	mole %			0.10	2.40	92.9	3.40	1.2	100.0	
3	kg mol/hr	85.93		1.55	39.70	1516.6	55.34	19.6	1718.7	1718.7
	mole %	5.0		0.09	2.31	88.24	3.22	1.14	100.0	
4	kg mol/hr	42.96		0.77	19.85	758.28	27.67	9.80	859.34	
	mole %	5.00		0.09	2.31	88.24	3.22	1.14	100.0	
5	kg mol/hr	2525.5	60751	45.5	370	28.25	18.02			
	Steam	H_2O	$\bar{R}m^3/hr$	Te/hr	°C	bar	Mol Wt			
6	kg mol/hr	2331.5	436.59	258.5	19.85	153.6			3200.0	1573.5
	mole %	72.85	13.65	8.08	0.62	4.80			100.0	
7	kg mol/hr	4662.9	873.17	517.0	39.7	307.2	MG	Cond	6400.0	1171.3
	mole %	72.85	13.65	8.08	0.62	4.80	35.6	Te/hr	100.0	
					Sp Gr	Visc	Sp Ht			
	Te/hr	°C	bar	Mol Wt	Te/m^3	C/Pse	kJ/Te			
8	145.1	15	4.46	18.02	1000	1.0	4.19			
9	99.0	137	4.46	18.02	927	0.2	4.31			
10	35.6	133	18.93	18.02						
11	237.0	105	87.29	18.02	951.5	0.25	4.19			
12	65.0	161	80.32	18.02	905.8	0.175	4.52			
13	53.5	161	80.32	18.02	905.8	0.175	4.52			
14	227.0	460	63.06	18.02	19.83	0.031	2.41			

Fig. 7.6. The reformers are fed with preheated desulphurized natural gas and steam. The reformer furnace flue gas serves to preheat the reactants coming from the hydro-desulphurizer, and then to part energize a steam generator. The remainder of the steam generator, apart from final superheat, is energized by the 'make gas'. The natural gas and hydrogen feed reactants are furnace heated from ambient temperature before entry to a desulphurizer, outputting via a flue gas preheater to the reformers. The same furnace adds final superheat to the steam cycle. The latter arrangement gives control of the temperature of the mixed flue gases to a level avoiding condensation of corrosive acids.

The natural gas reforming operation is part of a complex, including a methanol production process, and a pressure swing adsorption plant, which (*inter alia*) provides the hydrogen feed to the reformer. Methanol production and pressure swing adsorption are pressurized by a compressor driven by the turbine in Fig. 7.7. For the purposes of this chapter the natural gas reforming process is isolated. The Chapter 6 Japanese fuel cell hydrogen production process is doubtless an ingenious adaptation and miniaturization of a related Japanese industrial scheme.

7.16 Reformer description

The centre piece of the example plant is, of course, the reformer. In the interest of high reaction rate, and maximum hydrocarbon conversion, the reformer tubes have to operate with a catalyst at high temperature. The natural gas feed must be desulphurized to avoid poisoning the reformer catalyst. An excess of steam is added and the reactants are then flue gas preheated to the reformer inlet temperature (flowsheet value 514 °C). Preheat continues along the first third or so of the length of the catalyst-filled reformer tubes, without soot formation. The reforming reaction rate becomes significant at about 780 °C. The products ('make gas') with some unreacted hydrocarbons, leave at 850 °C. The steam feed per reformer is 2525.5 kg.mol/hr and the effluent steam 1573.46. The ratio of actual steam flow to stoichiometric is 2525.4/(2525.4 – 1573.46) = 265 percent. The same excess is met in the modern and smaller reformers associated with fuel cells.

The reformer reaction conditions are an application of Le Chatelier's principle (**42**), namely that the response of a reacting system to change is to minimize the effect of that change. The steam excess causes the system to minimize the steam concentration, in other words to favour the consumption of steam and minimize the unconsumed reactants. In an endothermic reaction, increased temperature pushes the equilibrium

composition (**42**) in the direction of the products and away from the reactants. The 850 °C exit temperature optimized the process, within the material limitations of the day.

Figure 7.6 and its data Table 7.1 give the details of the reformer reaction, its reactants 4 and 5, preheated to 514 °C, and its products 6 at 850 °C. In this chapter and book the scope does not include further examination of reformer chemistry. Disequilibrium-driven reaction kinetics is described via the Aarhenius equation in (**42**). Rather our interest is in process integration.

7.17 Heat exchanger network

The data of Figs. 7.6 and 7.7 and associated tables do not include pipe work pressure and temperature losses. On the other hand the heat exchanger loadings or 'absorptions' are based on the pressures and temperatures right at the heat exchanger inlets and outlets, and are accurate. They can only be checked approximately with the information given. The task is to graph the individual stream cooling and heating curves on the temperature enthalpy diagram, Fig. 7.8, and assemble them into composite cold (Fig. 7.9) and hot plots (Fig. 7.10). The design flow sheet unit used for the loadings is the Te.J., which is the heat required to raise 1 Te of water through 1 °C, that is 100 kJ or 1 MJ.

Figure 7.8 states the flow sheet information in graphical form. It shows the individual process streams and the performance of the heat exchanger network. It embraces the control heater and the reformer, the flue gas and make-gas hot streams, and the reactants and feed water/steam cold streams. The tiny load of the steam de-aeration process is not shown in detail, although it is responsible for an upward jump in the water temperature (left/above 200 MJ/sec).

The designer started Fig. 7.8 with the reformer conditions SABC and thereafter a plethora of alternatives from which to select a solution.

The remainder of the diagram is the designer's choice, of 1968/70. Motive power from a heat cycle was needed for pumps and to compress the products. The nature of the production complex complementary to the reformer caused the selection of a simple non-regenerative back pressure cycle.

In terms of heat the control heater is a small operation. The diagram is dominated by the cooling of reformer flue gas, with a significant contribution from cooling 'make gas'. The heating of reactants has to be interrupted for desulphurization and for the introduction of reformer steam at matched temperature. The full flow sheet shows measurement

Table 7.2 Parameters for Fig. 7.7

		$\bar{R}m^3/hr$	*Te/hr*	°C	*bar*	*M Wt*	*Sp Gr* Te/m^3	*Visc C/Pse*	*Sp Ht kJ/Te*
1	Steam from drum	151 511	113.5	285	69.6	18.02	35.71	0.031	1.2
2	Steam from control heater	303 023	227	460	63.1	18.02	19.83	0.031	0.575
3	HP Steam to compressor turbine	260 840	195.4	460	63.1	18.02	19.83	0.031	0.575
4	LP Steam to compressor turbine	72 017	53.2	370	28.6	18.02	10.14	0.026	0.555
5	HP Steam to circulator turbine	28 834	21.6	460	63.1	18.02	19.83	0.031	0.575
6	Process steam	121 476	91	370	28.6	18.02	10.14	0.026	0.555
7	Boiler circulation pump turbine steam		0	370	28.6	18.02	10.14	0.026	0.555
8	Boiler feed pump turbine steam		0	370	28.6	18.02	10.14	0.026	0.555
9	Steam to let down	81 700	61.2	370	28.6	18.02	10.14	0.026	0.555
10	Steam to topping column/reboiler	35 375	26.5	150	4.46	18.02	2.39	0.016	0.575
11	Steam to refining column/reboiler	96 780	72.5	150	4.46	18.02	2.39	0.016	0.575
15	Boiler feed water to make gas condenser		118.5	105		18.02	954	0.252	1.0
16	Boiler feed water from make gas condenser		53.5	250		18.02	813.7	0.125	1.18
17	Boiler feed water to flue gas economizer		65	161		18.02	905.8	0.175	1.08
18	Feed water to boiler feed pump		237	108		18.02	951.5	0.25	1.0
19	Condensate to de-aerator		99.0	137		18.02	927	0.2	1.03
20	Steam to de-aerator	2 670	1.0	150	4.46	18.02	2.39	0.016	0.575
21	Demineralized water de-aerator	145.1	15		4.46	18.02	1000	1.0	1.0

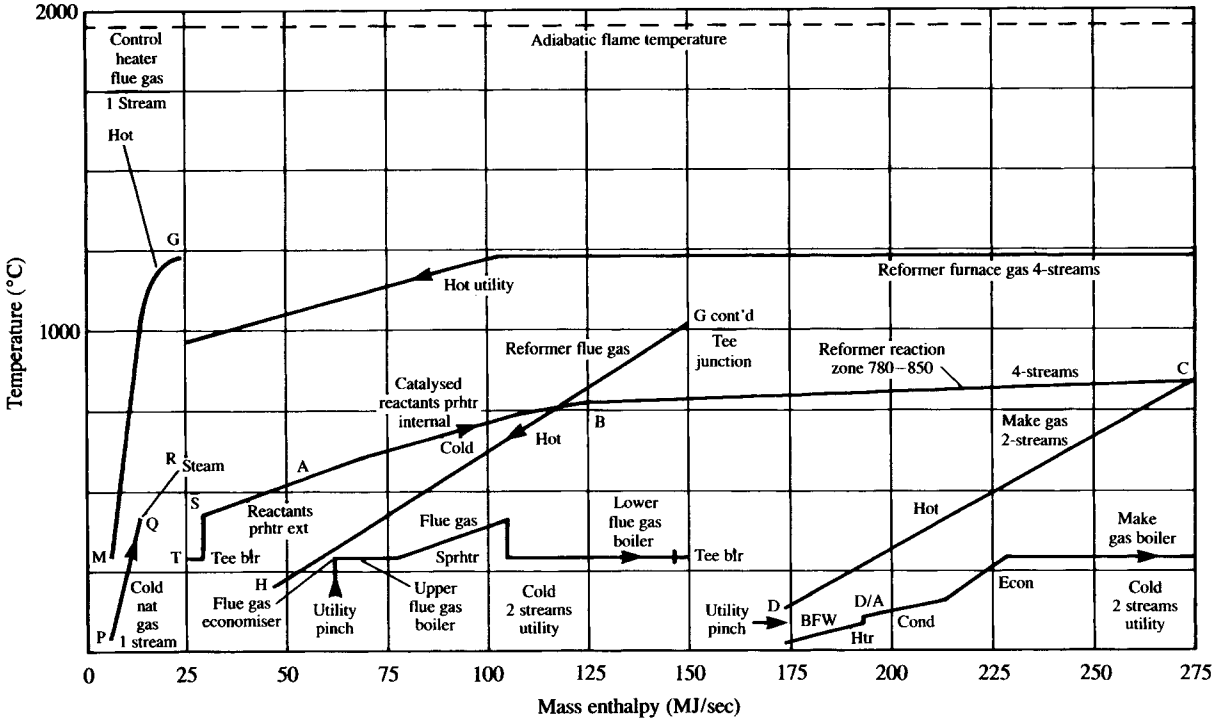

Fig 7.8 Process and utility streams

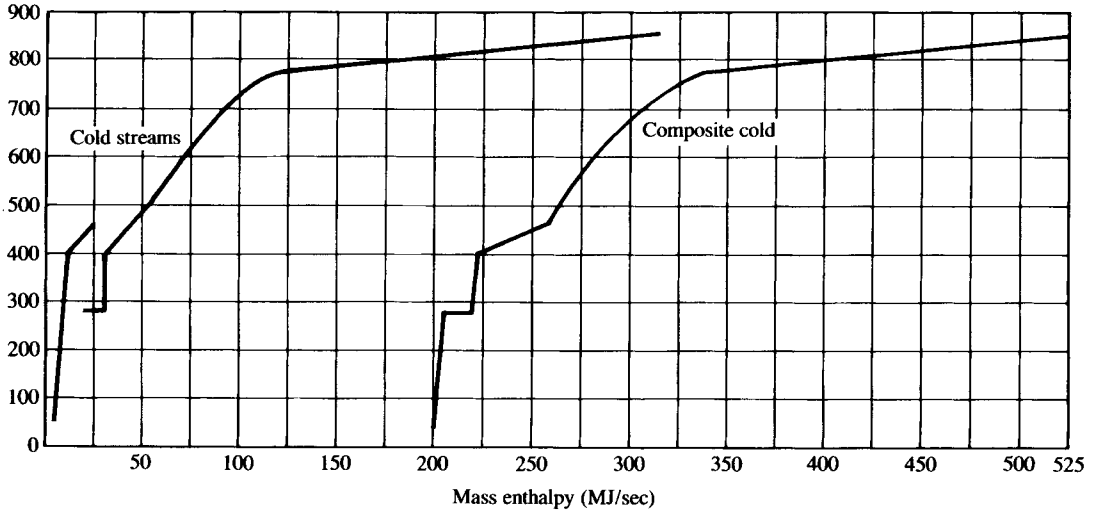

Fig 7.9 Composite cold curve

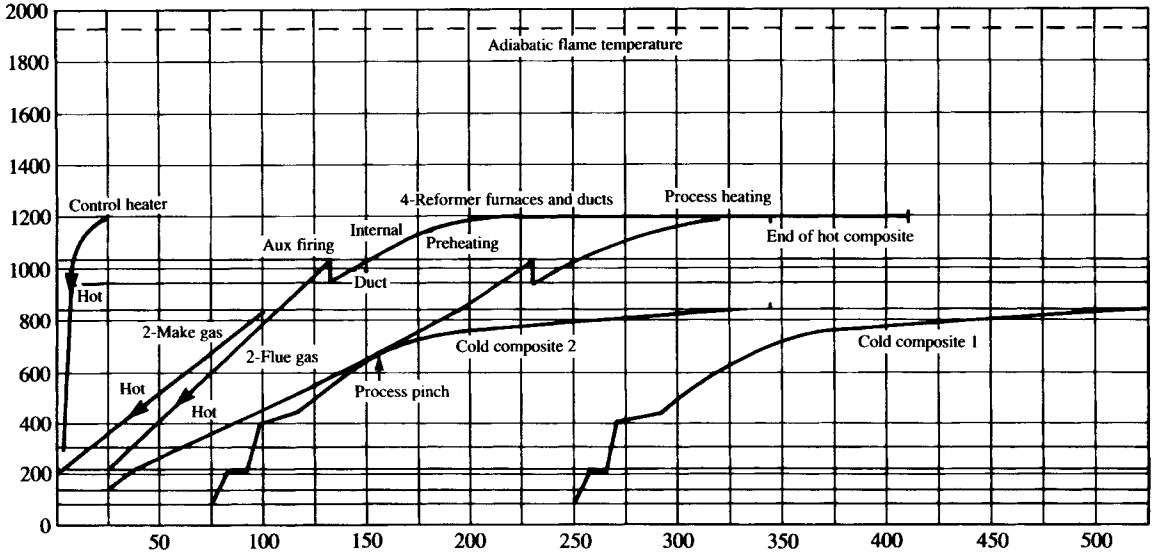

Fig 7.10 Hot and cold composite curves

sensors, control valves, safety equipment and the like, outside the scope of this chapter.

7.18 Steam pressures

The steam expansion path is from high-pressure 63 bars, to intermediate pressure 28 bars, to back-pressure 4.5 bars. The group of simple steam drive turbines are robust against heat cycle distortion considerations. Any intermediate steam pressures have to be provided by reducing and desuperheating stations; for example de-aerating steam, at 1.3 bar. The saturation temperature corresponding to 63 bars is 275 °C and there is a large gap between that temperature and both the flue gas and the 'make gas'. The related irreversibility is the price of simplicity.

7.19 Design options

A feasible option, available at the time, to fill the gap and get a better match between source and sink, would have been a double pressure heat cycle; as examined in Chapter 3 (feasible because the double heat source already breaks the steam generator into portions). The temperature enthalpy chart can portray the notional increased saturation temperature clearly, and by implication the improved cycle efficiency.

A less visible alternative is the use of regenerative feed heating. The water heating duty of the make gas BFW heater and of the make gas condenser could have been performed by much better matched bled steam, at the cost of redesigning the drive turbines with appropriate bleeds, but to the benefit of the cycle efficiency. At low temperatures, the non-linearity of the problem makes matching of temperatures disproportionately important. Going over the consequentials quickly and qualitatively: the 'make gas' could then take over some or all of the thermal duty of the control heater, heat the natural gas feed, and superheat the high pressure steam, albeit with more difficult control than burner adjustment. The T/H picture of the bled steam feed heaters would not show in Fig. 7.8. Something separate on the lines of Fig. 7.2 would be needed. The improved mean heat intake temperature/gain in cycle efficiency could be difficult to spot but the reduced size of the control heater and the transfer of some of its residual fuels to the reformer or elsewhere would be a sign that something useful had happened.

Another invisible loss is due to the heating of the substantial ambient temperature make-up by throttled steam and relatively hot make gas. An independent knowledge of the exergy analysis of heat cycles is, therefore,

a requirement when using pinch analysis. Any design alternative would, in 1968/70, have required detailed thermal performance appraisal and review from the viewpoint of start-up, control, and capital/operating cost, before being considered possible or profitable. A calculation of the overall exergetic efficiency of each alternative would establish the relative thermodynamic merits. In the 1990s there has merely been a point made about what can and cannot be seen on the temperature enthalpy chart, as used in pinch technology.

The problems of heat exchanger driving force are well displayed in Fig. 7.6 by the utility sink stream/heat cycle arrangements under the 'make gas' and flue gas hot streams. Utility pinches are visible.

In the early 1970s the reformer arrangement was the best available. Accordingly, design alternatives were not available for the above pinch region.

7.20 Hot and cold composite curves

Figure 7.9 shows the build up of the cold composite curve from its component process streams. Figure 7.10 shows the build up of the hot composite curve from its component streams. The cold composite curve is rescaled and shown touching the hot composite at the pinch point. The cold composite is then slid sideways to the right, to generate a large overlap and to illustrate the designer's problem in providing enough heat for his Rankine cycle. Very large temperature differentials are used in the reformer furnace. In fact with a far from equilibrium radiant reacting mixture in the furnace, the word 'temperature' is losing its meaning. The isothermal line indicating the furnace temperature says little more than that the burner arrangement has led to rather uniform well-mixed furnace conditions.

The graphical procedure is rather inaccurate, and Linnhoff (**64**) has evolved his problem table algorithm and grand composite curve for improved accuracy and productivity.

Although the use of grand composite curves has not been dealt with in this chapter, the technique is vital to the full practical application of process integration in industry. To enable the reader to move forward into the full scope a convenient source of references, all in one volume, is reference (**75**), the Proceedings of the First International Conference on Energy and the Environment, Vol. 1.

7.21 Exergy and pinch analysis

In (**67**) Linnhoff uses both the hot and cold composite curves, and the grand composite curve, to illustrate his comparison of (thermomechanical) exergy analysis and pinch analysis, although the word 'thermomechanical' is omitted. The author, on the other hand, is content for the purposes of exergy/pinch analysis comparison, with the presentation of Fig. 7.8.

Pinch analysis does deal with an important aspect of process optimization, via appropriate placement. However, chemical exergy is a notable absentee (**73**) which has been seen to be essential to a full understanding of the desalination and whisky distillation processes in this book, and indeed to any reactor or separator.

Some aspects of heat cycles are invisible to pinch analysis, notably heat cycle distortion; others are difficult to spot. In (**73**) (early definition of fuel chemical exergy) rational exergetic efficiencies are derived for large industrial processes, a commitment not undertaken in pinch analysis which strives toward improvement, stating what has been achieved in economic terms. Via the ongoing competitive comparisons the two approaches must surely be brought to coalescence, more particularly as the industrial perspective is one of initial attack on crippling waste of fuel and resources, with a very long way to go before diminishing returns are reached. The background is one in which the term 'thermal efficiency' is widely misunderstood and resources oddly allocated. Great opportunities are born in such tough situations: rewards await those who grasp those opportunities.

7.22 Closing remarks

In vegetation, the photosynthesis process provides a bountiful harvest of large organic molecules, but it is a harvest which is at risk. This is described in Chapter 4.

The thermonuclear furnace in the sun is utilized to provide the basis for life. The radiation does the *work* of creating large molecules from small. Nature, thereafter, is a frugal manager. The predatory carnivores, the herbivores, the scavengers – from eagles to termites, to maggots and moulds – are conservators of large molecules and the radiation derived exergy within them. Mankind has to look at nature's example: a preoccupation with heat is inadequate. Nature accomplishes its ends in the world of the living, using isothermal interactions, for motive power, for chemical processes, for all that is achieved, for the go of things. There must be a message there for us. The contemplation of nature and the

development of motive power from the products of photosynthesized molecules, in mere microbes, produces a feeling of inadequacy.

The fuel cell is one attempt at an isothermal route to motive power. An attempt is made to use the chemical exergy of the fuel. Moreover, heat is developed inside the cell pro rata to the reversible entropy change of the reaction and additionally as a result of imperfections in its working.

The provision of the hydrogen which motivates the cell involves the steam reforming process. This rescues the hydrogen from its combined state in steam and in the hydrocarbons of natural gas. The reformers of Chapters 6 and 7 involve crude combustion to yield Carnot limited energy in combustion products, which are organized in the reformer to provide the *work* involved in the reaction. Due to lack of detail in the relatively simple example of Chapter 6, and because the plant in Chapter 7 is part of an uncharted complex which includes methanol production, related exergy analysis has not been deployed.

In the Japanese example given in Chapter 6, the fuel cell and its fuel preparation equipment are self contained. The reject fuel from the cell is combustible and sufficient in quantity to drive the reformer. As the technology advances, and the cell efficiency improves, it will become increasingly difficult for the reformer to be driven in this way, and raw fuel will have to be used with crude combustion. Could the electrical output of the cell motivate some kind of reformer? Let us compress the natural gas/steam mixture in a near isentropic gas turbine compressor! Let compression continue after the achievement of 780 °C at which (Chapter 7) the catalysed reformer reaction rate becomes significant (the compressor internals will have to be coated with catalyst). The reaction will then withdraw heat and work from the surroundings, while the imperfect compressor supplies both commodities. Ideally the design compromise will achieve an outlet temperature of 850 °C, as in Chapter 7. The resulting 'make gas' will be turbine-expanded for the shift reaction. The reader can attempt to conceive another 'reaction pump', as the preceding apparatus might be called, for the shift reaction. The objective notionally achieved is the avoidance of crude combustion and Carnot limitation. The author's excuse for this very speculative exercise is to show that exergy analysis can generate alternative ideas for detailed thermodynamic and economic appraisal. With high-temperature fuel cells, the alternative of reform at the anode appears, Chapters 4 and 6. The reform can be a non-equilibrium reaction or, as in Chapter 4, an equilibrium reaction in a reformer analogous to a fuel cell.

More immediately, combined heat and power (CHP) is being encouraged on the specious grounds that the fuel utilization factor can

reach 80 percent, and can be quoted as an efficiency, which it is not. Whilst CHP is usually a major improvement on what it replaces and discourages the burning of electricity, it offers no exergetic advantage over combined cycle electricity generation using a gas turbine/condensing steam cycle. The latter, however, allows the consumer the choice of burning electricity, a choice which is not always frugal. Members of influential UK government committees can be heard condemning the steam cycle because it rejects much heat; heat which is in fact economically valueless (tomato growing apart) and thermodynamically squeezed dry. A valid objective would be to encourage large-scale combined or integrated power and process. (Integrated using all the resources of exergy analysis and pinch technology.) The necessary complexes should, in the interest of industrial efficiency, maximize electricity generation and be encouraged to export their surplus on a cost basis underlain by exergy analysis (thermoeconomics).

Meanwhile, for power, the natural gas-fired combined cycle is supreme on the basis of an exhaustible fuel. Coal gasification is the longer term alternative, to feed combined cycles. Integration of heat cycles with fuel cells, as in Chapter 6, brings the available technologies into cooperation. In the field of economics the traded good should be that which can be used, namely exergy, not indestructible energy. A layman asked to define energy will approximate to 'the potential to cause change'. He means exergy, the 'go of things': the go of heating buildings; the go of motors; the go of processes; the go of life itself.

References

(1) **Gibbs, J. W.** (1961) On the equilibrium of heterogeneous substances, *The scientific papers of J. Willard Gibbs*, Dover Publications, New York.

(2) **Fast, J. D.** (1962) *Entropy*, (Phillips Technical Library), Cleaver-Hulme Press, London.

(3) **Elwell, D.** and **Pointon, A. J.** (1986) *Physics for engineers and scientists*, Ellis Horwood Limited, Chichester.

(4) **Feynman, R. P. *et al.*** (1977) *The Feynman Lectures on Physics*, Addison-Wesley Publishing Company, Massachusetts.

(5) **Keenan, J. H.** (1970) *Thermodynamics*, MIT Press, Massachusetts.

(6) **Silver, R. S.** (1972) *Introduction to thermodynamics*, Cambridge University Press.

(7) **Atkins, P. W.** (1991) *Physical chemistry*, Oxford University Press.

(8) **Haller, B. R.** (1990) Improvements in the aerodynamics of large steam turbines, *Steam turbines for the 1990s*, IMechE Conference Publication 1990–4, Mechanical Engineering Publications Limited, London.

(9) **Mayhew, Y. R.** (1991) Does the methodology of teaching thermodynamics to engineers need changing for the 1990s?, *Proc. Instn Mech. Engrs, Part A*, **205**, 283–286.

(10) **Seippel, C.** (1950) The energy economy of steam power plants, *The Brown Boveri Review*.

(11) **Keller, A.** (1949) The evaluation of steam power plant losses by means of the entropy balance diagram, *ASME Paper 49–A–65*, ASME, New York.

(12) **Smith, P. F.** and **Player, M. A.** (1991) Deconvolution of bipolar signals using a modified maximum entropy method, *Journal of Appl. Physics D*, **24**.

(13) **Kotas, T. J.** (1985) *The exergy method of thermal plant analysis*, Butterworths London.

(14) **Reid, C. E.** (1990) *Chemical thermodynamics*, McGraw Hill Publishing Co, New York.

(15) **Zemansky, M. W.** (1962) *Heat and thermodynamics*, McGraw Hill Publishing Co, New York.

(16) **Obert, E.** and **Gaggioli, R.** (1962) *Thermodynamics*, McGraw Hill Publishing Co, New York.

(17) **Gaggioli, R. A.** (editor) (1982) *Thermodynamics – second law analysis*, American Chemical Society.

(18) **Kotas, T. J., Raichura, R. C.,** and **Mayhew, Y. R.** (1987) Nomenclature for exergy analysis, *Second law analysis of thermal systems* (edited by Moran and Sciubba), ASME, New York.

(19) **Keenan, J. H.** ***et al.*** (1978) Steam tables, SI units, Wiley Interscience Publication, John Wiley and Sons.

(20) **Keenan, J. H.,** ***et al.*** (1983) Gas tables, SI units, Wiley Interscience Publication, John Wiley and Sons.

(21) **Linhoff, B.** (1989) Pinch technology for the synthesis of optimal heat and power systems, *ASME J. Energy Res. Technol.*, **III**, 137.

(22) **Spiegler, K. S.** and **Laird, A. D.** (1980) *Principles of desalination*, (Second Edition, Parts A and B), Academic Press, New York.

(23) **Guggenheim, E. A.** (1933) *Modern thermodynamics by the methods of Willard Gibb*, Methuen, London.

(24) **Barclay, F. J.** (1995) Cheaper power and desalination, Proceedings of the IDA World Congress on Desalination and Water Sciences, Abu Dhabi, Vol III, p. 381.

(25) **Frankel, A.** (1960) Flash evaporators for the distillation of sea-water, *Proc. Instn Mech. Engrs*, **174**, 312.

(26) **Silver, R. S.** (1965) Fresh water from the sea, *Proc. Instn Mech. Engrs*, **179** (1), 135–154.

(27) **Darwish, M. A., Al-Najem, N. M.** and **Al-Ahmad, M.S.** (1993) Second-Law analysis of recirculating multistage-flash desalting system, *Desalination*, **89**, 289–309.

(28) **Koot, L. W.** (1968) Exergy losses in a flash evaporator, *Desalination*, **5**, 331–348.

(29) **Andrews, W. T.** and **Bergman, R. A.** (1986) The Malta sea water reverse osmosis facility, *Desalination*, **60**, 135–144.

(30) **Ophir, A.** (1990) Low temperature vapour compression and multiple effect distillation process developments and field experience, related to high quality and economical sea water desalination, European Desalination Association Symposium on Desalination Plant Operations, Las Palmas.

(31) **McGovern, J. A.** (1990) Exergy analysis, Parts 1 and 2, *Proc. Instn Mech. Engrs*, **204**, 253–268.

(32) **Rogers, G.** and **Mayhew, Y.** (1992) *Engineering thermodynamics,*

work and heat transfer, Longman Scientific and Technical, Harlow, England.

(33) **Gallow, W. L. R.** and **Milanez, L. F.** (1990) Choice of a reference state for exergetic analysis, *Energy*, **15**, 113–121.

(34) **Makita, T.** ***et al.*** (1993) The key technology development of a next generation high temperature gas turbine, Third Symposium on Combined Cycle Gas Turbines (CCGT), IMechE, London.

(35) **Muten, I. M.** (1993) Developments in emission monitoring, *ibid.*

(36) **Roberts, J. A.** (1993) Current and potential development in the use of aero derived gas turbines for power generation duties, *ibid.*

(37) **Pessarakli, M.** (1997) *Handbook of photosynthesis*, Marcel Dekker, New York.

(38) **Moran, M. H.** and **Shapiro, H. N.** (1995) *Fundamentals of engineering thermodynamics*, Second Edition (SI Units), John Wiley and Sons, Chichester.

(39) **Chase, M. W.** (1985) JANAF Thermochemical Tables *J. Phys. Chem. Ref. Data*, **14**, published for National Bureau of Standards by American Chemical/Physical Societies.

(40) **Barclay, F. J.** (1995) *Combined power and process – an exergy approach*, First Edition, Mechanical Engineering Publications, Bury St Edmunds.

(41) **Kotas, T. J.** (1995) *The exergy method of thermal plant analysis*, Second Edition. Krieger Publishing Company, Florida.

(42) **Atkins, P. W.** (1995) *Physical chemistry*, Fifth Edition, Oxford University Press, Oxford.

(43) **Gardner, J.** (1996) Papers S455 Thermodynamic processes in solid oxide and other fuel cells. *Fuel cells for power and propulsion* IMechE Seminar, London.

(44) **Smith, I. K.** (1992) Matching and work ratio in elementary power plant theory, *Proc. Instn Mech. Engrs*, **206** (A4), 257–262.

(45) **Dunbar, W. R.** and **Lior, N.** (1991) Understanding combustion irreversibility, *Second law analysis – industrial and environmental applications*, AES-VOL25/HTD-VOL191, ASME, New York.

(46) **Gaggioli, R. A.** and **Dunbar, W. R.** (1993) EMF, maximum power and efficiency of fuel cells, *Trans. ASME, J. Energy Res. Technol.*, **115**, 100–104.

(47) **Dunbar, W. R., Lior, N.** and **Gaggioli, R. A.** (1993) The effect of the fuel cell unit size on the efficiency of a fuel cell topped Rankine power cycle, *Trans. ASME, J. Energy Res. Technol.*, **115**, 105–107.

(48) **Rogers, G. F. C.** and **Mayhew, Y. R.** (1989) *Thermodynamic and transport properties of fluids*, (SI Units), Basil Blackwell, Oxford.

(49) **Monick, J. A.** (1969) *Alcohols: their chemistry, properties, and manufacture,* Rheinhold Publishing Corporation, New York.

(50) **Chalmers, E., Hodgett, D. L.** and **Mitchell, B. S.** (1985) A steam heat pump for increasing energy efficiency in distillation *British Electroheat Association Symposium Proceedings*, Aberdeen, Scotland.

(51) **Hodgett, D. L.** (1980) *The high temperature heat pump for waste heat recovery in the distillation process*, Scottish Hydroelectric, Perth.

(52) **Gaggioli, R. A.** and **Petit, P. J.** (1977) Use the second law first *Chem. Technol.*, (August) 496–506.

(53) **Beyer, J.** (1978) Einige Probleme der Praktischen Anwendung der Exergetischen Methode in Warmwirtschaftlichen Untersuchungen Industrieller Produktionprozesse – Teil 1, *Energieanwendung*, **27** 204–208.

(54) **Sama, D. A.** (1981) Biomass to ethanol has merit, *Hydrocarbon processing* (July) (Presented to the 73rd National meeting of the AIChE November 1980).

(55) Grove Anniversary Symposia, London, 1984–1997.

(55a) Proceedings of the First Grove Fuel Cell Symposium, London, 1990, *J. Power Sources*, **29**.

(55b) Proceedings of the Second Grove Fuel Cell Symposium, London, 1992, *J. Power Sources*, **37**.

(55c) Proceedings of the Third Grove Fuel Cell Symposium, London, 1994, *J. Power Sources*, **49**.

(55d) Proceedings of the Fourth Grove Fuel Cell Symposium, London, 1996, *J. Power Sources*, **61**.

(55e) Proceedings of the Fifth Grove Fuel Cell Symposium, London, 1997, *J. Power Sources*, **71**, nos 1 and 2.

(55f) **Appleby, A. J.** (editor) (1987) *Fuel cells, trends in research and applications*, Hemisphere Publishing Corporation.

(56) Fuel Cell RD & D in JAPAN, *August 1992 Annual Review*, Fuel Cell Information Development Centre, The Institute of Applied Energy, Shinbashi SY Building, 1–14–2, Nishishinbashi, Minato-Ku, Tokyo 105, Japan.

(57) **Scholz, W. H.** (1993) Processes for industrial production of hydrogen and associated environmental effects, *Gas separation and purification*, Vol. 7, Butterworth-Heinemann Ltd, pp. 131–139.

(58) **Bacon, F. T.** (1960) Fuel cells: will they soon become a major source of electrical energy?, *Nature*, (May), 589–592.

(59) **Appleby, A. J.** (1987) Phosphoric acid fuel cells, Symposium, Fuel Cells, Trends in Research and Application.

(60) **Simons, S. N.** (1983) Phosphoric acid fuel cells, status, and technology, *Fuel cells, status technology, and applications*, Institute of Gas Technology, Lewis Research Centre, Illinois, USA.

(61) **Koyashiki, T. *et al.*** (1992) Advanced fuel cell energy system for telecommunications use, *Intelec 14th International Telecommunications Conference*, IEEE, Washington DC, USA, pp. 4–11.

(62) **Take, T. *et al.*** (1992) Fuel substitution technology in phosphoric acid fuel cells, *NTT Rev.*, **4**, 39–45.

(63) **Scott, D. H.** (1993) Advanced power generation from fuel cells–implications for coal, *IEA Coal Research*, Gemini House, London, UK.

(64) **Linhoff, B. *et al.*** (1985) *A user guide on process integration for the efficient use of energy*, Institution of Chemical Engineers, Rugby.

(65) **Gundersen, T.** and **Naess, L.** (1988) The synthesis of cost optimal heat exchanger networks; an industrial review of the state of the art, *Computational Chemical Engineering*, **12**, 503–530.

(66) **Linhoff, B.** (1989) Pinch technology for the synthesis of optimal heat and power systems, *ASME J. Energy Resources Technol.*, **111**, 137–147.

(67) **Linnhoff, B.** (1993) Pinch analysis and exergy – a comparison *Energy Systems and Ecology Conference*, Cracow, Poland.

(68) **Linnhoff, B.** (1990) The optimization of process changes and utility selection in heat integrated processes, *Trans IChemE*, **68**, (A).

(69) **Bockris, J.** and **Srinivasan, S.** (1967) Predominantly electrochemical nature of biological power producing reactions, *Nature*, **215**, 197. (Letter).

(70) **Townsend, D. W.** and **Linnhoff, B.** (1983) Heat and power networks in process design, Parts 1 and 2, *AIChE J.*, **29**, 742–771.

(71) **Linnhoff, B.** and **Dunford, H.** (1983) Heat integration of distillation columns into overall processes, *Chem. Engng Sci.*, **38**, 1175–1188.

(72) **Linnhoff, B.** and **Eastwood, A. R.** (1983) Overall site optimization by pinch technology, *Chem. Engng Res. Des.*, **65**, 408–414.

(73) **Szargut, J. *et al.*** (1988) *Exergy analysis of thermal, chemical, and metallurgical processes*, Hemisphere Publishing Corporation/ Springer Verlag.

(74) **Seippel, C.** (1950) Some thermodynamic aspects of power production, *Fourth World Power Conference*, London, 1950, Section E3, Paper 9 (British Electricity Translation, 124).

(75) **Tassou, S. A.** (editor) (1997) Proceedings of the First International Conference on Energy and the Environment (ICEE '97), Vol. 1 Brunel University and IMechE, UK. See papers by: Marechal, F. and Kalitventzeff, B., pp. 72–82; Zhelev, T. K., pp. 82–89, Sarabchi, K. and Polley, G. T., pp. 110–120; and Berglin, N. and Berntsson, T., pp. 121–131.

(76) **Ralph, T. G. *et al.*** (1997) Low cost electrodes for proton exchange membrane fuel cells, *J. electrochem, Soc.*, **144**.

Appendix 1

Relative Exergy in a Water–Ethanol Mixture

1 Thermo-physical data and literature

The theory of a mixture of two volatile liquids is given in reference (**42**), along with details of the partial molar volumes of the water ethanol mixture, which exhibit complexities at low ethanol concentrations. Also there is a description of the water-surrounded ethanol molecule in a dilute mixture. The latter arrangement has been photographed and published in [**I**] and is doubtless associated with the complex partial molar volume behaviour.

In the Russian reference [**II**], for which the author is unaware of an English language equivalent, the thermo-physical properties of ethanol and the water–ethanol mixture are very extensively tabulated (British Library).

In the book [**III**] the departures of the water ethanol mixture from ideal are quoted as excess functions, and the difficulty in understanding this mixture remarked upon (Science Library).

A pioneer of the thermodynamics of binary mixtures and of exergy analysis was Bosnjakovic, whose German language book *Technical Thermodynamics* (Vol. 2 only) was translated into English in the USA, [**IV**] (British Library). Bosnjakovic's enthalpy concentration chart for the water ethanol mixture appears in [**V**]. His related entropy concentration chart is not obtainable from the British Library. The latter charts were the bases of Beyer's exergy concentration chart used in Chapter 5.

2 The water ethanol exergy concentration chart of Beyer

In the chart used in Chapter 5, exergy is referred to as an arbitrary dead state at 1 bar, 12 °C, 0.001kg/kg ethanol concentration. The latter conditions represents the throwaway parameters in a distillery, in a cool climate. Usually a dead state represents conditions in the environment, but that choice would not be relevant to the internal thermodynamics of a mixture. The dead state must be within the mixture, and mixture exergies are relative thereto.

In Chapter 1 of this book, there is a discussion of membrane equilibrium and desalination, which brings out the direct relation in a single substance, between concentration, chemical potential, and exergy.

In the water–ethanol mixture the concentration difference between the dead state and pure water is 0.001 kg/kg of water. Separate the reference mixture and the pure water using a hydrophilic membrane, and a modest compression of the mixture will result in equilibrium. Between the reference mixture and pure ethanol is a very large ethanol concentration difference, which is difficult to equilibrate across an organophilic membrane. A relatively large exergy for pure alcohol, as in Beyer's diagram, is therefore predictable, and could be calculated if osmotic pressure data were available. Beyer did not publish his exergy calculations, but submitted them to his sponsors, leaving us a problem, the more so because Beyer was dissatisfied with the accuracy of his diagram.

If water and ethanol are mixed isothermally in steady flow to produce the reference mixture, an entropy growth and the related heat of mixing results. The incoming relative chemical exergies are destroyed, and as the water exergy is small it should be possible to get an approximation to the ethanol value. Accurate heats of mixing are in Table 46 of [**II**]. However, the tabulation of the non-linear function is coarse, and graphical methods involving drawing tangents at the origin, do not yield an accurate answer. The order of things is from 370 to 470 kJ/kg, not out of line with Beyer at 438. Regression analysis could improve the accuracy.

In an unpublished communication T. J. Kotas (**13**) who originally supplied the author with Beyer's hard-to-get East German paper, obtained a value of 456 using analytic ideal solution theory, hopefully correct for a dilute solution. Beyer, on the other hand, asserts the necessity of using real solution theory. Moreover, paragraph 1 above draws attention to the complexity at low alcohol concentrations.

Finally the GASVLE computer program looked at the above mixing problem using equations of state, with the following results. A table of

thermodynamic properties of the mixture was produced and is reproduced overleaf, giving data for the liquid and vapour phases. The interpolated data for the dead state at 12 °C, are

Substance	*Specific entropy*	*Mass kg*	*Total entropy*
Water	0.1651	0.999	0.1649
Ethanol	−0.0927	0.001	−0.0000927
Mixture	0.1669	1.000	0.1669

Hence

entropy growth = 0.1669 − 0.1649927 = 0.0019723

and

heat of mixing = chemical exergy destroyed
= 285.15×0.0019723
= 0.5438665 per kg of mixture
= 543 per kg of alcohol,

which is not in close agreement with the above results, of around 438.

Note that the entropy growth of the water in being slightly diluted by alcohol is 0.002, leading to a water chemical exergy of 285.15×0.002 = 0.5, and confirming the qualitative thinking above via osmotic pressure.

In the GAS/VLE properties table, due to a programming error by the author, the thermomechanical exergies, which match well those of Beyer, have to be read as differences from the dewpoint line downwards.

In view of the above, Beyer's view that the accuracy of his table needs improvement has to be accepted. Moreover, accuracy can be seen as a substantial computational task outside the scope of this book. Witness the labour of producing the steam tables! However, it is not in doubt that the point made in Chapter 5 is valid, namely that the performance of the heat pump motivated distillation process can be viewed with clarity using Beyer's exergy concentration diagram.

References

[I] **Chieux, P.** (1994) How does water affect alcohol? *Physics World*, **7** (5).

[II] **Stabnikov, B. N.** ***et al.*** (1976) Ethyl spirit, *Pishevaya Promishlennost*, 113035, M35 Moscow.

[III] **Rowlinson, J. S.** and **Swinton, F. L.** (1982) *Liquids and liquid mixtures*, (Butterworths, London).

[IV] **Bosnjakovic, F.** (1960) *Technical thermodynamics*, Third Edition (Translated 1965, Blackshear, P. L., Holt Reinhardt Wilson, New York, Chicago, San Francisco, Toronto, London).

[V] **Wanheit, P. C.** (1988) *Separations in chemical engineering* (Elsevier, Oxford).

```
================================================================================
                GASVLE v2.3 12/ 1/1994 user: A.P.Laughton, GRC 03
================================================================================

>C BAR KG KJ M3                    Water and ethanol properties are referred to
>2                                  both the water triple point and each other.
>ETOH H2O
>0 1
>LRS KIJ -.067 MINI WF ETOH HM $M
>BUBP T=.01

 LRS  equation of state method (C for Costald liq. density)
 ------------------------------------------------------------------------------
   Pt Calc     Temp       Press  Wt.Fr.      Enthalpy     Entropy
              (C)        (bar)  (ETOH)       (kJ/kg)     (kJ/kg.C)
    1 BUBP C     .01       .006  .00000     -2528.5      -6.8964

>HBASE=-1 SBASE=-1
>COMP .001 1 FLSH T=12 P=1

 LRS  equation of state method (C for Costald liq. density)
 ------------------------------------------------------------------------------
   Pt Calc     Temp       Press  Wt.Fr.      Enthalpy     Entropy
              (C)        (bar)  (ETOH)       (kJ/kg)     (kJ/kg.C)
    2 SPHS C   12.00      1.000  .99900E-03   46.499       .16690

>#T=273.15+TT #G=N2-#T*N3 MINI $AME $N2-#T*N3-#G "Exergy kJ/kg"
>FOR 0(.1)1
>  COMP %X 1-XX
>  BUBT P=1
>  DEWT P=1
>  FLSH T=10 DT=10 NT=12 P=1
>LOOP

 LRS  equation of state method (C for Costald liq. density)
 ------------------------------------------------------------------------------
   Pt Calc     Temp       Press  Wt.Fr.      Enthalpy     Entropy    N2-#T*N3-#G
              (C)        (bar)  (ETOH)       (kJ/kg)     (kJ/kg.C)  Exergy kJ/kg

    5 SPHS C   10.00      1.000  .00000       38.607       .13834       .25052
    6 SPHS C   20.00      1.000  .00000       77.200       .27229       .64864
    7 SPHS C   30.00      1.000  .00000       115.88       .40202       2.3317
    8 SPHS C   40.00      1.000  .00000       154.67       .52792       5.2247
    9 SPHS C   50.00      1.000  .00000       193.61       .65031       9.2608
   10 SPHS C   60.00      1.000  .00000       232.72       .76951       14.384
   11 SPHS C   70.00      1.000  .00000       272.04       .88580       20.544
   12 SPHS C   80.00      1.000  .00000       311.60       .99944       27.702
   13 SPHS C   90.00      1.000  .00000       351.44       1.1107       35.821
    3 BUBT C   99.78      1.000  .00000       390.72       1.2174       44.665
    4 DEWT C   99.78      1.000  .00000       2665.3       7.3165       580.05
   14 SPHS    100.00      1.000  .00000       2665.7       7.3176       580.15
   15 SPHS    110.00      1.000  .00000       2684.7       7.3680       584.84
   16 SPHS    120.00      1.000  .00000       2703.9       7.4173       589.91

   19 SPHS C   10.00      2.000  .00000       38.715       .13826       .38241
   20 SPHS C   20.00      2.000  .00000       77.306       .27220       .78029
   21 SPHS C   30.00      2.000  .00000       115.98       .40193       2.4636
   22 SPHS C   40.00      2.000  .00000       154.77       .52782       5.3562
   23 SPHS C   50.00      2.000  .00000       193.71       .65021       9.3921
   24 SPHS C   60.00      2.000  .00000       232.82       .76940       14.515
   25 SPHS C   70.00      2.000  .00000       272.14       .88568       20.675
   26 SPHS C   80.00      2.000  .00000       311.70       .99932       27.833
   27 SPHS C   90.00      2.000  .00000       351.53       1.1106       35.951
   28 SPHS C  100.00      2.000  .00000       391.69       1.2196       45.002
```

29	SPHS	C	110.00	2.000	.00000	432.20	1.3268	54.963
30	SPHS	C	120.00	2.000	.00000	473.10	1.4321	65.817
17	BUBT	C	120.38	2.000	.00000	474.68	1.4361	66.251
18	DEWT	C	120.38	2.000	.00000	2701.0	7.0934	679.40
33	SPHS	C	10.00	1.000	.10000	54.486	.19507	-.47581E-01
34	SPHS	C	20.00	1.000	.10000	92.219	.32603	.34177
35	SPHS	C	30.00	1.000	.10000	130.07	.45300	1.9891
36	SPHS	C	40.00	1.000	.10000	168.07	.57633	4.8230
37	SPHS	C	50.00	1.000	.10000	206.25	.69635	8.7809
38	SPHS	C	60.00	1.000	.10000	244.65	.81335	13.810
39	SPHS	C	70.00	1.000	.10000	283.29	.92763	19.864
40	SPHS	C	80.00	1.000	.10000	322.21	1.0394	26.906
31	BUBT	C	84.55	1.000	.10000	340.01	1.0895	30.426
41	VLE	C	90.00	1.000	.10000	518.58	1.5850	67.723
32	DEWT	C	98.63	1.000	.10000	2506.6	6.9578	523.72
42	SPHS		100.00	1.000	.10000	2509.2	6.9647	524.32
43	SPHS		110.00	1.000	.10000	2528.1	7.0146	528.96
44	SPHS		120.00	1.000	.10000	2547.0	7.0634	533.98
47	SPHS	C	10.00	2.000	.10000	54.594	.19498	.85381E-01
48	SPHS	C	20.00	2.000	.10000	92.325	.32594	.47459
49	SPHS	C	30.00	2.000	.10000	130.17	.45290	2.1218
50	SPHS	C	40.00	2.000	.10000	168.17	.57622	4.9557
51	SPHS	C	50.00	2.000	.10000	206.35	.69624	8.9134
52	SPHS	C	60.00	2.000	.10000	244.75	.81324	13.942
53	SPHS	C	70.00	2.000	.10000	283.38	.92751	19.996
54	SPHS	C	80.00	2.000	.10000	322.30	1.0393	27.037
55	SPHS	C	90.00	2.000	.10000	361.54	1.1489	35.033
56	SPHS	C	100.00	2.000	.10000	401.13	1.2564	43.958
45	BUBT	C	105.67	2.000	.10000	423.76	1.3166	49.426
57	VLE	C	110.00	2.000	.10000	578.07	1.7216	88.242
46	DEWT	C	119.08	2.000	.10000	2541.7	6.7527	617.27
58	SPHS		120.00	2.000	.10000	2543.5	6.7572	617.75
61	SPHS	C	10.00	1.000	.20000	66.123	.22280	3.6828
62	SPHS	C	20.00	1.000	.20000	102.95	.35062	4.0629
63	SPHS	C	30.00	1.000	.20000	139.93	.47466	5.6724
64	SPHS	C	40.00	1.000	.20000	177.09	.59527	8.4438
65	SPHS	C	50.00	1.000	.20000	214.47	.71277	12.319
66	SPHS	C	60.00	1.000	.20000	252.11	.82746	17.248
67	SPHS	C	70.00	1.000	.20000	290.02	.93959	23.189
68	SPHS	C	80.00	1.000	.20000	328.26	1.0494	30.107
59	BUBT	C	81.33	1.000	.20000	333.35	1.0638	31.095
69	VLE	C	90.00	1.000	.20000	814.03	2.4052	129.27
60	DEWT	C	97.27	1.000	.20000	2347.7	6.5698	475.39
70	SPHS		100.00	1.000	.20000	2352.8	6.5835	476.57
71	SPHS		110.00	1.000	.20000	2371.4	6.6328	481.16
72	SPHS		120.00	1.000	.20000	2390.2	6.6812	486.14
75	SPHS	C	10.00	2.000	.20000	66.231	.22271	3.8173
76	SPHS	C	20.00	2.000	.20000	103.06	.35052	4.1974
77	SPHS	C	30.00	2.000	.20000	140.03	.47455	5.8067
78	SPHS	C	40.00	2.000	.20000	177.20	.59516	8.5782
79	SPHS	C	50.00	2.000	.20000	214.58	.71266	12.453
80	SPHS	C	60.00	2.000	.20000	252.20	.82733	17.382
81	SPHS	C	70.00	2.000	.20000	290.12	.93946	23.322
82	SPHS	C	80.00	2.000	.20000	328.35	1.0493	30.239
83	SPHS	C	90.00	2.000	.20000	366.94	1.1570	38.104
84	SPHS	C	100.00	2.000	.20000	405.94	1.2630	46.894
73	BUBT	C	101.92	2.000	.20000	413.49	1.2832	48.690
85	VLE	C	110.00	2.000	.20000	885.28	2.5289	165.27
74	DEWT	C	117.55	2.000	.20000	2382.0	6.3826	563.11
86	SPHS		120.00	2.000	.20000	2386.6	6.3944	564.37

89	SPHS	C	10.00	1.000	.30000	73.599	.23633	7.3015
90	SPHS	C	20.00	1.000	.30000	109.47	.36083	7.6717
91	SPHS	C	30.00	1.000	.30000	145.53	.48179	9.2415
92	SPHS	C	40.00	1.000	.30000	181.81	.59954	11.947
93	SPHS	C	50.00	1.000	.30000	218.35	.71438	15.734
94	SPHS	C	60.00	1.000	.30000	255.17	.82660	20.558
95	SPHS	C	70.00	1.000	.30000	292.32	.93645	26.378
96	SPHS	C	80.00	1.000	.30000	329.82	1.0442	33.164
87	BUBT	C	80.77	1.000	.30000	332.72	1.0524	33.724
97	VLE	C	90.00	1.000	.30000	1109.5	3.2255	190.81
88	DEWT	C	95.63	1.000	.30000	2188.3	6.1673	430.75
98	SPHS		100.00	1.000	.30000	2196.3	6.1890	432.61
99	SPHS		110.00	1.000	.30000	2214.8	6.2378	437.14
100	SPHS		120.00	1.000	.30000	2233.3	6.2857	442.07
103	SPHS	C	10.00	2.000	.30000	73.706	.23623	7.4373
104	SPHS	C	20.00	2.000	.30000	109.58	.36073	7.8074
105	SPHS	C	30.00	2.000	.30000	145.64	.48168	9.3774
106	SPHS	C	40.00	2.000	.30000	181.92	.59943	12.083
107	SPHS	C	50.00	2.000	.30000	218.45	.71426	15.870
108	SPHS	C	60.00	2.000	.30000	255.27	.82647	20.693
109	SPHS	C	70.00	2.000	.30000	292.41	.93632	26.513
110	SPHS	C	80.00	2.000	.30000	329.91	1.0440	33.298
111	SPHS	C	90.00	2.000	.30000	367.82	1.1499	41.023
112	SPHS	C	100.00	2.000	.30000	406.17	1.2541	49.668
101	BUBT	C	100.94	2.000	.30000	409.81	1.2638	50.530
113	VLE	C	110.00	2.000	.30000	1192.5	3.3361	242.29
102	DEWT	C	115.71	2.000	.30000	2221.8	5.9978	512.60
114	SPHS		120.00	2.000	.30000	2229.8	6.0184	514.78
117	SPHS	C	10.00	1.000	.40000	76.989	.23800	10.216
118	SPHS	C	20.00	1.000	.40000	111.86	.35903	10.576
119	SPHS	C	30.00	1.000	.40000	146.96	.47675	12.104
120	SPHS	C	40.00	1.000	.40000	182.31	.59148	14.740
121	SPHS	C	50.00	1.000	.40000	217.95	.70351	18.435
122	SPHS	C	60.00	1.000	.40000	253.92	.81312	23.146
123	SPHS	C	70.00	1.000	.40000	290.24	.92055	28.839
124	SPHS	C	80.00	1.000	.40000	326.97	1.0261	35.484
115	BUBT	C	80.70	1.000	.40000	329.56	1.0334	35.985
125	VLE	C	90.00	1.000	.40000	1404.9	4.0458	252.36
116	DEWT	C	93.62	1.000	.40000	2028.3	5.7526	389.03
126	SPHS		100.00	1.000	.40000	2039.8	5.7838	391.68
127	SPHS		110.00	1.000	.40000	2058.1	5.8321	396.16
128	SPHS		120.00	1.000	.40000	2076.5	5.8795	401.05
131	SPHS	C	10.00	2.000	.40000	77.096	.23789	10.353
132	SPHS	C	20.00	2.000	.40000	111.97	.35892	10.713
133	SPHS	C	30.00	2.000	.40000	147.06	.47663	12.241
134	SPHS	C	40.00	2.000	.40000	182.41	.59135	14.877
135	SPHS	C	50.00	2.000	.40000	218.05	.70338	18.572
136	SPHS	C	60.00	2.000	.40000	254.01	.81298	23.283
137	SPHS	C	70.00	2.000	.40000	290.34	.92041	28.975
138	SPHS	C	80.00	2.000	.40000	327.06	1.0259	35.619
139	SPHS	C	90.00	2.000	.40000	364.23	1.1297	43.194
140	SPHS	C	100.00	2.000	.40000	401.89	1.2320	51.685
129	BUBT	C	100.56	2.000	.40000	404.03	1.2377	52.189
141	VLE	C	110.00	2.000	.40000	1499.7	4.1434	319.32
130	DEWT	C	113.46	2.000	.40000	2060.9	5.6005	464.96
142	SPHS		120.00	2.000	.40000	2073.0	5.6317	468.22
145	SPHS	C	10.00	1.000	.50000	76.365	.22813	12.406
146	SPHS	C	20.00	1.000	.50000	110.19	.34552	12.755
147	SPHS	C	30.00	1.000	.50000	144.27	.45984	14.239

148	SPHS	C	40.00	1.000	.50000	178.64	.57139	16.803
149	SPHS	C	50.00	1.000	.50000	213.34	.68046	20.400
150	SPHS	C	60.00	1.000	.50000	248.40	.78731	24.993
151	SPHS	C	70.00	1.000	.50000	283.87	.89219	30.549
152	SPHS	C	80.00	1.000	.50000	319.77	.99532	37.046
143	BUBT	C	80.51	1.000	.50000	321.60	1.0005	37.400
153	VLE	C	90.00	1.000	.50000	1700.4	4.8661	313.90
144	DEWT	C	91.10	1.000	.50000	1867.5	5.3255	350.00
154	SPHS		100.00	1.000	.50000	1883.4	5.3686	353.61
155	SPHS		110.00	1.000	.50000	1901.4	5.4164	358.04
156	SPHS		120.00	1.000	.50000	1919.6	5.4633	362.88
159	SPHS	C	10.00	2.000	.50000	76.473	.22802	12.545
160	SPHS	C	20.00	2.000	.50000	110.29	.34540	12.894
161	SPHS	C	30.00	2.000	.50000	144.37	.45972	14.377
162	SPHS	C	40.00	2.000	.50000	178.74	.57126	16.941
163	SPHS	C	50.00	2.000	.50000	213.44	.68033	20.538
164	SPHS	C	60.00	2.000	.50000	248.50	.78717	25.130
165	SPHS	C	70.00	2.000	.50000	283.96	.89203	30.687
166	SPHS	C	80.00	2.000	.50000	319.86	.99515	37.182
167	SPHS	C	90.00	2.000	.50000	356.25	1.0968	44.598
168	SPHS	C	100.00	2.000	.50000	393.17	1.1971	52.922
157	BUBT	C	100.13	2.000	.50000	393.64	1.1983	53.033
169	VLE	C	110.00	2.000	.50000	1806.9	4.9506	396.35
158	DEWT	C	110.64	2.000	.50000	1899.0	5.1907	419.95
170	SPHS		120.00	2.000	.50000	1916.2	5.2349	424.52
173	SPHS	C	10.00	1.000	.60000	71.797	.20595	14.162
174	SPHS	C	20.00	1.000	.60000	104.52	.31953	14.500
175	SPHS	C	30.00	1.000	.60000	137.54	.43028	15.937
176	SPHS	C	40.00	1.000	.60000	170.88	.53849	18.424
177	SPHS	C	50.00	1.000	.60000	204.59	.64444	21.919
178	SPHS	C	60.00	1.000	.60000	238.70	.74838	26.387
179	SPHS	C	70.00	1.000	.60000	273.24	.85055	31.800
180	SPHS	C	80.00	1.000	.60000	308.27	.95116	38.138
171	BUBT	C	80.05	1.000	.60000	308.44	.95164	38.170
172	DEWT	C	87.81	1.000	.60000	1705.5	4.8845	313.73
181	SPHS		90.00	1.000	.60000	1709.3	4.8951	314.54
182	SPHS		100.00	1.000	.60000	1726.9	4.9430	318.52
183	SPHS		110.00	1.000	.60000	1744.7	4.9901	322.90
184	SPHS		120.00	1.000	.60000	1762.8	5.0366	327.69
187	SPHS	C	10.00	2.000	.60000	71.904	.20583	14.302
188	SPHS	C	20.00	2.000	.60000	104.63	.31941	14.640
189	SPHS	C	30.00	2.000	.60000	137.64	.43015	16.077
190	SPHS	C	40.00	2.000	.60000	170.98	.53835	18.564
191	SPHS	C	50.00	2.000	.60000	204.69	.64430	22.058
192	SPHS	C	60.00	2.000	.60000	238.79	.74822	26.526
193	SPHS	C	70.00	2.000	.60000	273.33	.85038	31.938
194	SPHS	C	80.00	2.000	.60000	308.36	.95098	38.275
195	SPHS	C	90.00	2.000	.60000	343.91	1.0503	45.522
185	BUBT	C	99.48	2.000	.60000	378.14	1.1433	53.218
196	VLE	C	100.00	2.000	.60000	780.18	2.2215	147.80
186	DEWT	C	106.99	2.000	.60000	1735.7	4.7666	377.61
197	SPHS		110.00	2.000	.60000	1741.2	4.7809	378.98
198	SPHS		120.00	2.000	.60000	1759.3	4.8277	383.81
201	SPHS	C	10.00	1.000	.70000	63.347	.16956	16.089
202	SPHS	C	20.00	1.000	.70000	94.923	.27915	16.416
203	SPHS	C	30.00	1.000	.70000	126.82	.38615	17.805
204	SPHS	C	40.00	1.000	.70000	159.09	.49086	20.211
205	SPHS	C	50.00	1.000	.70000	191.75	.59353	23.597
206	SPHS	C	60.00	1.000	.70000	224.85	.69439	27.933
207	SPHS	C	70.00	1.000	.70000	258.42	.79369	33.195

199	BUBT	C	79.38	1.000	.70000	290.38	.88556	38.953
202	VLE	C	80.00	1.000	.70000	948.49	2.7510	165.14
200	DEWT	C	83.36	1.000	.70000	1541.6	4.4263	280.55
209	SPHS		90.00	1.000	.70000	1553.1	4.4581	282.92
210	SPHS		100.00	1.000	.70000	1570.4	4.5053	286.84
211	SPHS		110.00	1.000	.70000	1588.1	4.5519	291.18
212	SPHS		120.00	1.000	.70000	1605.9	4.5979	295.92
215	SPHS	C	10.00	2.000	.70000	63.454	.16944	16.231
216	SPHS	C	20.00	2.000	.70000	95.027	.27902	16.557
217	SPHS	C	30.00	2.000	.70000	126.93	.38602	17.946
218	SPHS	C	40.00	2.000	.70000	159.19	.49072	20.352
219	SPHS	C	50.00	2.000	.70000	191.85	.59337	23.738
220	SPHS	C	60.00	2.000	.70000	224.94	.69422	28.074
221	SPHS	C	70.00	2.000	.70000	258.51	.79351	33.334
222	SPHS	C	80.00	2.000	.70000	292.60	.89144	39.503
223	SPHS	C	90.00	2.000	.70000	327.27	.98823	46.568
213	BUBT	C	98.64	2.000	.70000	357.74	1.0712	53.394
224	VLE	C	100.00	2.000	.70000	1282.5	3.5549	269.88
214	DEWT	C	102.14	2.000	.70000	1570.5	4.3252	338.25
225	SPHS		110.00	2.000	.70000	1584.5	4.3621	341.72
226	SPHS		120.00	2.000	.70000	1602.5	4.4085	346.50
229	SPHS	C	10.00	1.000	.80000	51.074	.11521	19.313
230	SPHS	C	20.00	1.000	.80000	81.448	.22063	19.628
231	SPHS	C	30.00	1.000	.80000	112.18	.32372	20.966
232	SPHS	C	40.00	1.000	.80000	143.31	.42474	23.288
233	SPHS	C	50.00	1.000	.80000	174.87	.52395	26.560
234	SPHS	C	60.00	1.000	.80000	206.91	.62157	30.757
235	SPHS	C	70.00	1.000	.80000	239.45	.71783	35.857
227	BUBT	C	78.64	1.000	.80000	268.04	.80009	40.983
228	DEWT	C	79.28	1.000	.80000	1378.7	3.9551	251.98
236	SPHS		80.00	1.000	.80000	1379.9	3.9586	252.21
237	SPHS		90.00	1.000	.80000	1396.8	4.0057	255.66
238	SPHS		100.00	1.000	.80000	1414.0	4.0524	259.53
239	SPHS		110.00	1.000	.80000	1431.4	4.0984	263.81
240	SPHS		120.00	1.000	.80000	1449.1	4.1440	268.50
243	SPHS	C	10.00	2.000	.80000	51.180	.11508	19.456
244	SPHS	C	20.00	2.000	.80000	81.552	.22049	19.770
245	SPHS	C	30.00	2.000	.80000	112.28	.32357	21.109
246	SPHS	C	40.00	2.000	.80000	143.41	.42459	23.430
247	SPHS	C	50.00	2.000	.80000	174.97	.52378	26.702
248	SPHS	C	60.00	2.000	.80000	207.00	.62139	30.898
249	SPHS	C	70.00	2.000	.80000	239.54	.71763	35.998
250	SPHS	C	80.00	2.000	.80000	272.65	.81273	41.988
251	SPHS	C	90.00	2.000	.80000	306.37	.90688	48.861
241	BUBT	C	97.77	2.000	.80000	333.05	.97958	54.814
242	DEWT	C	98.46	2.000	.80000	1407.5	3.8743	303.87
252	SPHS		100.00	2.000	.80000	1410.2	3.8815	304.50
253	SPHS		110.00	2.000	.80000	1427.8	3.9280	308.82
254	SPHS		120.00	2.000	.80000	1445.6	3.9740	313.55
257	SPHS	C	10.00	1.000	.90000	35.031	.34605E-01	26.255
258	SPHS	C	20.00	1.000	.90000	64.149	.13566	26.556
259	SPHS	C	30.00	1.000	.90000	93.659	.23465	27.841
260	SPHS	C	40.00	1.000	.90000	123.60	.33181	30.075
261	SPHS	C	50.00	1.000	.90000	154.00	.42737	33.227
262	SPHS	C	60.00	1.000	.90000	184.91	.52157	37.277
263	SPHS	C	70.00	1.000	.90000	216.37	.61461	42.207
255	BUBT	C	78.08	1.000	.90000	242.25	.68914	46.831
256	DEWT	C	78.12	1.000	.90000	1220.8	3.4751	230.99
264	SPHS		80.00	1.000	.90000	1223.9	3.4839	231.58
265	SPHS		90.00	1.000	.90000	1240.5	3.5303	234.97

```
  266 SPHS      100.00      1.000   .90000      1257.5       3.5763       238.78
  267 SPHS      110.00      1.000   .90000      1274.7       3.6218       243.02
  268 SPHS      120.00      1.000   .90000      1292.2       3.6669       247.66

  271 SPHS C     10.00      2.000   .90000      35.137      .34471E-01    26.399
  272 SPHS C     20.00      2.000   .90000      64.253       .13552       26.701
  273 SPHS C     30.00      2.000   .90000      93.759       .23449       27.986
  274 SPHS C     40.00      2.000   .90000      123.69       .33164       30.219
  275 SPHS C     50.00      2.000   .90000      154.09       .42719       33.371
  276 SPHS C     60.00      2.000   .90000      185.00       .52138       37.419
  277 SPHS C     70.00      2.000   .90000      216.45       .61440       42.349
  278 SPHS C     80.00      2.000   .90000      248.51       .70648       48.149
  279 SPHS C     90.00      2.000   .90000      281.22       .79782       54.817
  269 BUBT C     97.09      2.000   .90000      304.86       .86228       60.072
  270 DEWT C     97.15      2.000   .90000      1248.8       3.4116       277.07
  280 SPHS      100.00      2.000   .90000      1253.7       3.4248       278.21
  281 SPHS      110.00      2.000   .90000      1271.1       3.4708       282.49
  282 SPHS      120.00      2.000   .90000      1288.8       3.5163       287.17

  285 SPHS C     10.00      1.000   1.0000      15.263       -.11201      48.296
  286 SPHS C     20.00      1.000   1.0000      43.069      -.15512E-01   48.584
  287 SPHS C     30.00      1.000   1.0000      71.297      .79170E-01    49.813
  288 SPHS C     40.00      1.000   1.0000      99.984       .17227       51.954
  289 SPHS C     50.00      1.000   1.0000      129.17       .26400       54.980
  290 SPHS C     60.00      1.000   1.0000      158.89       .35459       58.874
  291 SPHS C     70.00      1.000   1.0000      189.20       .44422       63.624
  283 BUBT C     78.06      1.000   1.0000      214.09       .51590       68.070
  284 DEWT C     78.06      1.000   1.0000      1064.8       2.9380       228.07
  292 SPHS       80.00      1.000   1.0000      1067.9       2.9470       228.67
  293 SPHS       90.00      1.000   1.0000      1084.3       2.9927       232.01
  294 SPHS      100.00      1.000   1.0000      1101.0       3.0380       235.77
  295 SPHS      110.00      1.000   1.0000      1118.0       3.0830       239.95
  296 SPHS      120.00      1.000   1.0000      1135.3       3.1277       244.55

  299 SPHS C     10.00      2.000   1.0000      15.369       -.11216      48.442
  300 SPHS C     20.00      2.000   1.0000      43.171      -.15664E-01   48.730
  301 SPHS C     30.00      2.000   1.0000      71.396      .79006E-01    49.959
  302 SPHS C     40.00      2.000   1.0000      100.08       .17209       52.099
  303 SPHS C     50.00      2.000   1.0000      129.26       .26381       55.124
  304 SPHS C     60.00      2.000   1.0000      158.98       .35438       59.018
  305 SPHS C     70.00      2.000   1.0000      189.28       .44400       63.767
  306 SPHS C     80.00      2.000   1.0000      220.22       .53287       69.365
  307 SPHS C     90.00      2.000   1.0000      251.86       .62121       75.814
  297 BUBT C     96.93      2.000   1.0000      274.22       .68219       80.782
  298 DEWT C     96.93      2.000   1.0000      1091.9       2.8918       268.44
  308 SPHS      100.00      2.000   1.0000      1097.2       2.9059       269.65
  309 SPHS      110.00      2.000   1.0000      1114.4       2.9513       273.88
  310 SPHS      120.00      2.000   1.0000      1131.9       2.9964       278.52

>END
```

Index